Does exposure to ionising radiation and chemotherapy damage mitochondria within oocytes?

Qiaochu Wang

Thesis submitted for the degree of Doctor of Philosophy

at the Department of Anatomy & Developmental Biology,
Faculty of Medicine, Nursing and Health Sciences,
Monash University

Supervisors:

Associate Professor Karla J. Hutt

Professor John Carroll

Submitted June 2021

Copyright Notice

Table of contents

Abstract 5
Thesis including papers work declaration 9
Publications and Conferences 11
Acknowledgements 12
List of Figures 14
List of Abbreviations 16
Chapter 1. Literature review 18
1.1 Introduction 19
1.2 Structure and function of the ovary 19
1.2.1 Formation and maintenance of the ovarian follicular reserve 19
1.2.2 Folliculogenesis 21
1.3 Cancer treatments 26
1.3.1 Radiotherapy 27
1.3.2 Chemotherapy 27
1.4 Mitochondria 28
1.4.1 Structure and function 28
1.4.2 Dynamics 29
1.4.3 Mitochondria DNA 30
1.5 Irradiation damages mitochondria 32
1.5.1 Irradiation affects mitochondrial mass 32
1.5.2 Irradiation affects mitochondrial DNA 32
1.5.3 Irradiation affects the electron transport chain 33
1.5.4 Irradiation affects the intracellular levels of reactive oxygen species (ROS) 33
1.6 Cisplatin damages mitochondria 34
1.6.1 Cisplatin induces mtDNA damage 34
1.6.2 Cisplatin affects the electron transport chain 35
1.6.3 Cisplatin affects ROS level 35
1.7 ROS and antioxidants 35
1.7.1 ROS generation in mitochondria 36
1.7.2 ROS and protein peroxidation 36
1.7.3 ROS and lipid peroxidation 37

1.7.4 ROS and DNA damage....37
1.7.5 Antioxidants....38
1.8 Overall Significance....41
1.9 Aims and Hypothesis....41
Chapter 2. Evaluation of mitochondria in oocytes following γ-irradiation....42
Chapter 3. Evaluation of mitochondria in oocytes following cisplatin exposure....53
Chapter 4. Investigation of the potential of MitoQ to protect against ovarian damage caused by ionising radiation....64
4.1 Introduction....65
4.2 Materials and Methods....67
4.2.1 Mice and treatments....67
4.2.2 Chemicals....68
4.2.2 Histology....68
4.2.3 Quantification of primordial and primary follicles....68
4.2.4 Quantification of secondary follicles, antral follicles, atretic follicles and corpora lutea....69
4.2.5 Immunofluorescence....69
4.2.6 Statistical analysis....70
4.3 Results....70
4.3.1 5 mg/kg MitoQ supplementation caused swollen intestines and suppressed ovulation, but these impacts were not observed when 2 mg/kg was used....70
4.3.3 MitoQ protected primary follicle loss 3 hours after 0.45Gy whole body γ-irradiation....74
4.3.4 MitoQ did not prevent the depletion of primordial and primary follicles 5 days after 0.45Gy whole body γ-irradiation....76
4.3.5 γ-Irradiation did not enhance DNA/RNA oxidative damage to the ovary....78
4.3.6 γ-Irradiation did not enhance lipid oxidative damage to the ovary....81
4.3.7 γ-Irradiation did not enhance protein oxidative damage to the ovary....83
4.4 Discussion....85
4.5 Conclusion....90
Chapter 5. General discussion....93
References....102

Abstract

The female reproductive lifespan is determined by the size of the primordial follicle pool established in the ovary before or just after birth. Primordial follicles eventually develop into mature hormone producing follicles and ovulatory oocytes. Primordial follicles are non-renewable, even if the pool is depleted by exposure to radiotherapy and cytotoxic chemotherapy, causing infertility and premature menopause. With an increasing survival rate for most cancers, and concerns about female fertility after life-saving treatment, it is important to comprehensively understand the mechanisms underlying follicle depletion and to devise novel strategies to preserve the future fertility of females. Numerous studies have demonstrated that apoptosis induced by oocyte nuclear DNA damage is responsible for the loss of ovarian follicles following exposure to radiation or cytotoxic chemotherapies. However, the potential contribution of mitochondrial damage to cancer-treatment induced follicle depletion has received only limited attention.

Since mammalian oocytes have a limited capacity for glycolysis, their main source of energy is the mitochondria via a process called oxidative phosphorylation (OXPHOS). To meet their high-energy requirements, the number of mitochondria in oocytes increases dramatically during oogenesis and folliculogenesis. Studies in somatic cells show that exposure to ionizing radiation or chemotherapeutic drugs like the platinum-based chemotherapeutic cisplatin, results in damage to mitochondrial structure, function and mtDNA, and causes the excessive production of ROS due to the malfunction of OXPHOS, all of which can trigger apoptosis or compromise cell function. Thus, it was hypothesized that mitochondrial damage within oocytes could contribute follicle depletion or loss of oocyte quality caused by cancer treatments, and in turn, protecting mitochondria could represent a novel therapeutic strategy to alleviate the ovotoxicity of cancer treatments. To begin to address this hypothesis, this thesis evaluated the characteristics of mitochondria in oocytes following γ-irradiation exposure (Chapter 2) and cisplatin treatment (Chapter 3), and investigated the potential of the mitochondrial antioxidant, MitoQ, to mitigate the follicle depletion caused by radiation (Chapter 4), using mice as a model.

In Chapter 2, the short and long-term impact of γ-irradiation on mitochondria in oocytes at different stages of development was investigated. Whilst mitochondria in growing oocytes exhibited largely

normal characteristics, acute mitochondrial damage, which was manifested by the loss of mitochondrial membrane potential, was detected in small immature oocytes at 3 and 6 hours after γ-irradiation. Loss of mitochondrial membrane potential is a well-described characteristic of cell death mediated by the intrinsic apoptosis pathway and is consistent with the rapid depletion of primordial and primary follicles after exposure to γ-irradiation. Importantly, all those small immature oocytes that survived at 24 hours after γ-irradiation, had a mitochondrial mass, distribution and quality similar to controls. Depletion of the ovarian reserve of primordial and growing follicles was supported by the finding that 3 weeks after γ-irradiation, mice ovulated significantly fewer mature oocytes than age-matched untreated controls. However, mitochondrial localization, mtDNA copy number and ATP levels in those fully-grown oocytes were normal (despite a slight reduction in mitochondrial mass), consistent with normal mitochondrial function. Overall, the observations reported in this chapter suggest that mitochondrial damage (either via direct mitochondrial membrane damage, or indirectly through the induction of intrinsic apoptosis) contributes to primordial and primary follicle depletion, but long-lasting impacts on mitochondrial function appear to be minor or completely absent. Indeed, previous studies indicate that mature oocytes from apoptosis-deficient mice exposed to γ-irradiation have normal meiotic and developmental competence, consistent with the presence of healthy mitochondria.

In Chapter 3, the short and long-term impacts of two different doses of cisplatin on mitochondria in oocytes were evaluated. Cisplatin was found to induce mitochondrial damage and deplete the ovarian reserve in a dose dependent manner. Small immature oocytes from pre-pubertal mice lost mitochondrial membrane potential at 24 hours after 2mg/kg and 4mg/kg cisplatin treatment, but oocyte death was triggered in large numbers of oocytes only after exposure to the higher dose of cisplatin. Furthermore, pre-pubertal mice treated with the 2mg/kg dose of cisplatin ovulated reduced numbers of mature oocytes compared to saline treated controls 5 weeks after cisplatin treatment, however, the pre-pubertal mice treated with 4mg/kg cisplatin did not ovulate any mature oocytes. This observation is consistent with the dramatic depletion of the ovarian reserve of primordial follicles previously reported in cisplatin-treated mice. Of note, adult mice were more tolerant to cisplatin ovotoxicity than pre-pubertal mice, as ovulation was not affected when mice were treated as adults with 4mg/kg cisplatin. Importantly, mitochondria localisation, mass, membrane potential and ATP levels were similar in mature oocytes harvested from saline and cisplatin (4mg/kg) treated mice. Thus, cisplatin-induced mitochondrial

dysfunction in immature oocytes may contribute to the loss of ovarian follicles after treatment, but there was no evidence of persistent mitochondrial dysfunction in those oocytes that survive and mature.

MitoQ is a powerful nontoxic mitochondrial targeted antioxidant that has previously been shown in rats to protect against testicular damage caused by γ-irradiation. Based on this information, and the findings presented in Chapter 2 and 3, Chapter 4 was designed to investigate the possibility that MitoQ could prevent follicle loss and oxidative damage after γ-irradiation. Unexpectedly, in an initial pilot study, severe intestinal swelling was observed in mice 5 days after four doses of 5mg/kg MitoQ delivered by intraperitoneal (i.p.) injection. In addition, corpora lutea number dropped dramatically in MitoQ treated mice, while follicle numbers remained unaffected, indicating suppression of ovulation. To avoid these undesirable side effects, 2mg/kg MitoQ was subsequently used. As expected, primordial and primary follicles were completely depleted in the ovaries of mice 5 days after exposure to γ-irradiation, while secondary and antral follicles remained unaffected. MitoQ (2mg/kg) supplementation did not prevent the loss of primordial and primary follicles. Interestingly, when follicle numbers were analysed at 3 hours after γ-irradiation, primary follicle numbers were found to be reduced compared to untreated controls, and this was completely mitigated by MitoQ treatment, suggesting that MitoQ delayed depletion of this follicle class. In addition, given that radiation treatment can increase the production of reactive oxygen species (ROS) by mitochondria, DNA/RNA, lipid, and protein oxidative damage was analysed in ovarian tissue sections from untreated and γ-irradiated mice at 3 hours and 5 days after exposure. The percentage of follicles at each stage of development staining positively for the three oxidative damage markers analysed, was similar in untreated and γ-irradiated mice, and administration of MitoQ did not alter this. Thus, whether γ-irradiation causes DNA/RNA, lipid, and protein oxidative damage in ovaries remains unconfirmed.

Overall, the findings of this thesis show that γ-irradiation and cisplatin treatment cause loss of mitochondrial membrane potential and death of a cohort of small immature oocytes from primordial and primary follicles. Notably, however, those immature oocytes that survive γ-irradiation and cisplatin exposure are able to develop to the ovulatory stage and appear to contain mitochondria with normal characteristics. Thus, there was no evidence from these studies to suggest that mitochondria sustained ongoing damage or dysfunction. Under the conditions used in this study, MitoQ was unable to prevent

primordial and primary follicle depletion caused by γ-irradiation. Further studies, trialing different supplementation regimens, will be required to fully evaluate the potential of MitoQ as a possible follicle protectant.

Thesis including papers work declaration

I hereby declare that this thesis is an original work of my research and contains no material which has been accepted for the award of any other degree or diploma at any university or equivalent institution and that, to the best of my knowledge and belief, this thesis contains no material previously published or written by another person, except where due reference is made in the text of the thesis.

Thesis chapter	Publication title	Status	Nature and % of student contribution	Co-author name(s) Nature and % of Co-author's contribution	Co-author(s), Monash Student Y/N
2	Evaluation of mitochondria in oocytes following γ-irradiation	Published	Designed and performed the experiments; collected and analyzed data; drafted the manuscript (70%)	1. Jessica M. Stringer, assisted with oocytes collection (5%) 2. Jun Liu, assisted with mtDNA copy number and immunofluorescent images analysis (10%) 3. Karla J. Hutt designed the experiment and edited the manuscript (15%)	Y

3	Evaluation of mitochondria in oocytes following cisplatin exposure	published	Designed and performed the experiments; collected and analyzed data; drafted the manuscript (85%)	1. Karla J. Hutt designed the experiment and edited the manuscript (15%)	N

Publications and Conferences

Publications

1. Qiaochu Wang, Hutt KJ. Evaluation of mitochondria in mouse oocytes following cisplatin exposure. J Ovarian Res. 2021 May 10;14(1):65. doi: 10.1186/s13048-021-00817-w. PMID: 33971923; PMCID: PMC8111953.

2. Qiaochu Wang, Stringer JM, Liu J, Hutt KJ. Evaluation of mitochondria in oocytes following γ-irradiation. Sci Rep. 2019 Dec 27;9(1):19941. doi: 10.1038/s41598-019-56423-w. PMID: 31882895; PMCID: PMC6934861.

Conferences

1. Qiaochu Wang, Jessica Stringer, John Carroll, Karla Hutt. Does exposure to ionising radiation damage mitochondria within oocytes? 2018 Annual Scientific Meeting of the Society for Reproductive Biology (SRB) (Poster)

2. Qiaochu Wang, Jessica Stringer, John Carroll, Karla Hutt. Does exposure to ionising radiation damage mitochondria within oocytes? Australian Conference for Mitochondrial Research, Melbourne (AussieMit) (Poster)

Acknowledgements

First and foremost, I would like to express my deepest gratitude to my supervisors Associated Professor Karla Hutt and Professor John Carroll. Without the recommendation from John and the acceptance by Karla, I would not have the chance to do my PhD in the Ovarian Biology Laboratory. Karla has provided me with professional guidance in research and continuous support in life in the past 4 years. She always gave positive feedbacks and constructive advice on my experiments and the manuscripts, which encouraged and inspired me. She also offered flexible working time to me after I came back from the maternity leave, so that I had enough time to take care of my child. I cannot think of anyone better than her as a supportive and thoughtful supervisor. Thank you so much for everything during this memorable journey.

I would like to thank all the lab members in Hutt and Carroll's lab for their help during my PhD. To Jessica Stringer, thank you for teaching me how to collect oocytes and to do immunofluorescence on ovarian sections. To Nadeen Zerafa, thank you for injecting mice when I was on maternity leave and thank you for all the sample submissions and mouse orders. To Carolina Lliberos, thank you for teaching me how to do stereology and immunohistochemistry. To Urooza Sarma, thank you for the facetime when I had trouble with the microscope. To Jun Liu, thank you for the help on the qPCR and immunofluorescent intensity analysis. To Meaghan Griffiths, thank you for teaching me how to culture cells and testing cisplatin for me. To Amy Winship, Qinghua Zhang, Deepak Adhikari, Wai Shan Yuen, Lauren Alesi, and Quynh-Nhu Nguyen, thank you for the help and advice when needed. Specially, I need to thank Carolina Lliberos, Urooza Sarma, Martin Estermann, Zahida Yesmin Roly, Ming Shen Tham, Inwon Lee and Xuebi Cai for making my PhD full of joy. It is my pleasure to provide chocolate to you guys!

Last but not least, I would like to sincerely thank my family. To my perfect husband, who is also my PhD mate at Monash, thank you for the help and advice in the experiments and the love, patience and care in life. To my mother-in-law, thank you for taking care of our baby in the last year of my PhD. To my 2-year-old daughter, thank you for all the naive talks and laughs, which relieving my pressure before the thesis submission. To my parents, thank you for your continuous support throughout my PhD. This

thesis would not have existed without all of you having my back.

List of Figures

Chapter 1

Figure 1. Timeline of the developmental process from primordial germ cell migration to the beginning of folliculogenesis in mouse and human.

Figure 2. Outline of the main steps of folliculogenesis.

Figure 3: Morphology of ovarian folliculogenesis stages.

Figure 4. Mitochondrial structure.

Figure 5. Diagrammatic representation of changes in estimate number of mitochondria during development of female germ line.

Figure 6. Mitochondrial genome. CO, cytochrome oxidase; Cyt, ubiquinone-cytochrome c reductase; ND, NADH dehydrogenase; ATPase, ATP synthase. tRNAs are represented as points.

Figure 7. Overview of molecular mechanisms of cisplatin in cancer treatment.

Figure 8. Mitochondrial electron transport chain and electron leakage.

Figure 9. Antioxidative mechanism of SS-31.

Figure 10. Structure and mechanism of MitoQ.

Chapter 2

Figure 1. The distribution of mitochondria in small and growing immature oocytes from untreated and γ-irradiated mice.

Figure 2. Membrane potential of mitochondria in small immature oocytes from untreated and γ-irradiated mice.

Figure 3. Membrane potential of mitochondria in growing immature oocytes from untreated and γ-irradiated mice.

Figure 4. Mitochondria in mature oocytes.

Supplemental Figure 1. Classification of oocytes according to size.

Chapter 3

Figure 1. The distribution of mitochondria in small and growing immature oocytes from saline and cisplatin (2 and 4 mg/kg) treated mice.

Figure 2. Membrane potential of mitochondria in small immature oocytes from saline and cisplatin (2 and 4 mg/kg) treated mice.

Figure 3. Membrane potential of mitochondria in growing immature oocytes from saline and cisplatin (2 and 4 mg/kg) treated mice.

Figure 4. Mitochondria in mature oocytes (2 mg/kg cisplatin injected at PN10).

Figure 5. Mitochondria in mature oocytes (4 mg/kg cisplatin injected at PN50).

Chapter 4

Figure 1. Effects of 5mg/kg/day MitoQ on the intestine and ovaries of mice.

Figure 2. Effects of 2mg/kg/day MitoQ on the intestine and ovaries of mice.

Figure 3. Ovarian morphology and follicle numbers in mice supplemented with MitoQ (2mg/kg/day) and exposed to whole-body γ-irradiation (0.45Gy) at the 3-hour collection time point.

Figure 4. Ovarian morphology and follicle numbers of mice supplemented with MitoQ (2mg/kg/day) and exposure to whole-body γ-irradiation (0.45Gy) at the 5-day collection time point.

Figure 5. DNA/RNA oxidative damage of ovarian follicles after 0.45Gy γ-irradiation.

Figure 6. Lipid oxidative damage of ovarian follicles after 0.45Gy γ-irradiation.

Figure 7. Protein oxidative damage of ovarian follicles after 0.45Gy γ-irradiation.

Supplemental Figure 1. Diagram of MitoQ and γ-irradiation treatments.

Supplemental Figure 2. Representative images of negative control of the oxidative damage markers.

List of Abbreviations

FSH	Follicle-Stimulating Hormone
LH	Luteinizing Hormone
AMH	Anti-Müllerian Hormone
PN	Postnatal Day
DFs	Dominant Follicles
SFs	Subordinate Follicles
COC	Cumulus-oOcyte Complex
TNF	Tumor Necrosis Factor
POI	Premature Ovarian Insufficiency
ER	Endoplasmic Reticulum
ATP	Adenosine Triphosphate
OXPHOS	Oxidative Phosphorylation
ETC	Electron Transport Chain
TCA	Tricarboxylic Acid
co Q	Coenzyme Q
ROS	Reactive Oxygen Species
GTPase	Guanosine Triphosphates
Mfn1	Mitofusion 1
Mfn2	Mitofusion 2
PGC-1α	Peroxisome Proliferator-activated Receptor γ Coactivator-1α
MtDNA	Mitochondrial DNA
H-strand	Heavy Strand
L-strand	Light Strand
tRNA	Transfer RNAs
CHO-K1	Chinese Hamster Ovarian Cells
HPV-G	Human Keratinocytes
RTK	Receptor Tyrosine Kinases
PTK	Protein Tyrosine Kinases

NTY	3-Nitrotyrosin
PUFAs	Polyunsaturated Fatty Acids
PTPs	Permeability Transition Pores
4-HNE	4-Hydroxynonenal
MDA	Malondialdehyde
OS	Oxidative Stress
DDR	DNA Ddamage Response
BER	Base Excision Repair
NER	Nucleotide Excision Repair
HR	Homologous Recombination
NHEJ	Nonhomologous End Joining
SOD	Superoxide Dismutase
CAT	Catalase
GPx	Glutathione Peroxidase
TPP	Triphenylphosphonium
HCV	Hepatitis C Virus
PCOS	Polycystic Ovary Syndrome
nDNA	Nuclear DNA
mtROS	Mitochondrial Reactive Oxygen Species
DMSO	Dimethyl Sulfoxide
PAS	Periodic Acid-Schiff
BSA	Bovine Serum Albumin
TNT	Tris-NaCl-Tween
DCFDA	2’,7’-Dichlorofluorescin Diacetate
TMRM	Tetramethylrhodamine Methyl Ester

Chapter 1. Literature review

1.1 Introduction

Standard cytotoxic cancer treatments, including radiation and chemotherapy, can damage the oocytes and somatic cells within the ovary, leading to a reduction in the size of the ovarian follicular reserve, which predisposes females to infertility and premature menopause later in life [1]. With improving survival rates for many cancers, there is a growing need to avoid this undesirable side-effect and devise new strategies to improve the long-term fertility and health of women post-treatment [2]. In order to achieve this goal, it is necessary to fully understand the mechanisms by which specific anti-cancer treatments damage the ovary and induce oocyte death. Recent studies have largely focused on the damage that radiation and chemotherapy cause to the genomic DNA in oocytes, which includes the induction of DNA double or single strand breaks and formation of DNA crosslinks and adducts [3]. However, it is likely that radiation and chemotherapy also damage organelles within the oocyte that are vital for oocyte function. In particular, radiation and chemotherapies, such as cisplatin, may damage mitochondria. Mitochondrial damage can trigger oocyte death or compromise oocyte quality [4]. This is especially important to consider in the context of fertility preservation for female cancer patients, as these organelles are maternally inherited [5]. This literature review summarizes our current understanding of the impact of cancer treatments, in particular irradiation and cisplatin, on the ovary, with a focus on their potential effects on mitochondria as demonstrated in somatic cells.

1.2 Structure and function of the ovary

The ovaries are the primary functional organs of the female reproductive system, the functions of which are to support the growth and development of female germ cells, and to synthesize, release, and control the production of hormones necessary for the development of secondary sex characteristics and support pregnancy [6]. The ovaries are composed of an inner medulla and outer cortex. The inner medulla is made up of connective and interstitial tissue, vasculature, nerve innervation, and lymphatics. The outer cortex is where oocytes reside, which are maintained in structures called ovarian follicles.

1.2.1 Formation and maintenance of the ovarian follicular reserve

The majority of oocytes are maintained in the ovary in the form of primordial follicles, each of which

is comprised of a small, immature oocyte that is both growth and meiotically arrested, surrounded by the single layer of squamous granulosa cells. The ovarian reserve of primordial follicles is formed by a series of highly coordinated events that occurs during embryonic development in humans and mice (Fig.1) [6]. In mice, it begins with the specification of primordial germ cells at the allantois of the proximal epiblast at ~E6.0 [7]. These cells then proliferate and migrate to colonize the undifferentiated gonadal ridge at ~ E11.5 and become oogonia. The oogonia continue to proliferate and form the nest like structures of interconnected cells as a consequence of incomplete cytokinesis [8, 9]. Oogonia cease proliferating at around E13.5, transit into meiosis and then subsequently arrest at diplotene of the first meiotic prophase at E17.5. Coincident with the meiotic arrest, nests begin to breakdown and individual oocytes become engulfed in a single layer of granulosa cells, forming primordial follicles. The process of follicle formation is completed by postnatal day (PN) 8. A similar sequence of events occurs in humans, with colonization of the urogenital ridge occurred at around 7 weeks gestation and follicle formation completed before birth. Once formed, primordial follicles enter a state of growth arrest, referred to as quiescence [10]. The period of primordial quiescence may span up to 18 months in mice, or decades in humans [11].

The transition from mitosis to meiosis is a significant developmental event because it marks the time at which it is no longer possible to make new female germ cells. Consequently, the initial pool of primordial follicles formed before (in humans) or just after birth (in mice) represents the entire stockpile of gametes available to support female fertility, endocrine function and reproductive health. The number of primordial follicles is progressively depleted over the reproductive lifespan by their gradual activation to resume growth and begin folliculogenesis, or as a consequence of follicle death [12]. Although some studies have suggested that new oocytes may be generated from a population of ovarian stem cells that remain in the ovary postnatally [13-15], this hypothesis remains controversial [16]. Thus, the finite supply of primordial follicles established early in life significantly influences a woman's future fertility and consequently, exogenous stimuli, such as anti-cancer treatments that damage primordial follicles and induce their loss, significantly compromise female fertility.

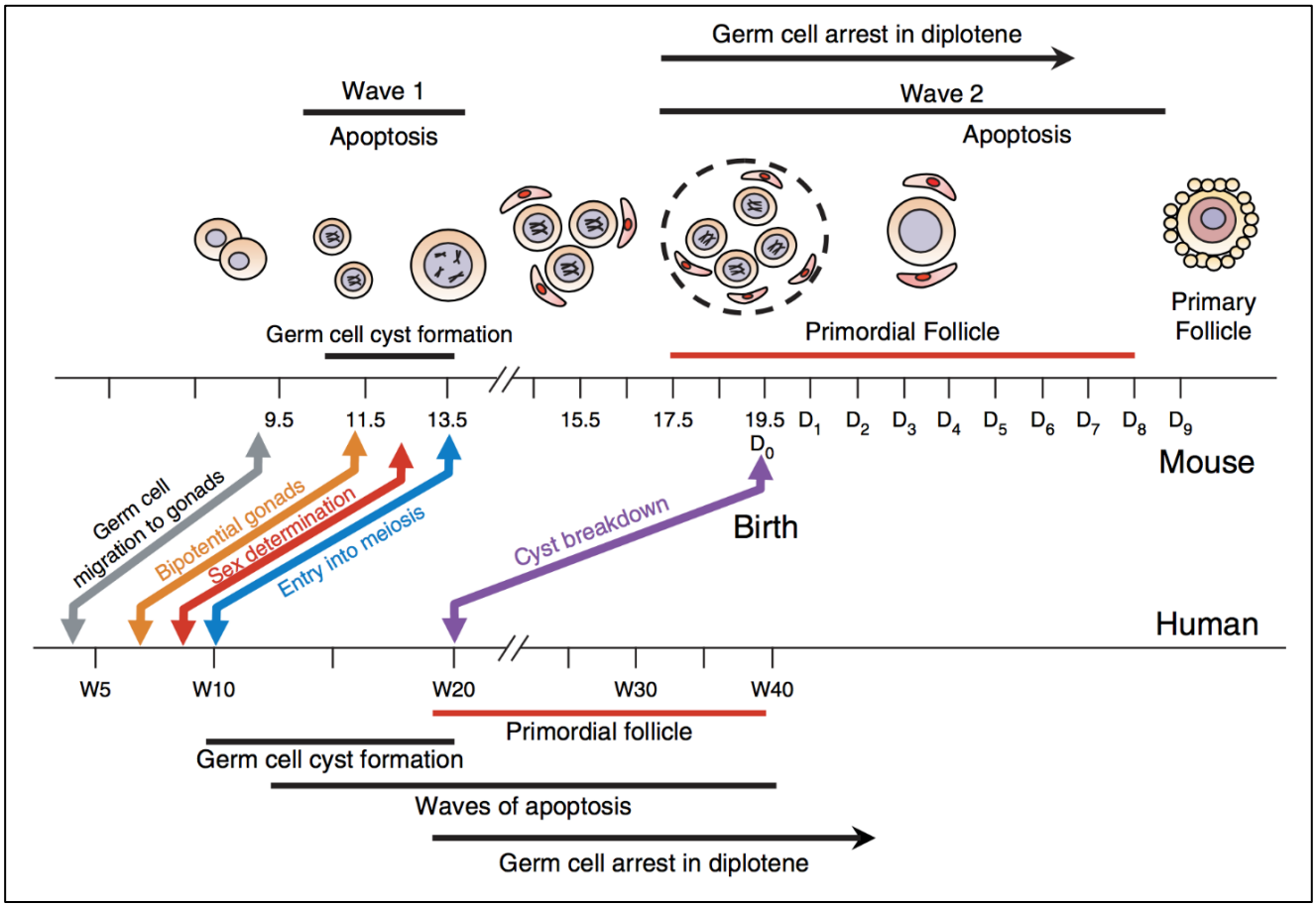

Figure 1. Timeline of the developmental process from primordial germ cell migration to the beginning of folliculogenesis in mouse and human. Human development is listed in weeks post coitus, mouse development in days post coitus [17].

1.2.2 Folliculogenesis

Folliculogenesis refers to the process of the development of primordial follicles to the ovulatory stage [18]. The whole process takes approximately 12 months in humans [12] and 3 weeks in mice [19]. Once primordial follicles are released from dormancy and begin developing in a step wise and cyclical manner, folliculogenesis continues until the supply reaches a critical lower threshold, and the pool becomes exhausted [20].

Folliculogenesis, in both mice and humans, is characterised by two major phases [21]. The first phase is gonadotropin independent and is primarily regulated by locally produced factors acting in an autocrine and paracrine fashion. It includes the activation and development of the primordial follicle to the secondary/pre-antral stages. The second phase is dependent on the cyclic release of pituitary-

gonadotropic factors, Follicle Stimulating Hormone (FSH) and Luteinizing Hormone (LH), and is characterised by a dramatic increase in follicle size, formation of a follicular antrum and cytoplasmic and meiotic maturation of the oocytes [21, 22].

Folliculogenesis is separated into 5 stages characterised by distinct morphological changes: primordial, primary, secondary, antral and pre-ovulatory follicles (Fig. 2), the main characteristics of which are described below.

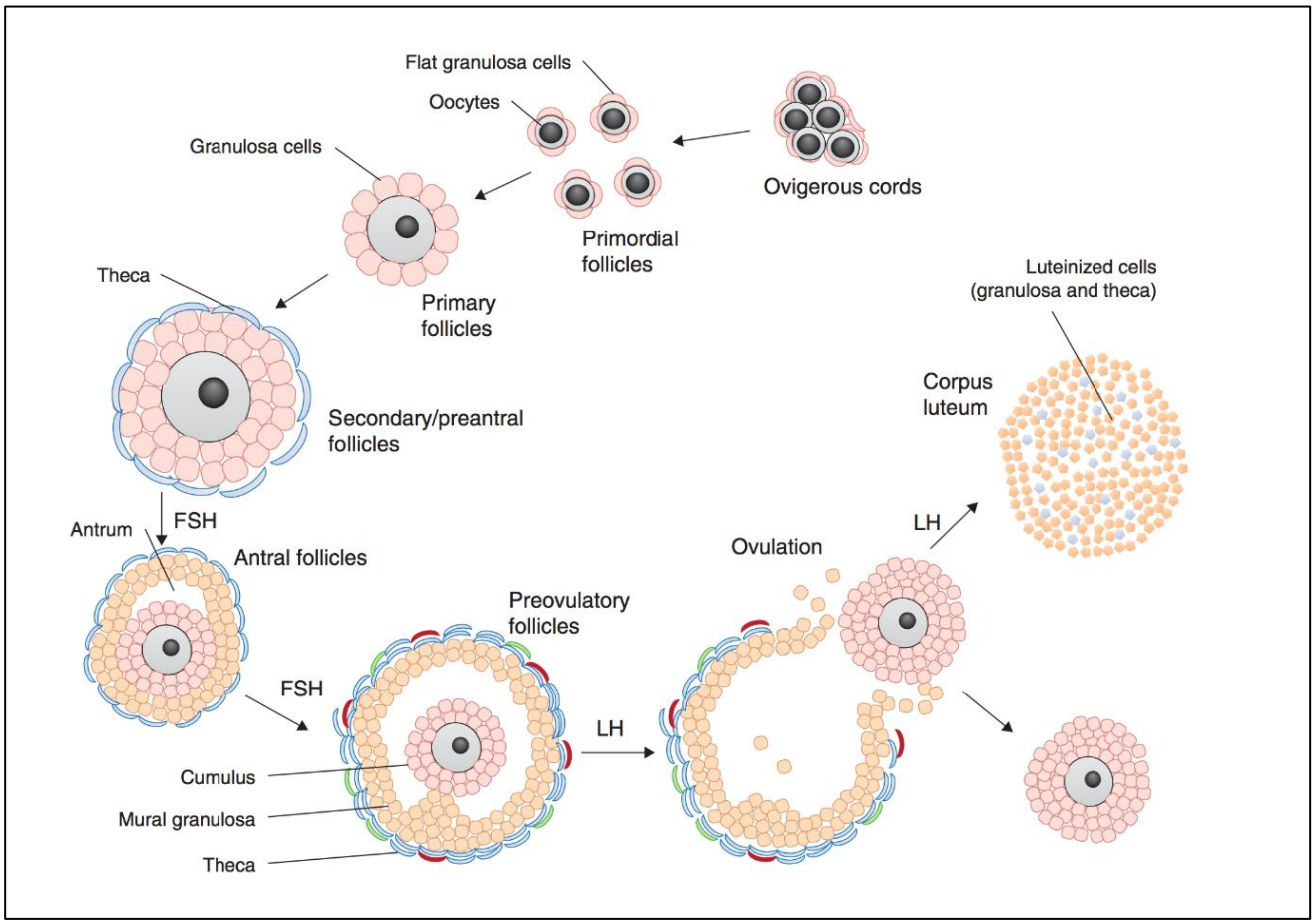

Figure 2. Outline of the main steps of folliculogenesis [23].

1.2.2.1 Primordial follicles

Primordial follicles are comprised of a quiescent oocyte surrounded by a complete or partial single layer of squamous granulosa cells with very low mitotic potential (Fig. 3a, red arrow). The follicles are relatively small, measuring approximately 25µm in diameter in humans, and 12µm in mice [24]. The pool of primordial follicles defines the female fertile potential, and is known as the 'ovarian reserve'

[25]. The first morphological evidence that a primordial follicle has been activated to enter folliculogenesis is the growth of the oocyte and the transition of the squamous granulosa cells into a cuboidal morphology along with their proliferation (Fig. 3a, green arrow) [26].

1.2.2.2 Primary follicles

Primary follicles are characterised by a growing oocyte completely enclosed in a single layer of cuboidal granulosa cells (Fig. 3b). At this stage, granulosa cells begin to express FSH receptors, which act to escalate later stage follicular growth in response to high levels of serum FSH [12]. Additionally, immediately following activation, follicles begin to produce Anti-Müllerian Hormone (AMH), which is thought to play an important role in regulating folliculogenesis [27]. The oocyte grows rapidly, accumulating mRNAs, proteins and organelles, including mitochondria [12]. At this point, the zona pellucida, a thick glycoprotein matrix begins to assemble around the oocyte [28].

1.2.2.3 Secondary follicles

At the secondary stage, the continued proliferation of granulosa cells results in formation of a second layer surrounding the oocyte (Fig. 3c, d) [22]. The stromal cells surrounding primary follicles coalesce into a layer of theca cells [29]. Cross-talk between thecal cells and granulosa cells plays an essential role in folliculogenesis, because the androgen synthesized by the thecal cells is aromatized by granulosa cells, resulting in the production of mitogenic oestrogens [21]. This is referred to as the ‘two-cell, two-gonadotropin’ model. Following the formation of new small blood vessels, the follicle no longer relies on passive diffusion of nutrients and oxygen from stromal vasculature, but is instead associated with an individual network of capillaries for nourishment [12, 30].

1.2.2.4 Antral follicles

Antral follicles are characterized by the formation of a fluid-filled cavity (or antrum) between the granulosa cell layers in response to FSH stimulation (Fig. 3e, f). This follicular fluid is primarily comprised of plasma and factors, such as FSH, LH, estradiol and progesterone, secreted by the oocyte and associated granulosa cells [12, 31]. As the antrum increases in size (ranging in volume from 0.02-

7ml in humans), the follicle enlarges rapidly and the granulosa cells differentiate into two populations, cumulus cells that surround the oocyte and mural granulosa cells that form the inside wall of the follicle [11, 12, 32]. Thecal cells undergo extensive proliferation and differentiate into two distinct layers: the theca interna, made up of richly vascularized thecal interstitial cells, and the theca externa, made up of smooth muscle [12].

1.2.2.5 Pre-ovulatory follicles

The pre-ovulatory follicle possesses an oocyte surrounded by layers of cumulus cells (Fig. 3e) [26]. With further proliferation of granulosa cells, expansion of the antrum and richer vascularization of the theca cells, the pre-ovulatory follicle turns into the largest follicle in the ovary [33]. However, among the pool of growing follicles, only a minority of the selected antral follicles will reach this stage. These follicles are also called dominant follicles (DFs). Compared to the subordinate follicles (SFs), the DFs contain more estrogen and FSH receptors, which help the DFs survive and thrive in an environment of declining FSH [34].

1.2.2.6 Ovulation and Corpus Luteum

In response to the LH surge generated by the hypothalamus-pituitary-ovary axis, DFs rupture and release the cumulus-oocyte complex (COC), which contain a meiosis II arrested and fertilizable oocyte [34]. Humans are mono-ovulatory, typically ovulating a single oocyte each reproductive cycle [23], whereas mice release 8-12 oocytes each cycle [35].

Once the COC is released from DFs into the oviduct, the residual granulosa and thecal cells of ruptured follicles develop into corpora lutea, which provides embryo-supporting progesterone following fertilization [21]. The corpus luteum is a large and transient endocrine structure in the ovary. In humans, the diameter of the corpus luteum reaches up to 40mm during the luteal phase and degenerates around 12 weeks gestation or 10 days after ovulation [36, 37]. If fertilization does not occur, the corpus luteum degenerates to form the corpus albicans, leading to a drop in progesterone levels, and subsequent menstruation in humans and a new ovarian cycle. Mice lack menstruation, but instead rely on cyclic degeneration and regeneration of the endometrium [12, 38].

1.2.2.7 Follicle Atresia

Follicle atresia is a continuous process during folliculogenesis, which causes 99.9% of the follicles die in mammals [12]. In human, follicle number reaches a peak of approximately 6.8 million at around 20 weeks of gestation. Thereafter, it falls dramatically to around 2 million at birth, 400,000 by the onset of puberty, and only approximately 450 follicles develop to the ovulatory stage throughout the female reproductive lifespan [17, 39]. When less than 1,000 follicles remains in the ovary, menopause occurs, indicating exhaustion of the ovarian reserve [20]. In C57/BL6 mice, the number of primordial follicles drops sharply from about 7,000 by PN3 to around 2,000 by PN7, and less than 500 remain in the ovary by PN200 [1, 40].

Follicular atresia is crucial for the control of oocyte quality and quantity [17, 41]. The atresia of growing follicles is thought to be initiated by the apoptosis of granulosa cells [41]. Two apoptotic pathways are likely involved in this process: 1) the extrinsic apoptosis pathway, which is triggered by Fas ligand and Tumor Necrosis Factor (TNF), and 2) the intrinsic apoptosis pathway (also known as the mitochondrial pathway), which is controlled by proteins belonging to the Bcl2 family [12].

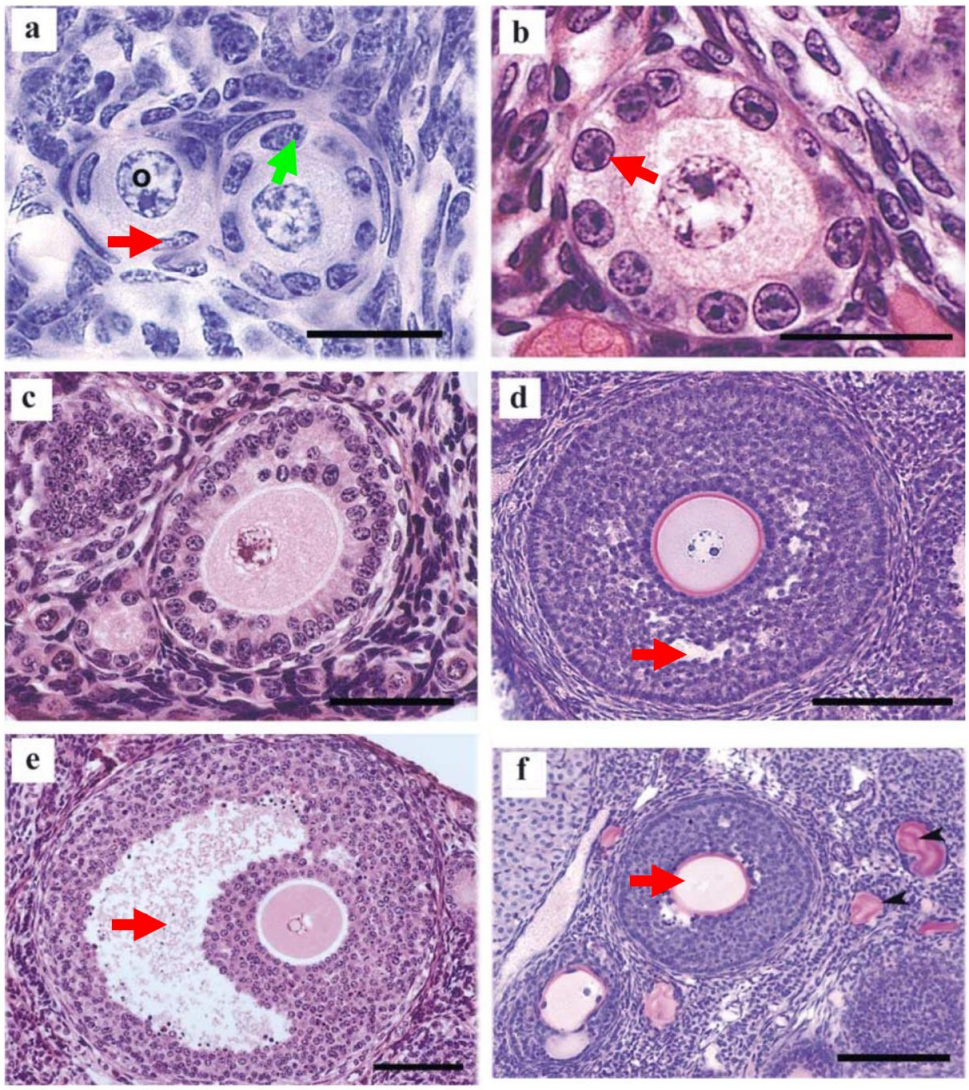

Figure 3: The morphology of ovarian follicles at different stages of development. (A) Red arrow indicates squamous granulosa cells of primordial follicle, green arrow indicates cuboidal granulosa cells of primary follicle bar = 20µm. (B) Primary follicle, arrow indicates cuboidal granulosa, bar = 20µm. (C) Secondary follicle, bar = 50µm. (D) Early antral follicle, small antral cavities indicated by arrow, bar = 100µm. (E) Late antral follicle, arrow indicates large antral cavity, bar = 100µm. (F) Atretic follicle, bar = 100µm. [26]

1.3 Cancer treatments

Standard cancer treatments, including radiation and chemotherapy, have significantly improved the survival rates of cancer patients. However, these treatments can damage normal cells, resulting in off-target effects on healthy tissue, such as the ovary [42]. Many studies have demonstrated that cytotoxic cancer treatments directly damage the DNA in oocytes and somatic cells within the ovary, leading to a reduction in the size of the ovarian follicular reserve, which eventually results in acute ovarian failure

or premature ovarian insufficiency (POI) [1]. Typically, acute ovarian failure refers to the instant loss of ovarian function during or after cancer treatment, whereas POI refers to the failure of ovarian function years after cancer treatment, and leads to permanent amenorrhea in women before the age of 40 [43, 44]. In addition to compromised fertility, POI is associated with poor mental health, cardiovascular disease and low bone mineral density [45-47]. Thus, taking into account the broad adverse effects of cancer therapies, it is important to understand the mechanisms underlying follicle depletion and ovarian damage in order to devise new strategies to preserve female fertility.

1.3.1 Radiotherapy

Radiotherapy takes advantage of high energy rays to directly induce DNA damage. It can also indirectly cause DNA damage by elevating the levels of reactive oxygen species (ROS) [48]. Although an efficient DNA repair system exists in mammalian oocytes, exposure to radiation accelerates the depletion of the ovarian reserve, resulting in acute ovarian failure or POI [49-51]. The risk of developing acute ovarian failure increases if women are exposed to pelvic, abdominal or spinal irradiation [44]. In addition, due to the natural decline of the ovarian reserve with age, pre-pubertal females are more resistant to radiation than adults [52]. For example, POI results from a 20.3 Gy dose at birth, but the POI-inducing dose decreases to 18.4 Gy at 10 years, 16.5 Gy at 20 years and 14.3 Gy at 30 years [52, 53].

1.3.2 Chemotherapy

There are more than 100 chemotherapeutic agents used in routine oncological practice, which can be categorized into alkylating agents, antimetabolites, anthracyclines, platinum-based drugs, anti-tumor antibiotics and topoisomerase inhibitors [53]. To achieve the best therapeutic outcome, chemotherapeutic drugs are administrated in combination based on their anti-tumor actions [53]. The main predictive factors of ovarian damage after chemotherapy are 1) the age of the individual at treatment, 2) the drug type and 3) the cumulative dosage administrated [54]. In general, the rates of acute ovarian failure and POI after chemotherapy are significantly higher in older women [55]. In addition, the risk of POI after antimetabolites treatment is lower than when platinum-based and alkylating agents are used [56]. It is now well-established that radiotherapy and chemotherapy are capable of inducing follicle depletion via nuclear DNA damage and apoptosis [57, 58]. Recent evidence

suggests that these treatments may also damage the ovarian stroma such that it becomes unable to support follicle growth [56].

1.4 Mitochondria

As the powerhouse of the cell, mitochondria make up for approximately 30% of total cell volume in eukaryotes [5, 59] and fully mature oocytes contain the largest number of mitochondria among different cell types [60]. Their abundance, structure and function make them possible targets of the cytotoxic treatments, and in this regard, it has been shown in somatic cells that irradiation has direct effects on cellular organelles other than the nucleus, including mitochondria [5, 61, 62].

1.4.1 Structure and function

Mitochondria are maternally inherited, double membrane organelles, present in most eukaryotic cells [63]. Mitochondria have two essential roles within the cell: 1) to provide metabolic energy, and 2) the control of apoptosis. The outer membrane of mitochondria cooperates with the endoplasmic reticulum (ER) to regulate Ca^{2+} signaling [64]. The inner membrane folds into cristae, which house several complexes involved in ATP production, and encloses the matrix, which contains vital proteins and the mitochondrial genome [65, 66]. The inner membrane is impermeable to almost all molecules in order to ensure normal mitochondrial function [67]. The space between the outer and inner membrane of mitochondria is called intermembrane space, which is where cytochrome c located (Fig. 4)[68, 69].

In eukaryotes, mitochondria produce about 95% of the adenosine triphosphate (ATP) for cellular metabolism via oxidative phosphorylation (OXPHOS) [70]. OXPHOS takes place at the inner membrane of mitochondria, and involves the transfer of electrons along a series of complexes called the electron transport chain (ETC) via redox reactions [71]. The ETC consists of complex I (NADH-ubiquinone oxidoreductase), complex II (succinate-quinone oxidoreductase), complex III (cytochrome b), complex IV (cytochrome c oxidase) and complex V (ATP synthase) [70, 72]. Complex I accepts electrons from the tricarboxylic acid (TCA) cycle and passes them to coenzyme Q (co Q), which carries electrons from complex II and passes them to complex III. Complex III transfers electrons to cytochrome c, and then to complex IV, to reduce molecular oxygen to water. The energy released by the

ETC is essential for the transport of protons across the mitochondrial inner membrane, and it enables complex V to phosphorylate ADP to form ATP (Fig. 5) [73]. Normally, one electron at a time is transported via a redox reaction to generate ATP [74]. However, electrons may leak and interact with oxygen, resulting in the formation of superoxide radical ($O^{\bullet 2}$) [74]. Thus, ROS are normal byproducts of ATP generation [75].

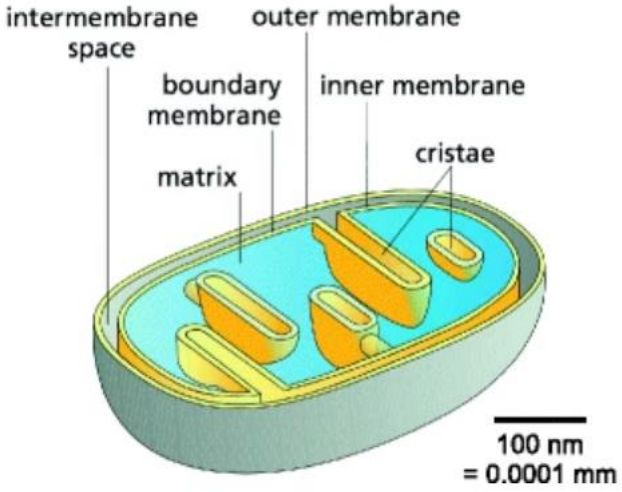

Figure 4. Mitochondrial structure [69].

1.4.2 Dynamics

Mitochondria vary considerably in morphology and numbers within the cell [76]. For example, fibroblast mitochondria are long filaments; whereas hepatocyte mitochondria are spheres [75]. Under metabolic or environmental stimuli, mitochondria undergo more frequent fission and fusion to maintain normal function [75]. Both of these processes are controlled by large guanosine triphosphates (GTPase) in mammals [77]. Mitochondrial fission is a process that involves transcription and translation of mtDNA, recruitment of proteins and lipids, and expansion of the mitochondrial reticulum [78, 79]. Mitochondrial fusion is mainly mediated by Mitofusion 1 and 2 (Mfn1 and Mfn2), located on the outer membrane, and Dynamin-related gene (Opa1), located on the inner membrane [75]. Peroxisome proliferator-activated receptor γ coactivator-1α (PGC-1α) has been identified as a master regulator of mitochondrial biogenesis [80]. Fusion and fission play a role in controlling mitochondrial quality. Fusion helps exchange genes and proteins to complement dysfunctional mitochondria, whereas fission eliminates damaged mitochondria and facilitates apoptosis and mitophagy [81, 82]. Furthermore, fusion of the mitochondrial inner membrane has been found in apoptotic cells, highlighting the role of

mitochondria in apoptosis [83]. Of note, mitochondrial biogenesis is quiescent in germ cells during early embryogenesis, with approximately 10 mitochondria in each primordial germ cell. It then restarts during the migration of primordial germ cells through the developing embryo to the gonadal ridge, such that a few thousand mitochondria are present in the oocytes of primordial follicles (Fig. 5) [84].

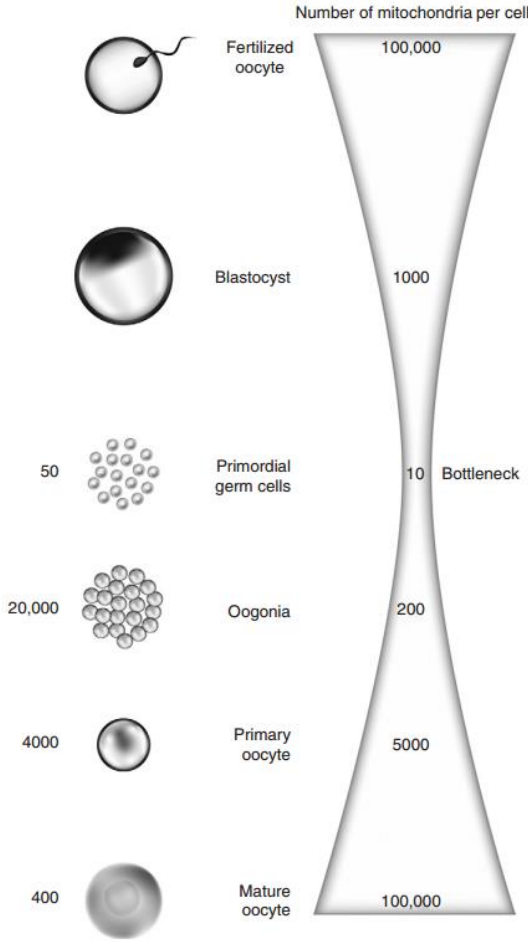

Figure 5. Diagrammatic representation of changes in the estimated number of mitochondria during the development of female germ line [84].

1.4.3 Mitochondria DNA

Mitochondrial DNA (mtDNA) is a double-stranded, compact and circular DNA molecule that is approximately 17 kb in size, located within the mitochondrial matrix [85]. The complementary mtDNA consist of the heavy (H-strand) light strands (L-strand) [83]. mtDNA contains 22 transfer RNAs (tRNA) genes, 2 ribosomal RNAs (rRNA) genes and 13 protein-encoding genes [65, 86], including genes for the electron transport chain enzyme complex subunits (complex I, III, IV, V) (Fig. 6) [87, 88].

mtDNA content varies dramatically in different cell types. In general, cells with high energy requirements, such as neurons and muscle cells, contain more mtDNA copies compared to leukocytes [65]. The development of sensitive techniques, such real-time quantitative PCR, makes it feasible to quantify mtDNA copies in single oocyte [89]. It has been reported that oocytes possess the largest number of mtDNA copies, which varies from 100,000 to 310,000 in mouse, cow and human oocytes [90-92]. Even within the same species, oocyte mtDNA content appears to be highly variable. For examples, in human oocytes, mtDNA copy number ranges from 11,000 to 903,000 copies, which could be related to the exceptional rate of cytoplasmic growth [93]. During folliculogenesis, mtDNA copy number increases with oocytes growth, with an average of 5,000 copies in mouse primary oocytes (oocyte diameter, φ=20μm) increasing to 150,000 copies in mature MII oocytes (φ=80μm) [89]. Importantly, studies indicate that mtDNA copy number is intimately connected to oocytes quality [41]. In this regard, many studies on the relationship between oocyte mtDNA copy number in mature oocytes and fertilizability have demonstrated that low mtDNA content correlates with fertilization failure and ovarian insufficiency [93, 94].

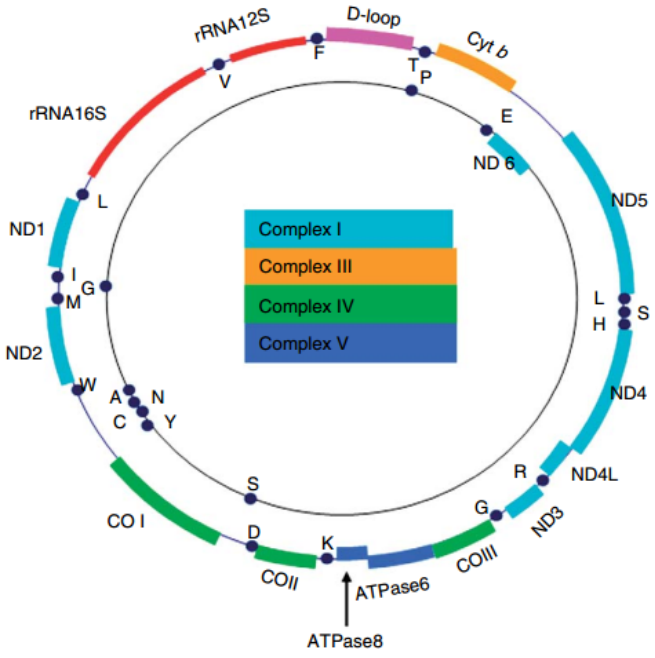

Figure 6. The mitochondrial genome. CO, cytochrome oxidase; Cyt, ubiquinone-cytochrome c reductase; ND, NADH dehydrogenase; ATPase, ATP synthase. tRNAs are represented as points [65].

1.5 Irradiation damages mitochondria

Radiotherapy, using X-ray and γ-radiation, is a standard treatment for many cancers [95]. Ionising radiation is a type of high energy radiation that causes DNA strand breaks and overproduction of reactive oxygen species (ROS) in tumour cells, as well as in normal cells, ultimately resulting in cell death [95]. Numerous studies have demonstrated that radiotherapy near to the ovaries poses a significant risk to female fertility [50]. Whilst many studies have shown that γ-radiation induces DNA double strand breaks in the nucleus of primordial follicle oocytes, leading to their apoptosis [3], the potential for γ-radiation to damage mitochondria within oocytes has not been evaluated. Damage to mitochondria may contribute to the extreme sensitivity of primordial follicle oocytes to γ-radiation and could result in reduced quality of those that survive the treatment [96]. A survey of the somatic cell literature provides evidence that mitochondria can be damaged by radiation, and it has been proposed that the damage incurred to mitochondrial DNA, and changes in mitochondrial function, have a key role in radiation toxicity within normal tissue [97]. Some of the reported mitochondrial responses to ionizing radiation are described below.

1.5.1 Irradiation affects mitochondrial mass

An increase in mitochondrial mass is commonly observed following exposure to irradiation [98-100]. For example, in human lung carcinoma A549 cells, mitochondrial mass was increased and correlated with the promotion of mitochondrial respiration and increased ATP production after 10 Gy irradiation [100]. Similarly, in Chinese Hamster Ovarian cells (CHO-K1) and human keratinocytes (HPV-G), an increase of mitochondrial mass and oxygen consumption rate were observed 4-12 hours post exposure to 5 Gy γ-radiation [99]. In the human breast cancer cell line MCF-7, a 1.5~3.8-fold increase in mitochondrial mass was observed after X-radiation [101]. An increase in mitochondrial mass following exposure to radiation has been proposed to be a mechanism of compensation for oxidative defects [98].

1.5.2 Irradiation affects mitochondrial DNA

Due to lack of histone protection and an efficient DNA repair system, mtDNA is more susceptible than nuclear DNA to ionising radiation [102, 103]. Ionising radiation is capable of inducing a variety of

lesions in mtDNA, including strand breaks [104], base mis-matches [105], and large deletions [103, 106]. In mice, a 3,860-bp region of mtDNA that encodes tRNA genes, cytochrome c oxidase and complex I genes, is prone to deletion and is referred to as the 'murine common deletion' site [107]. Deletion of this region is associated with exposure to irradiation and a similar 4,977-bp deletion is found in human cells exposed to radiation, and is associated with ageing and other pathologies [107, 108]. In addition to mtDNA deletions, *in vivo* and *in vitro* studies have shown that mtDNA copy number increases dramatically and rapidly following irradiation [5, 101, 109-112]. It has been reported that mtDNA content increases dramatically within 1 hour in mice subjected to X-irradiation (1Gy) and the mtDNA/nDNA ratio was increasd by 3 fold after a 10 Gy dose in nucleated blood cells [109, 110]. The observed increase of mtDNA copy number is likely a compensatory mechanism or adaptive response to radiation-induced mtDNA damage to maintain mitochondrial function [109].

1.5.3 Irradiation affects the electron transport chain

As described above, mitochondria are the energy-transducing organelles responsible for generating ATP through the process of OXPHOS. It has been reported that the activity of the ETC complex decreases significantly 4 hours after exposure to 5 Gy γ-irradiation in CHO-K1 cells [98]. In human osteosarcoma cells, γ-radiation exposure also led to a deficiency of the ETC complexes and this was associated with reduced ATP content. However, the ATP content returned to normal levels 3 hours later, indicating that the effects on energy production were transient [113]. In other contexts, persistent damage to the ETC and mitochondrial functions was found after radiation exposure. For example, partial deactivation of Complex I and III in the heart cells of mice, coupled with decreased respiratory capacity and increased ROS, were observed 4 weeks after treatment with 2 Gy X-radiation [114].

1.5.4 Irradiation affects the intracellular levels of reactive oxygen species (ROS)

The overproduction of intracellular ROS has adverse effects on mitochondrial membrane potential, ATP production and DNA structure, eventually leading to apoptosis [100, 115]. Water comprises a large proportion of the cell content and its radiolysis results in generation of free radicals [116]. Even though these free radicals have a very short half-life, they are a significant cause of persistent oxidative stress after irradiation [117]. In addition, irradiation also increases ROS levels within mitochondria [41].

Using MitoSOX, which selectively reacts with mitochondrial ROS, Kobashigawa and colleagues found a sustained increase of mitochondrial ROS levels in human fibroblast-like cells within 72 hours of 2 Gy γ-irradiation [118].

1.6 Cisplatin damages mitochondria

Cisplatin, and other platinum-based antineoplastic drugs, are widely used for the treatment of a variety of cancers, such as lung cancer, ovarian cancer, bladder cancer, breast cancer and other solid tumours in both adults and children [119]. The anticancer activity of cisplatin is attributed to its ability to form crosslinks with the purine bases on DNA, causing DNA damage and inducing apoptosis, and also by increasing the levels of reactive oxygen species (ROS) (Fig. 7) [119, 120].

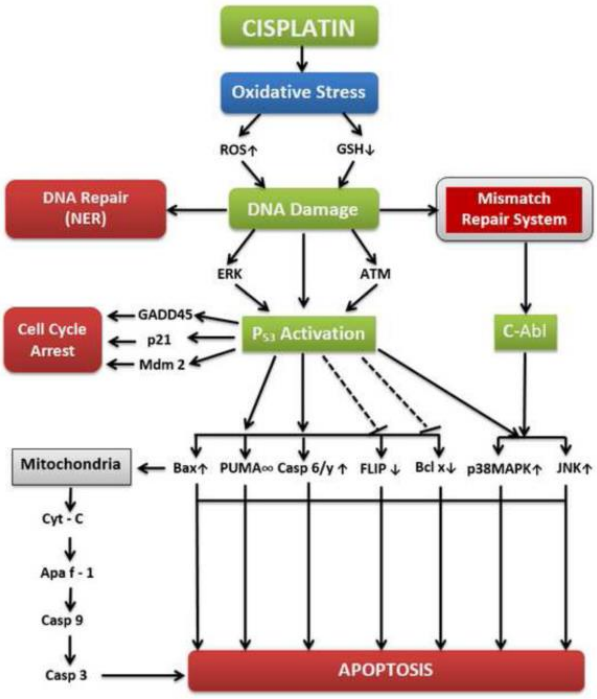

Figure 7. Overview of molecular mechanisms of cisplatin in cancer treatment [119].

1.6.1 Cisplatin induces mtDNA damage

The circular DNA maintained within mitochondria (mtDNA) can be directly targeted by cisplatin and this activity may be at least partly responsible for its anticancer effects [121, 122]. For example, in melanoma cells, cisplatin preferentially binds and forms adducts with mtDNA relative to genomic DNA,

leading to inhibition of NADH-ubiquinone reductase and reduced ATP generation [123]. Indeed, a study in CHO cells showed a four to six fold higher incorporation of cisplatin into mtDNA as compared to genomic DNA [122]. mtDNA damage and overproduction of ROS caused by cisplatin treatment are thought to contribute to hippocampal damage, peripheral neuropathy in dorsal root ganglion neurons, and ototoxicity in the cochlea [124-127].

1.6.2 Cisplatin affects the electron transport chain

Similar to the situation described above for irradiation, a number of studies have reported that cisplatin exposure compromises the activity and function of the ETC. In cultured porcine proximal tubule cells, the activity of Complex I and IV declined by approximately 15 to 55%, and significantly reduced ATP level was observed 20 minutes after incubation with cisplatin [128]. In rat livers, the activity of Complex I and II were significantly decreased after cisplatin treatment [129]. Likewise, a significant decrease in the activity of the ETC and ATP levels were observed in fibroblasts from older men after treatment with platinum-based chemotherapy [130].

1.6.3 Cisplatin affects ROS level

Similar to other chemotherapeutic drugs, cisplatin can lead to an increase of ROS level in cells [131]. For instance, excessive ROS generation was found in colon carcinoma and melanoma cell lines after high doses of cisplatin treatment [132]. Elevated mitochondrial ROS levels were also observed using MitoSOX Red in human renal proximal tubular cells treated with cisplatin [120]. The elevation of ROS levels in response to cisplatin treatment can result in the activation of both the extrinsic apoptosis pathway, mediated by tumor necrosis factors (TNF), and the mitochondria regulated intrinsic apoptosis pathways [133-138].

1.7 ROS and antioxidants

ROS consist of several highly reactive molecules, such as hydroxyl ($^{\bullet}OH$), superoxide ($^{\bullet}O_2^-$) and hydrogen peroxide (H_2O_2), which are normal byproducts of cellular metabolism [139]. A moderate level of cellular ROS is beneficial to cell growth, protein phosphorylation and is anti-inflammatory, but excessive ROS is harmful to proteins, lipids and DNA [140, 141]. Based on the fact that a high metabolic

rate and low scavenging efficiency contribute to high levels of ROS in tumor cells, emerging evidence has shown that manipulation of ROS levels by antioxidants is a promising strategy of anti-cancer therapy [140, 142].

1.7.1 ROS generation in mitochondria

The mitochondrial electron transport chain (ETC) is the principal source of endogenous ROS in eukaryotic cells (Fig. 8). The ETC comprises five complexes that can pump the protons (H^+) across the inner membrane and transfer electrons via redox reactions to synthesize ATP [143]. However, 0.2-2% of electrons will leak from the chain and directly interact with O_2, generating superoxide ($^{\bullet}O_2^-$) [144]. Complex I, II and III are the main sites of electron leakage. Under pathological conditions, complex I, which converts NADH to ubiquinone (coenzyme Q), is the main source of ROS; whereas under normal conditions, complex II, which links the Krebs cycle with ETC, produces more ROS [144, 145]. Unlike complex I and II, which only generate ROS within the mitochondrial matrix, complex III produces ROS in the matrix and intermembrane space, which can then be more easily released into cytoplasm [146].

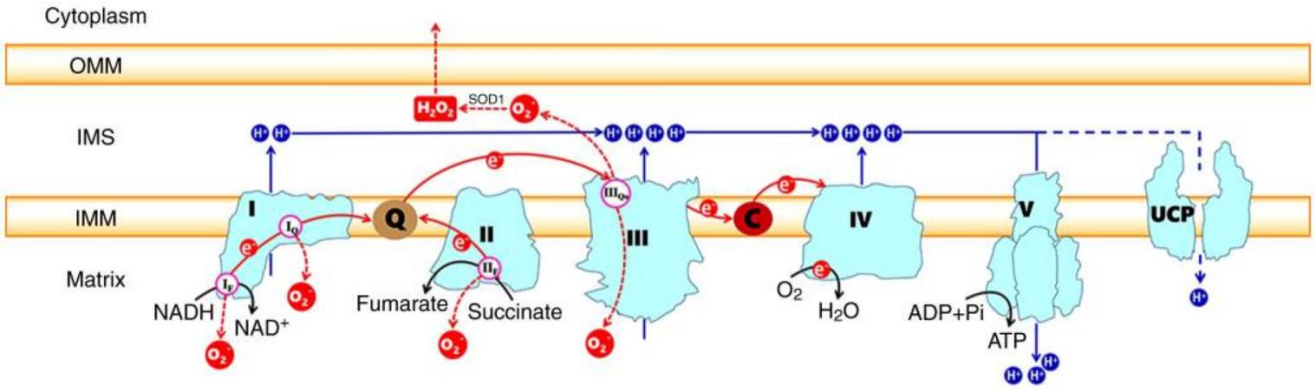

Figure 8. The mitochondrial electron transport chain and electron leakage [144].

1.7.2 ROS and protein peroxidation

Due to the cellular abundance and instant their reaction to ROS, proteins are considered the main targets of oxidative stress [147]. In general, ROS cause irreversible protein modifications by carbonylation and tyrosine nitration, or reversible modifications by disrupting the redox balance of cysteine and tyrosine residues [148]. Thus, a wide variety of cellular events, such as phosphorylated kinase mediated signaling, can be affected [140]. In particular, receptor tyrosine kinases (RTK) and the non-receptor protein tyrosine kinases (PTK) activated by ROS are related to apoptosis [140, 149].

The tyrosine residues of proteins are prone to be nitrated by free radicals, such as peroxynitrite ($ONOO^-$), producing the 3-Nitrotyrosin (NTY) [150]. Compared to peroxynitrite, NTY is a more stable protein peroxidative product. High levels of NTY are commonly detected in pathological conditions, including inflammation, aging and cardiovascular diseases [150]. Thus, the presence of NTY in proteins is considered a biomarker of oxidative stress and an indicator of disease [150].

1.7.3 ROS and lipid peroxidation

Lipid peroxidation refers to a process involving the removal of electrons from unsaturated lipids by free radicals [151]. Bio-membranes have a high content of polyunsaturated fatty acids (PUFAs), making them targets for ROS-mediated modification [152]. ROS can destroy the lipid bilayer of mitochondria, a double membrane organelle, and compromise the permeability transition pores (PTPs), resulting in the release of cytochrome c, and eventually cell death via triggering the intrinsic apoptosis pathway [140]. Lipid peroxidation is initiated by the production of free fatty acid radicals under the stimuli of ROS, propagated by the formation of lipid peroxyl radicals and is terminated by the formation of a non-radical product [152]. The products of lipid peroxidation, such as 4-hydroxynonenal (4-HNE) and malondialdehyde (MDA) are easily detected and are key regulators of cell survival [152].

4-HNE, a highly active lipidic electrophile, is widely used as a maker of oxidative stress damage [153]. 4-HNE can form adducts with protein and DNA to regulate a wide range of signaling pathways [153, 154]. Of note, mitochondria are principal sites of 4-HNE generation and the HNE protein adducts formed in mitochondria are involved in the intrinsic apoptosis pathway [155]. In an *in vitro* study on mice oocytes, 4-HNE was shown to damage the spindle and chromosomes, but oocyte quality could be preserved by supplementation with melatonin, an effective antioxidant [156].

1.7.4 ROS and DNA damage

Within eukaryotic cells, DNA is insulted by various stimuli each day. In the case of oxidative stress, where ROS levels increase beyond the scavenging capacity, cells activate the DNA damage response to deal with any deleterious DNA lesions that arise [157]. In general, ROS can directly oxidize DNA,

especially at the 8-oxoguanine site, resulting in DNA mispairing and it can further affect DNA methylation [140, 158]. The base excision repair, nucleotide excision repair, homologous recombination and nonhomologous end joining pathways are involved in DDR [157]. Dysfunction of the repair mechanisms can cause genome instability, resulting in oncogenesis [159]. In addition, accumulation of ROS in mitochondria induces mtDNA damage and reduces the efficiency of the electron transport chain, which in turn results in the production of more ROS [140, 160].

1.7.5 Antioxidants

Excessive ROS is associated with cardiovascular disease, neurological disease, lung disease, kidney diseases and ovotoxicity [139, 161-165]. Based on their activities, cellular antioxidant systems can be categorized into enzymatic and non-enzymatic antioxidants to combat the overproduction of ROS [141]. The enzymatic antioxidants include superoxide dismutase (SOD), catalase (CAT) and glutathione peroxidase (GPx). The non-enzymatic antioxidants include vitamin E, glutathione and coenzyme Q10 (CoQ10) [166]. Despite a number of reported failures in clinical settings, supplementation of exogenous antioxidants are still considered important and effective ROS scavengers with therapeutic potential [141, 167]. Of note, mitochondria are the main sites of ROS production, and the intrinsic ROS scavenging activity within mitochondria is insufficient to eliminate the excessive ROS produced under conditions of oxidative stress [139, 168]. In this regard, various mitochondrial-targeted antioxidants, such as Szeto-Schiller (SS) peptides and MitoQ, have been developed and they have proven to be more effective than un-targeted antioxidants in the treatment of diseases involving mitochondrial dysfunction [169, 170].

1.7.5.1 Mitochondrial targeted antioxidant-Szeto-Schiller (SS) peptides

Szeto-Schiller (SS) peptides are a range of synthetic antioxidative peptides that contain a cationic motif, which allows them to penetrate membranes and accumulate in mitochondria [171, 172]. As a member of the SS peptides family, SS-31 has been shown to specifically react with cardiolipin, an essential mitochondrial inner membrane lipid, to decrease mitochondrial ROS production (Fig. 9) [173]. *In vitro* experiments have proven that SS-31 is a promising therapy for aging, heart failure and other mitochondrial related disorders [174, 175].

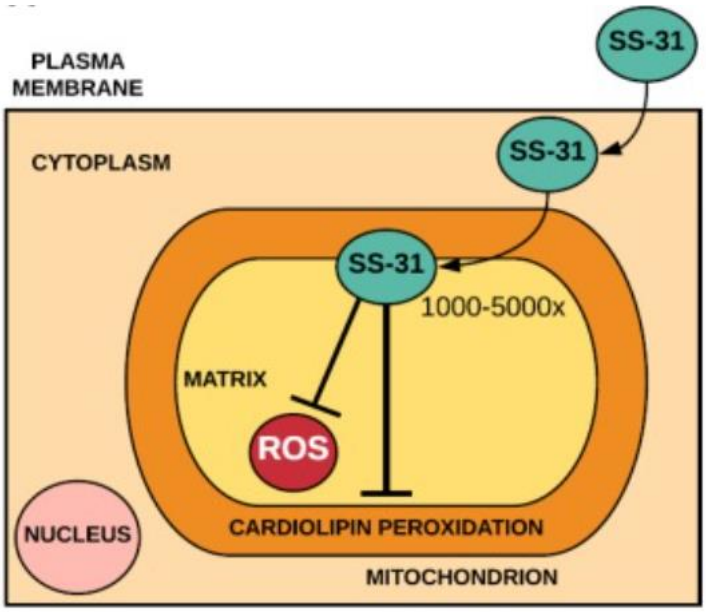

Figure 9. The antioxidative mechanism of SS-31 [173]. SS-31 can penetrate and accumulate within mitochondria, acting as the antioxidant by preventing the peroxidation of mitochondrial cardiolipin [173].

1.7.5.2 Mitochondrial targeted antioxidant-MitoQ

CoQ10 (or Ubiquinone) is a natural hydrophobic antioxidant that participates in ATP generation in mitochondria [176]. To avoid the hydrophobicity and the non-specific mitochondrial targeted character of CoQ10 and its derivatives, MitoQ was synthesized by coupling the ubiquinone part of CoQ10 with the lipophilic triphenylphosphonium (TPP) cation (Fig. 10) [141]. MitoQ is one of the most effective derivatives of CoQ10 that can be directly delivered to mitochondria [177]. The positively charged lipophilic cation (TPP^+), and the mitochondrial membrane potential, mean that MitoQ can easily and preferentially penetrate the phospholipid bilayer of mitochondria and accumulate within the mitochondrial matrix [178]. Once within the mitochondrial inner membrane, the ubiquinone part of MitoQ can be utilized by complex II to produce ubiquinol; the quinol form acts as an antioxidant, which can be oxidized back to quinone by ROS and be recycled by the respiratory chain [179]. Of note, MitoQ can only be efficiently utilized by complex II, thus it cannot restore mitochondrial function in the absence of complex II [178].

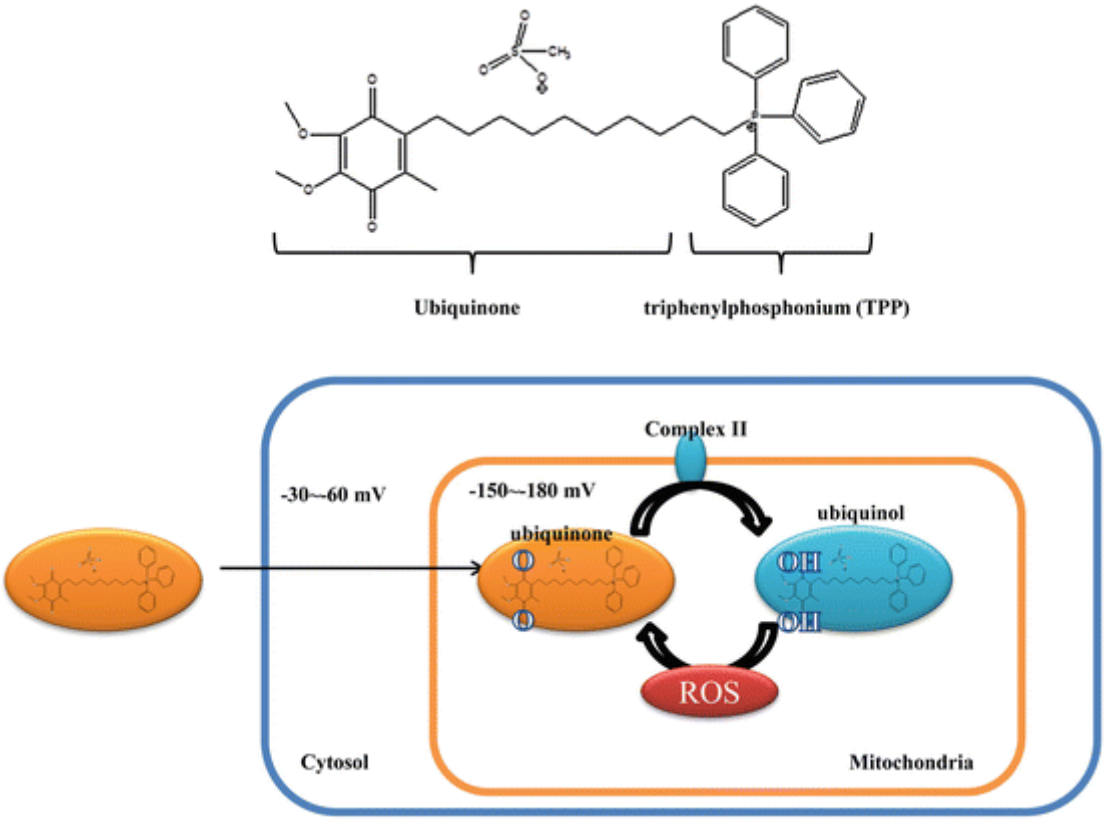

Figure 10. Structure and mechanism of MitoQ [141].

1.7.5.3 Protection against oxidative stress by MitoQ

MitoQ can penetrate lipid bilayers and accumulate within mitochondria, so the main oxidative effect of MitoQ is to prevent peroxidation of the lipids in the mitochondrial membrane [180, 181]. Some studies suggest that by protecting cardiolipin, a mitochondrial specific phospholipid, MitoQ might interfere with the intrinsic (mitochondrial mediated) apoptosis pathway to prevent cell death [182]. In addition, the reaction between MitoQ and peroxynitrite ($ONOO^-$), a damaging oxidative molecule, can possibly protect DNA, proteins and lipids from oxidative damage [178, 183, 184]. Thus, the excellent antioxidative performance of MitoQ has meant that it has been broadly used in numerous mitochondrial related diseases since its synthesis in the 1990s [185]. In human trials, MitoQ alleviated liver damage in hepatitis C virus (HCV) patients and improved vascular function in healthy elders [186, 187]. In mouse models, MitoQ has shown promise as an attractive therapeutic drug to treat Alzheimer's disease, cardiovascular disease, diabetic kidney disease and reproductive disorders [188-192]. Of note, MitoQ also plays protective role in the reproductive system under oxidative stress. For instance, studies in rats show that MitoQ alleviates γ-irradiation induced testicular damage by inhibiting the intrinsic apoptosis

pathway [193], and administration of MitoQ and Vitamin D protected mice from polycystic ovary syndrome (PCOS) [191].

1.8 Overall Significance

Premature ovarian failure and infertility are common side effects of anticancer therapies, largely due to the extreme sensitivity of the ovarian follicles to radiation and chemotherapies. Current methods to preserve future fertility in cancer patients are invasive and not suitable for all patients. The development of adjuvant therapies capable of protecting oocytes from the deleterious effects of such drugs would represent a significant advancement in our ability to preserve fertility and endocrine function in women with cancer. Despite significant evidence described above that radiation and cisplatin treatment damage mtDNA and mitochondrial function within somatic cells, the possibility that these treatments damage mitochondria within oocytes has not been evaluated. In the long term, protecting mitochondria may mitigate against radiation and cisplatin-induced insults to oocytes. Agents, such as MitoQ, that shield the mitochondria from insults without compromising the anti-tumour actions of radiation and the platinum-based drugs could serve as useful fertile-protective agents.

1.9 Aims and Hypothesis

Based on the known knowledge elaborated in the literature, it was hypothesized that radiotherapy and chemotherapy could compromise mitochondrial function, eventually resulting in cell death and the depletion of the ovarian reserve, or loss of oocyte quality. In addition, protecting mitochondria by the supplementation of MitoQ during cytotoxic cancer treatments could preserve the ovarian reserve and eliminate cellular oxidative damage in mice. Thus, the following chapters addressed the following aims:

1. To determine if γ-irradiation damages mitochondria in oocytes.
2. To determine if cisplatin damages mitochondria in oocytes.
3. To explore the possibility that the supplementation of Mito Q can prevent follicle loss and alleviate oxidative damage in mouse ovaries after cancer treatments.

Chapter 2. Evaluation of mitochondria in oocytes following γ-irradiation

SCIENTIFIC REPORTS
nature research

OPEN

Evaluation of mitochondria in oocytes following γ-irradiation

Qiaochu Wang, Jessica M. Stringer, Jun Liu & Karla J. Hutt*

Standard cytotoxic cancer treatments, such as radiation, can damage and deplete the supply of oocytes stored within the ovary, which predisposes females to infertility and premature menopause later in life. The mechanisms by which radiation induces oocyte damage have not been completely elucidated. The objective of this study was to determine if γ-irradiation changes mitochondrial characteristics in oocytes, possibly contributing to a reduction in oocyte number and quality. Immature oocytes were collected from postnatal day (PN) 9–11 C57Bl6 mice 3, 6 and 24 hours after 0.1 Gy γ-irradiation to monitor acute mitochondrial changes. Oocytes were classified as small (>20 µm) or growing (40–60 µm). Mitochondrial membrane potential was lost in 20% and 44% of small oocytes (~20 µm) at 3 and 6 hours after γ-irradiation, respectively, consistent with the induction of apoptosis. However, mitochondrial mass, distribution and membrane potential in the surviving small oocytes were similar to the non-irradiated controls at both time points. At 24 hours after γ-irradiation, all mitochondrial parameters analysed within immature oocytes were similar to untreated controls. Mitochondrial parameters within growing oocytes were also similar to untreated controls. When mice were superovulated more than 3 weeks after γ-irradiation, there was a significant reduction in the number of mature oocytes harvested compared to controls (Control 18 ± 1 vs 0.1 Gy 4 ± 1, n = 6/16 mice, $p < 0.05$). There was a slight reduction in mitochondrial mass in mature oocytes after γ-irradiation, though mitochondrial localization, mtDNA copy number and ATP levels were similar between groups. In summary, this study shows that γ-irradiation of pre-pubertal mice is associated with loss of mitochondrial membrane potential in a significant proportion of small immature oocytes and a reduction in the number of mature oocytes harvested from adult mice. Furthermore, these results suggest that immature oocytes that survive γ-irradiation and develop through to ovulation contain mitochondria with normal characteristics. Whether the oocytes that survive radiation and eventually undergo meiosis can support fertility remains to be determined.

Conventional cytotoxic cancer treatments, including radiation and chemotherapy, can damage the oocytes and somatic cells within the ovary, leading to a reduction in the size of the ovarian follicular reserve, which predisposes females to infertility and premature menopause later in life[1]. With improving survival rates for many cancers, it is desirable to avoid these side-effects and devise new strategies to protect the long-term fertility and health of women post-treatment[2]. In order to achieve this goal, it is necessary to understand the mechanisms by which specific cancer treatments damage the ovary and induce oocyte death.

Studies have shown that ionising radiation induces DNA double strand breaks in the genomic DNA of oocytes, leading to their apoptosis[3,4]. Interestingly, evidence from somatic cells and cancer cell lines suggest that radiation may also damage mitochondria[5,6]. However, radiation-induced mitochondrial damage has not been evaluated in oocytes. It has also been proposed that lack of histones and limited capacity for DNA repair may make mitochondrial (mt) DNA more susceptible to radiotherapy than nuclear DNA[7,8]. Previous studies indicate that damage of mitochondria and mtDNA plays a key role in radiation toxicity in human fibroblasts[9]. Decreased ATP levels and deficiencies in the activity of the electron transport chain (ETC) complexes are commonly observed in different cell types after radiation, indicating mitochondrial damage[10,11]. Furthermore, an increase in mitochondrial mass and mtDNA content (copy number) has been observed after radiation treatment and is thought to be a compensatory mechanism to maintain normal mitochondrial function[12].

Mitochondria are the powerhouse of the cell and comprise approximately 4–25% of total cell volume in eukaryotes and mature oocytes contain the largest number of mitochondria among different cell types[13,14]. Mitochondria play many important roles within the oocyte during maturation, fertilisation and preimplantation

Biomedicine Discovery Institute, Department of Anatomy and Developmental Biology, Monash University, Melbourne, Australia. *email: karla.hutt@monash.eu

embryonic development, including synthesizing adenosine triphosphate (ATP), regulating redox and Ca2+ homeostasis and controlling apoptosis[15]. Because of this, alterations in mitochondrial number and function in oocytes may reduce oocyte quality and subsequently compromise embryonic development[16]. Furthermore, as mitochondria are maternally inherited, mtDNA damage, such as point mutations, may transferred to the next generation[17]. Therefore, it is important to examine the characteristics of mitochondria in oocytes following exposure to γ-irradiation. If cancer treatment-induced mitochondrial damage contributes to depletion of the ovarian reserve or loss of oocyte quality, then protection of mitochondria may represent a novel strategy for alleviating radiation and chemotherapy-mediated insult to the ovary[18].

The objective of this study was to investigate the impact of γ-irradiation on mitochondria in immature oocytes. To do this, we used a mouse model in which prepubertal (PN9–11) female C57BL6 mice were untreated (controls) or exposed to whole body γ-irradiation at 0.1 Gy. At 3, 6 and 24 hours after treatment, immature oocytes were collected to monitor acute changes in mitochondrial mass and distribution, function (ATP levels) and mtDNA copy number. In addition, γ-irradiated mice were held for a minimum of 3 weeks to determine if damage inflicted on immature oocytes persists in mature oocytes.

Results

Mitochondrial distribution and mass were not affected by γ-irradiation in immature oocytes.

Immature oocytes were collected from mice 3, 6 and 24 hours following γ-irradiation (or from untreated controls) and classified according to the size. Oocytes with a diameter ~20 μm (range 12–21 μm) were defined as small oocytes from primordial or primary follicles (Supplemental Fig. 1A,B). Oocytes with a diameter ~50 μm (range 39–62 μm) were defined as growing oocytes from secondary follicles (Supplemental Fig. 1).

To assess mitochondrial distribution, live immature oocytes were incubated with the fluorescent dye MitoTracker Green. In small oocytes, mitochondria were distributed throughout the cytoplasm and no differences were observed in the localisation pattern between oocytes from untreated and γ-irradiated mice at any time point (Fig. 1a). In growing oocytes, mitochondria were distributed in two distinct patterns; either evenly distributed in the cytoplasm or aggregated close to nucleus (Fig. 1b,c). The homogenous and aggregated distribution patterns appeared in both control and γ-irradiated oocytes and no differences in the percentage of oocytes with aggregated mitochondria were observed between groups at any time point (Fig. 1d).

To assess whether mitochondrial abundance was affected by γ-irradiation, relative MitoTracker Green fluorescence intensity was quantified. There was no significant difference γ-irradiated groups relative to the control for small and growing oocytes at 3, 6 and 24 hours (Fig. 1e,f).

Mitochondrial membrane potential was transiently impaired in immature oocytes following γ-irradiation. We next determined whether mitochondrial membrane potential ($\Delta\Psi m$) was altered in immature oocytes from γ-irradiated mice by staining with TMRM, a cell-permeant dye that accumulates in active mitochondria with intact membrane potential (Figs. 2a and 3a). Oocytes were simultaneously stained with MitoTracker Green to confirm to presence of mitochondria and normalise TMRM levels to mitochondrial abundance.

Whilst TMRM staining was detectable in all control small oocytes, at 3 and 6 hours after γ-irradiation, mitochondrial membrane potential was lost in 20% and 44% of small oocytes, respectively (Fig. 2b). Loss of mitochondrial membrane potential is consistent with apoptosis[19]. In contrast, at the later time point of 24 hours after γ-irradiation, all oocytes analysed retained mitochondrial membrane potential (Fig. 2b) as indicated by detectable TMRM staining. We then quantified TMRM intensity in those small oocytes with detectable TMRM staining. No significant differences were observed between control and γ-irradiated groups at each time point ($p > 0.05$) (Fig. 2c).

TMRM staining was observed in all growing oocytes in both control and γ-irradiated groups (Fig. 3a). A slight decrease in TMRM intensity relative to controls was observed at 6 hours after γ-irradiation (Fig. 3b). We also evaluated ATP levels in growing oocytes. No differences were observed in the relative ATP content in control and γ-irradiated groups at any time point (Fig. 3c).

Mitochondrial characteristics were similar in mature oocytes ovulated by control mice or mice γ-irradiated 3 weeks earlier. To determine if γ-irradiation of immature oocytes generated changes in mitochondria that persist in mature oocytes, mice were super ovulated more than 3 weeks after γ-irradiation and MII oocytes were collected. Notably, the number of mature oocytes harvested from γ-irradiated mice was dramatically reduced compared to controls (Control 18 ± 1 vs 0.1 Gy 4 ± 1, $n = 6/16$ mice, $p < 0.01$), with 2 mice failing to ovulate (Fig. 4a). Staining with MitoTracker Green revealed a relatively homogeneous distribution pattern of mitochondria in the ovulated oocytes from control and γ-irradiated mice. A slight decrease in MitoTracker Green intensity relative to controls was observed in the γ-irradiated group (Fig. 4b,c). This likely resulted in the slight increase in TMRM staining intensity relative to MitoTracker Green that was observed in ovulated oocytes from γ-irradiated mice compared to controls (Fig. 4b,d).

Notably, we found that mtDNA copy number was similar in MII oocytes from control and γ-irradiated mice. Similarly, ATP level in γ-irradiated mice was not significantly different from controls (Fig. 4f).

Discussion

The goal of this study was to evaluate the impact of γ-irradiation on the mitochondria in oocytes. Mitochondrial distribution is thought to be important for meeting the energy requirements of cellular activities[20], therefore we used MitoTracker Green to localise mitochondria in small and growing oocytes from control and irradiated mice. We found that mitochondria were distributed evenly throughout the cytoplasm of small oocytes, consistent with a previous report[21], and we did not observe any change of mitochondrial localisation following γ-irradiation. In growing oocytes, mitochondria were found to be distributed in either a homogeneous or an aggregated pattern,

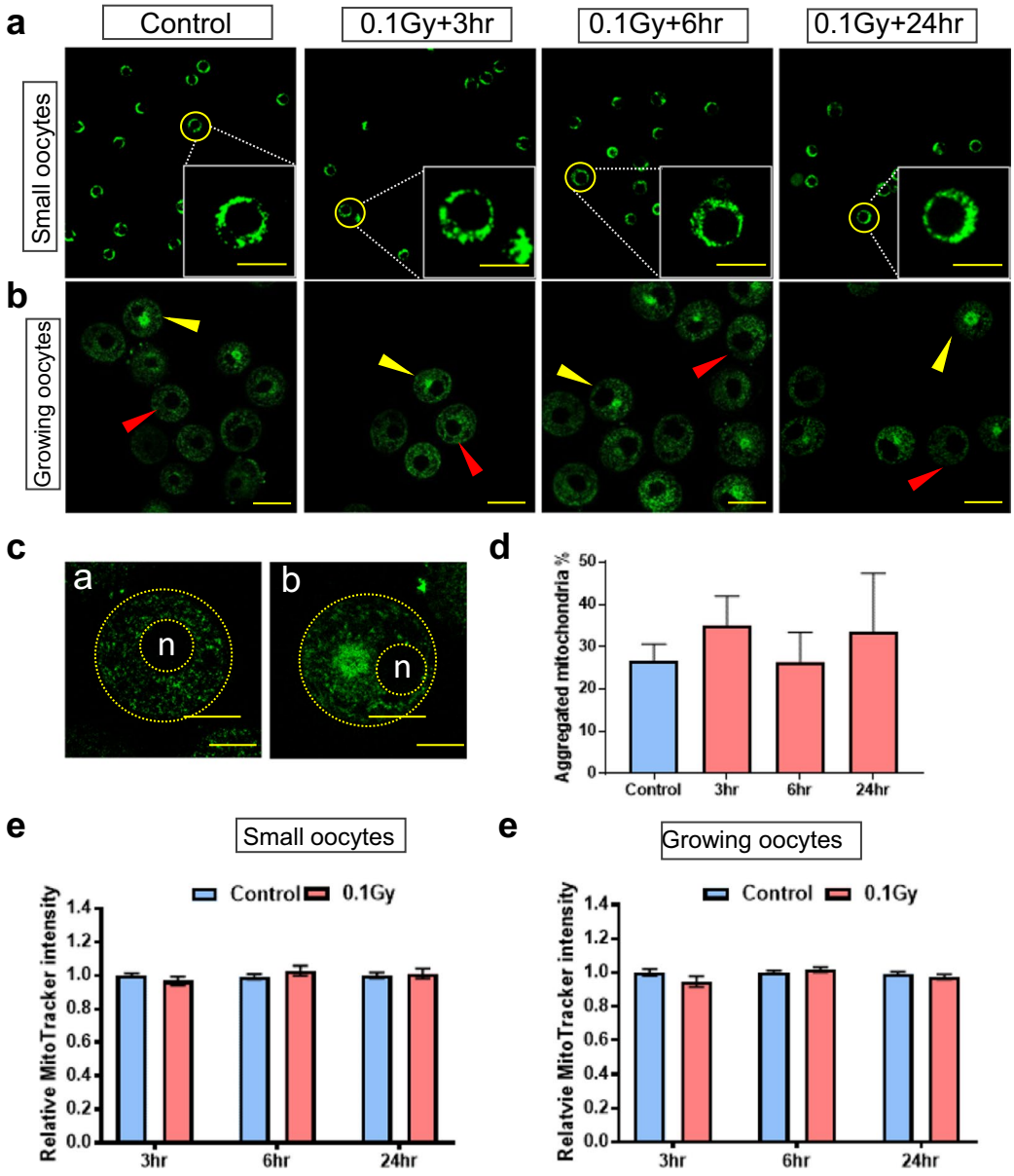

Figure 1. The distribution of mitochondria in small and growing immature oocytes from untreated and γ-irradiated mice. Immature oocytes were isolated from untreated control mice, or 3, 6 and 24 hours after γ-irradiation and mitochondrial distribution was assessed using MitoTracker Green (green) (n = 3–4 mice per group). (**a**) Mitochondria were distributed throughout the cytoplasm in small oocytes. Scale bar = 20 μm. (**b**) Mitochondria were either evenly distributed in the cytoplasm (red arrow head) or aggregated close to nucleus (yellow arrow head) in growing oocytes. Scale bar = 50 μm. (**c**) Enlarged view of homogenous mitochondrial distribution (**a**) and aggregated distribution (**b**). n = nucleus. Scale bar = 20 μm. (**d**) Percentage of growing oocytes with aggregated mitochondria for controls (n = 158) and 3 (n = 61), 6 (n = 54), 24 (n = 36) hours after γ-irradiation. No significant differences were observed (Kruskal-Wallis test, p-value > 0.05). (**e**) Relative MitoTracker intensity in small oocytes at 3 (n = 41/32), 6 (n = 59/21) and 24 (n = 39/23) hours after γ-irradiation compared to control. No significant differences were observed between control and γ-irradiated groups (*t*-test, p-value > 0.05). (**f**) Relative MitoTracker intensity in growing oocytes, at 3 (n = 48/42), 6 (n = 59/64) and 24 (n = 61/63) hours after γ-irradiation compared to control. No significant differences were observed between control and γ-irradiated groups (*t*-test, p-value > 0.05).

though the functional significance of the two patterns is not clear. Importantly, the proportion of oocytes with each localisation pattern in growing oocytes from control and γ-irradiated mice was similar.

Mitochondria are highly dynamic organelles in eukaryotes, continually undergoing fusion and fission[22]. The balance of these two processes maintains the overall population of mitochondria and is related to mtDNA stability, energy production, apoptosis[22]. It is proposed that an increase in mitochondrial abundance (number) is a mechanism of compensation for oxidative defects and is commonly observed in somatic cells following exposure to γ-irradiation[5,23]. In contrast, we did not detect any changes in mitochondrial abundance as indicated by MitoTracker

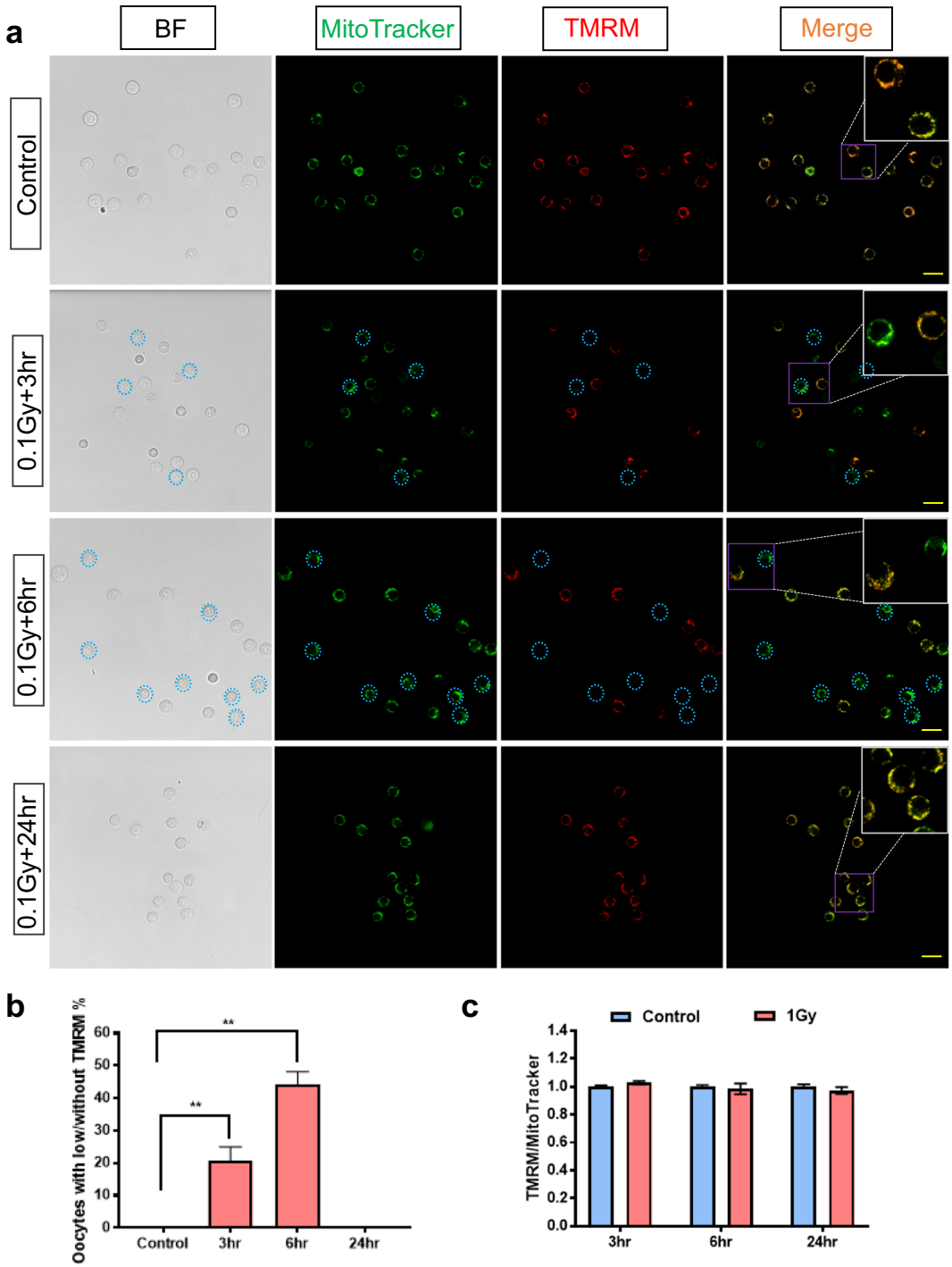

Figure 2. Membrane potential of mitochondria in small immature oocytes from untreated and γ-irradiated mice. Small oocytes were isolated from untreated control mice, or 3, 6 and 24 hours after γ-irradiation and mitochondrial membrane potential was assessed using TMRM. (**a**) Representative confocal images of small oocytes from untreated mice and γ-irradiated mice at 3, 6 and 24 hours after treatment. Scale bar = 40 μm. (**b**) Percentage of small oocytes with low or without TMRM in untreated oocytes (n = 124) and γ-irradiated oocytes at 3 (n = 32), 6 (n = 39) and 24 (n = 24) hours after γ-irradiation. Ordinary one-way ANOVA, Dunnett's multiple comparisons test, **p-value < 0.01. (**c**) Relative TMRM/MitoTracker ratio in small oocytes with TMRM signal at 3 (n = 41/26), 6 (n = 59/21) and 24 (n = 39/23) hours after irradiation. No significant differences were observed between control and γ-irradiated groups (*t*-test, p-value > 0.05).

fluorescent intensity in small oocytes at 3, 6 or 24 hours after γ-irradiation. However, it is possible that the timeframe we picked in our study was too late, as one previous study of mouse oocytes found that mitochondrial number dropped 2 minutes after whole body x-irradiation at 200r and was restored in the next few minutes[24].

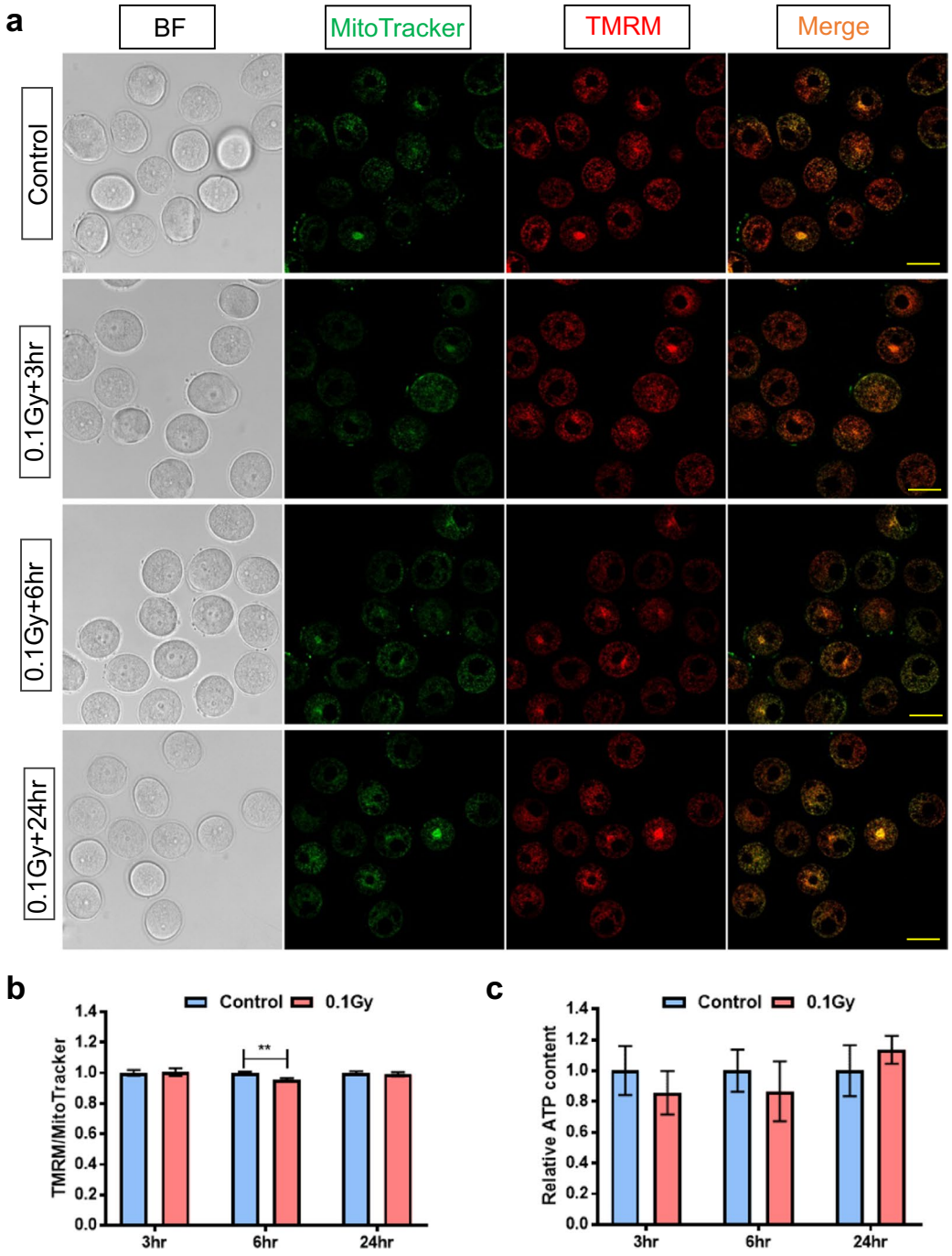

Figure 3. Membrane potential of mitochondria in growing immature oocytes from untreated and γ-irradiated mice. Growing oocytes were isolated from untreated control mice, or 3, 6 and 24 hours after γ-irradiation and mitochondrial membrane potential was assessed using TMRM. (**a**) Representative confocal images of growing oocytes from untreated mice and γ-irradiated mice at 3, 6 and 24 hours after treatment. Scale bar = 50 μm. (**b**) Relative TMRM/MitoTracker ratio in growing oocytes at 3 (n = 48/42), 6 (n = 59/64) and 24 (n = 61/63) hours after irradiation. Experiments were performed in triplicate. A significant decrease of TMRM intensity was observed only at 6 hours after γ-irradiation. Mann-Whitney test, **p-value < 0.01. No significant differences were observed between control and γ-irradiated groups at 3 and 24 hours (Mann-Whitney test and *t*-test, respectively, p-value > 0.05). (**c**) Relative ATP content in growing oocytes 3 (n = 7/7), 6 (n = 7/8) and 24 (n = 4/4) hours after γ-irradiation. No significant differences were observed between control and γ-irradiated groups (*t*-test, p-value > 0.05).

Mitochondrial membrane potential generated by proton pumping is essential for ATP synthesis and storage[25]. Thus, a sharp and persistent change of mitochondrial membrane potential may reduce cellular viability[19,26]. In this study, we found that the TMRM fluorescent signal emitted by cells was lost in 20% and 44% of small oocytes at 3

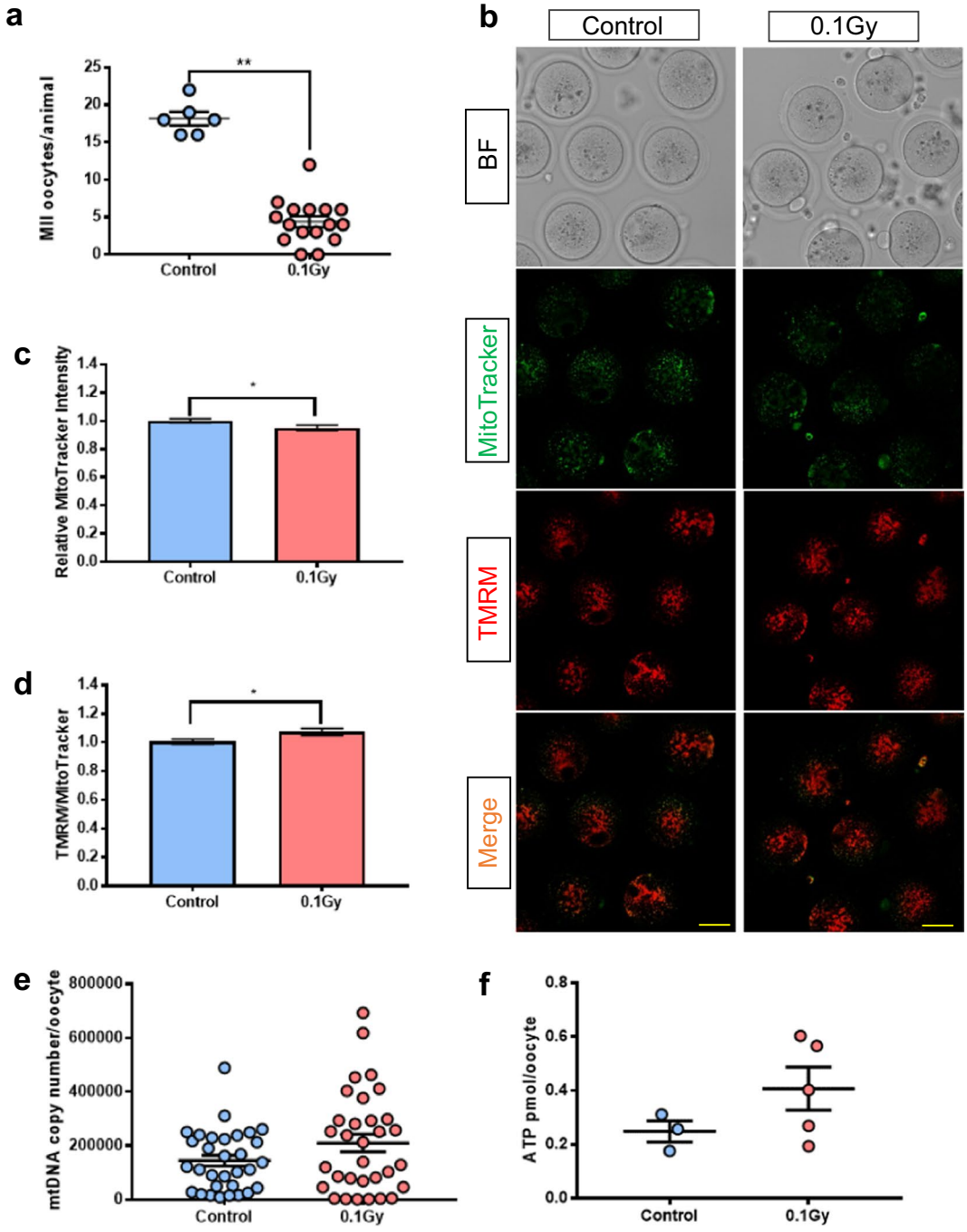

Figure 4. Mitochondria in mature oocytes. Mice were untreated (controls) or γ-irradiated at PN9-11 and then allowed to develop to sexual maturity before being super ovulated. mtDNA copy number was assessed in individual mature oocytes. (**a**) Number of oocytes harvested from adult mice. Each dot represents one animal, animal number n = 6/16 for control and γ-irradiated groups respectively. *t*-test, **p-value < 0.01. (**b**) Representative confocal images of mature oocytes. Scale bar = 50 μm. (**c**) Relative MitoTracker intensity of mature oocytes from untreated control mice (n = 44 oocytes) and γ-irradiated mice (n = 36 oocytes). *t*-test, p-value > 0.05. (**d**) TMRM to MitoTracker ratio in mature oocytes, oocytes number n = 44 in control group and n = 36 in irradiated group. *t*-test, *p-value < 0.05. (**e**) mtDNA copy number in mature oocytes in control (n = 31 oocytes) and γ-irradiated (n = 32 oocytes) groups. No significant differences were observed, Mann-Whitney test, p-value > 0.05. (**f**) ATP content in mature oocytes. Oocytes were pooled into groups of 10 ATP measurement. Oocytes were collected from three and five biological replicates for control and γ-irradiated groups respectively. No significant differences were observed, *t*-test, *p-value < 0.05.

and 6 hours after γ-irradiation, respectively. This finding indicates that the mitochondria in a cohort of oocytes were compromised by γ-irradiation and these oocytes were likely undergoing apoptosis[19]. Additional studies are required to determine if this is due to direct damage of the mitochondria by γ-irradiation or by the induction of apoptosis (e.g. as a result of damage to nuclear DNA). Interestingly, all small oocytes had detectable TMRM staining at 24 hours after γ-irradiation, suggesting the surviving oocytes can repair damage sustained by the mitochondria, or that the mitochondria of the surviving oocytes were in fact not damaged by the 0.1 Gy dose of γ-irradiation used in this study. Quantification of the relative TMRM intensity in the small oocytes showed no differences at any time point, suggesting the latter possibility may be true.

In contrast to small oocytes, γ-irradiation did not appear to be associated with lethal loss of mitochondrial membrane potential in growing oocytes, highlighting well-documented intrinsic differences in the radio-sensitivities of these two populations[20]. The ratio of TMRM to MitoTracker showed a very slight decrease at 6 hours after γ-irradiation in the growing oocyte population, but the subtlety of the change makes it unclear if this would have a meaningful biological consequence. Indeed, ATP levels were maintained in growing oocytes after γ-irradiation, indicating that mitochondria were functionally similar to non-irradiated controls.

To determine if damage inflicted on immature oocytes persists in mature oocytes, γ-irradiated mice were held for a minimum of 3 weeks (the period that required for immature oocytes to fully develop) before being superovulated. We found the number of mature oocytes from γ-irradiated mice was significantly lower than controls. This observation is in keeping with previous work demonstrating a reduction in the size of the ovarian reserve following γ-irradiation due to oocyte apoptosis[3]. It is also possible that γ-irradiation reduces the ability of mice to respond to exogenous hormonal stimulation, perhaps by damaging the hypothalamic–pituitary–gonadal axis, though the low dose of γ-irradiation used in this study make this hypothesis unlikely. We did observe a slight decrease in MitoTracker staining intensity, and concomitant increase in TMRM staining intensity, in γ-irradiated ovulated oocytes relative to controls, but whether such a small relative change is biologically or functionally meaningful is unclear. Furthermore, mitochondrial localisation, mtDNA copy number and ATP levels in these oocytes were similar to oocytes from non-irradiated mice. Overall, the results suggest that mitochondria function was not impaired in mature oocytes from γ-irradiated mice.

There were some limitations associated with this study. For example, this model used a very low dose of γ-irradiation. This was necessary to ensure that a cohort of oocytes survived to allow evaluation. Notably, girls and women would receive much higher doses and we cannot rule out the possibility that higher doses would lead to persistent effects on the mitochondria in oocytes. Furthermore, whilst we determined that mitochondria were capable of generating levels of ATP in γ-irradiated similar to controls, we did not evaluate ROS levels or other impacts, such as calcium signalling. Additionally, damage to mtDNA was not directly assessed. Thus, further work is required to determine if mitochondria are fully functional and undamaged.

In conclusion, our study demonstrated immature oocytes that survived γ-irradiation and developed through to ovulation contained apparently healthy mitochondria, at least to the extent of generating normal levels of ATP. Future studies should focus on establishing whether these oocytes can support normal healthy pregnancy. These promising findings may provide guidance to preserve female fertility when making therapeutic regimen for female cancer patients.

Materials and Methods

Animals, treatments and oocyte collection. C57BL/6J mice were housed in a high-barrier facility (Monash University ARL) with controlled temperature and 12 h light: 12 h dark cycle. All mice had free access to water and food. All animal procedures and experiments were performed in accordance with the NHMRC Australian Code of Practice for the Care and Use of Animals and approved by the Monash Animal Research Platform Animal Ethics Committee. Prepubertal female mice (PN9-11, n = 3–4 mice/control and time point post γ-irradiation), an age at which ovaries contain an abundance of small oocytes, were exposed to whole body γ-irradiation at 0.1 Gy. This dose of γ-irradiation has been shown to induce nuclear DNA damage in oocytes, but approximately 50% survive[27]. To collect immature oocytes, ovaries were harvested 3, 6, 24 hours after γ-irradiation and digested in 0.25% trypsin (SM-203-C, Merck) for 13 minutes and then 200 μl 10% FBS (12003 C, Sigma-Aldrich) in M2 (M7167; Sigma-Aldrich) was added to cease digestion. Oocytes were measured using Las x software (Leica). Oocytes with a diameter ~20 μm were defined as small oocytes from primordial or primary follicles. Oocytes with a diameter ~50 μm were defined as growing oocytes from secondary follicles. To collect mature oocytes, untreated control and γ-irradiated mice were held for a minimum of 3 weeks (the period that required for immature oocytes to fully develop) and then treated with an intraperitoneal injection of with pregnant mare serum gonadotrophin (5IU PMSG; Intervet) followed 44–48 hours later by human chorionic gonadotropin (5 IU hCG; Intervet). After 12–16 hours, cumulus-oocyte complexes were collected from oviducts and mature oocytes (MII stage) were denuded by digestion in M2 media containing 0.3% hyaluronidase (Sigma-Aldrich).

Assessment of mitochondrial membrane potential. Mitochondrial membrane potential was measured in single live oocytes using the low toxicity fluorescent dye tetramethyl rhodamine methyl ester perchlorate (TMRM, T668, ThermoFisher)[28]. TMRM is a cell-permeant dye that accumulates in active mitochondria with intact membrane potential. Briefly, denuded oocytes were incubated with 25 nM TMRM diluted in M2 medium at 37 °C for 30 minutes, washed 3 times in fresh M2 medium, mounted on the dish with glass bottom and then observed under a laser-scanning confocal microscope (SP8, Leica). TMRM was excited using the 552 nm laser line and fluorescence measured using a 563–627 nm band pass filter. A region encompassing the entire oocyte diameter was used to provide an average intensity of fluorescence within the oocyte. An identical region was used for each oocyte in all experiments. The plane of focus in which the oocyte diameter was largest was assumed to be the centre and was selected for image capture and analysis. The acquired images were processed and analysed using the ImageJ (NIH) open source software. For each image, the fluorescence intensity per single cell was

calculated and expressed as the ratio of actual intensity to the mean intensity of control group. Experiments were repeated a minimum of three separate times (representing biological replicates) and data are expressed as mean +/− SEM. The number of oocytes analyzed is stated in the appropriate figure legend.

Assessment of mitochondrial distribution and mass. Mitochondrial distribution and mass were evaluated using MitoTracker Green (M7514, ThermoFisher), which stains mitochondria regardless of mitochondrial membrane potential. Briefly, denuded oocytes from unprimed or gonadotropin-stimulated mice were incubated with 200 nM MitoTracker diluted in M2 at 37 °C for 30 minutes, washed 3 times in fresh M2, mounted on the dish with glass bottom and then observed under a laser-scanning confocal microscope (SP8, Leica). Mitotracker Green was excited using the 488 nm laser line and fluorescence measured using a 495–523 nm bandpass filter. The acquired images were processed and analysed using the ImageJ (NIH) open source software as described above. For each image, the fluorescence intensity per single oocyte was calculated and expressed as the ratio of actual intensity to the mean intensity of control group. Experiments were repeated a minimum of three separate times and data are expressed as mean +/− SEM for experiment.

ATP quantification. Denuded oocytes (10 pooled/group) collected from unprimed or gonadotropin-stimulated mice were collected in 50 μl filtered ultrapure water and stored at −80 °C until use. To prepare standards, 10^{-7} M ATP standard stock was obtained from ENLITEN® ATP Assay System Bioluminescence Detection Kit (Promega) and was diluted with filtered ultrapure water. ATP levels were assayed using the Adenosine 5¢-triphosphate (ATP) bioluminescent somatic cell assay kit (FLASC, Sigma) according to the manufacturer's instructions. Briefly, 100 μl ATP Assay Mix Working Solution was added to a 96-well plate (reaction vial) (M0187, Greiner) and allowed to stand at room temperature for 3 minutes. Somatic Cell ATP Releasing Reagent (100 μl), 50 μl filtered ultrapure water and 50 μl sample were added to a new tube and 100 μl was transferred to the reaction vial. ATP concentration was measured immediately using a luminometer (BMG, Clariostar, 76G58). Data are expressed as ATP content relative to the mean of controls or pmol/oocyte. Experiments were repeated a minimum of three separate times.

Quantification of mtDNA copy number. mtDNA copy number was assayed on single oocytes as previously described[29] with some modifications. Briefly, total DNA of single oocytes were isolated using 10 μl lysis buffer containing 50 mM tris-HCl (pH 8.5), 0.1 mM EDTA, 0.5% Tween-20 and 200 μg/ml proteinase K. Samples were incubated at 55 °C for 2 hours and then 95 °C for 10 minutes to inactivate the proteinase K. Six serial dilutions of stock plasmid (a.pngt from Rebecca Robker, The Robinson Research Institute, School of Medicine, The University of Adelaide, Australia) were used to generate the standard curve. Real-time quantitative PCR was performed in triplicate using 5′-CGTTAGGTCAAGGTGTAGCC-3′ and 5′-CCAAGCACACTTTCCAGTATG-3′ primers and SYBR green PCR master mix (Qiagen) and a 384-well real-time PCR machine (CFX384, Bio-Rad). The reaction conditions were 95 °C for 2 minutes and then 40 cycles of 95 °C for 5 seconds and 60 °C for 10 seconds. The number of oocytes analyzed is stated in the appropriate figure legend.

Statistical analysis. Data were analysed using with GraphPad Prism Software. For comparison of two groups, normally distributed data were analysed by *t*-test, whilst non-normally distributed data were analysed by Mann-Whitney test. More than two groups of normally distributed data were analysed by ordinary one-way ANOVA followed by Dunnett's multiple comparisons test, whilst non-normally distributed data were analysed by Kruskal-Wallis test. All data were presented as mean ± SEM. Statistical significance was denoted by *p-value < 0.05, **p-value < 0.01.

Data availability

Materials, data and associated protocols are available on request.

Received: 6 September 2019; Accepted: 3 December 2019;
Published online: 27 December 2019

References

1. Kerr, J. B. *et al*. Quantification of healthy follicles in the neonatal and adult mouse ovary: evidence for maintenance of primordial follicle supply. *Reproduction* **132**(1), 95–109 (2006).
2. Hutt, K. *et al*. How to best preserve oocytes in female cancer patients exposed to DNA damage inducing therapeutics. *Cell Death Differ* **20**(8), 967–8 (2013).
3. Kerr, J. B. *et al*. DNA damage-induced primordial follicle oocyte apoptosis and loss of fertility require TAp63-mediated induction of Puma and Noxa. *Mol Cell* **48**(3), 343–52 (2012).
4. Livera, G. *et al*. p63 null mutation protects mouse oocytes from radio-induced apoptosis. *Reproduction* **135**(1), 3–12 (2008).
5. Nugent, S. M. *et al*. Increased mitochondrial mass in cells with functionally compromised mitochondria after exposure to both direct gamma radiation and bystander factors. *Radiat Res* **168**(1), 134–42 (2007).
6. Zhou, X. *et al*. Effects of X-irradiation on mitochondrial DNA damage and its supercoiling formation change. *Mitochondrion* **11**(6), 886–92 (2011).
7. Richter, C., Park, J. W. & Ames, B. N. Normal oxidative damage to mitochondrial and nuclear DNA is extensive. *Proc Natl Acad Sci USA* **85**(17), 6465–7 (1988).
8. Larsen, N. B., Rasmussen, M. & Rasmussen, L. J. Nuclear and mitochondrial DNA repair: similar pathways? *Mitochondrion* **5**(2), 89–108 (2005).
9. Shimura, T. *et al*. A comparison of radiation-induced mitochondrial damage between neural progenitor stem cells and differentiated cells. *Cell Cycle* **16**(6), 565–573 (2017).
10. Nugent, S. *et al*. Altered mitochondrial function and genome frequency post exposure to γ-radiation and bystander factors. *Int J Radiat Biol* **86**(10), 829–41 (2010).

11. Yoshida, K. *et al.* Mitochondrial genotypes and radiation-induced micronucleus formation in human osteosarcoma cells *in vitro*. *Oncol Rep* **8**(3), 615–9 (2001).
12. Evdokimovskii, E. V. *et al.* [Sharp changes in the copy number of mtDNA and its transcription in the blood cells of X-ray irradiated mice are observed, and mtDNA fragments appear in the blood serum]. *Radiats Biol Radioecol* **47**(4), 402–7 (2007).
13. Kam, W. W. *et al.* Predicted ionisation in mitochondria and observed acute changes in the mitochondrial transcriptome after gamma irradiation: a Monte Carlo simulation and quantitative PCR study. *Mitochondrion* **13**(6), 736–42 (2013).
14. Polyak, K. *et al.* Somatic mutations of the mitochondrial genome in human colorectal tumours. *Nat Genet* **20**(3), 291–3 (1998).
15. Dumollard, R., Duchen, M. & Carroll, J. The role of mitochondrial function in the oocyte and embryo. *Curr Top Dev Biol* **77**, 21–49 (2007).
16. Babayev, E. & Seli, E. Oocyte mitochondrial function and reproduction. *Curr Opin Obstet Gynecol* **27**(3), 175–81 (2015).
17. Alston, C. L. *et al.* The genetics and pathology of mitochondrial disease. *J Pathol* **241**(2), 236–250 (2017).
18. Kam, W. W. & Banati, R. B. Effects of ionizing radiation on mitochondria. *Free Radic Biol Med* **65**, 607–19. (2013).
19. Zorova, L. D. *et al.* Mitochondrial membrane potential. *Anal Biochem* **552**, 50–59 (2018).
20. Adriaens, I., Smitz, J. & Jacquet, P. The current knowledge on radiosensitivity of ovarian follicle development stages. *Hum Reprod Update* **15**(3), 359–77 (2009).
21. Pepling, M. E. *et al.* Mouse oocytes within germ cell cysts and primordial follicles contain a Balbiani body. *Proc Natl Acad Sci USA* **104**(1), 187–92 (2007).
22. Chan, D. C. Fusion and fission: interlinked processes critical for mitochondrial health. *Annu Rev Genet* **46**, 265–87 (2012).
23. Yamamori, T. *et al.* Ionizing radiation induces mitochondrial reactive oxygen species production accompanied by upregulation of mitochondrial electron transport chain function and mitochondrial content under control of the cell cycle checkpoint. *Free Radic Biol Med* **53**(2), 260–70 (2012).
24. Parsons, D. F. An electron microscope study of radiation damage in the mouse oocyte. *J Cell Biol* **14**, 31–48 (1962).
25. Perry, S. W. *et al.* Mitochondrial membrane potential probes and the proton gradient: a practical usage guide. *Biotechniques* **50**(2), 98–115 (2011).
26. Shonai, T. *et al.* MEK/ERK pathway protects ionizing radiation-induced loss of mitochondrial membrane potential and cell death in lymphocytic leukemia cells. *Cell Death Differ* **9**(9), 963–71 (2002).
27. Suh, E. K. *et al.* p63 protects the female germ line during meiotic arrest. *Nature* **444**(7119), 624–8 (2006).
28. Duchen, M. R., Surin, A. & Jacobson, J. Imaging mitochondrial function in intact cells. *Methods Enzymol* **361**, 353–89 (2003).
29. Kameyama, Y. *et al.* Asymmetrical allocation of mitochondrial DNA to blastomeres during the first two cleavages in mouse embryos. *Reprod Fertil Dev* **22**(8), 1247–53 (2010).

Acknowledgements

This work was supported by the National Health and Medical Research Council (KJH (#1050130, 1100219). This work was made possible through Victorian State Government Operational Infrastructure Support and Australian Government NHMRC IRIISS.

Author contributions

K.J.H. and Q.W. designed the experiments; Q.W. and J.L. performed the experiments; Q.W., J.S. and K.H. analysed the data; Q.W. and K.J.H. wrote the manuscript. All authors edited the manuscript.

Competing interests

The authors declare no competing interests.

Additional information

Supplementary information is available for this paper at https://doi.org/10.1038/s41598-019-56423-w.

Correspondence and requests for materials should be addressed to K.J.H.

Reprints and permissions information is available at www.nature.com/reprints.

Publisher's note Springer Nature remains neutral with regard to jurisdictional claims in published maps and institutional affiliations.

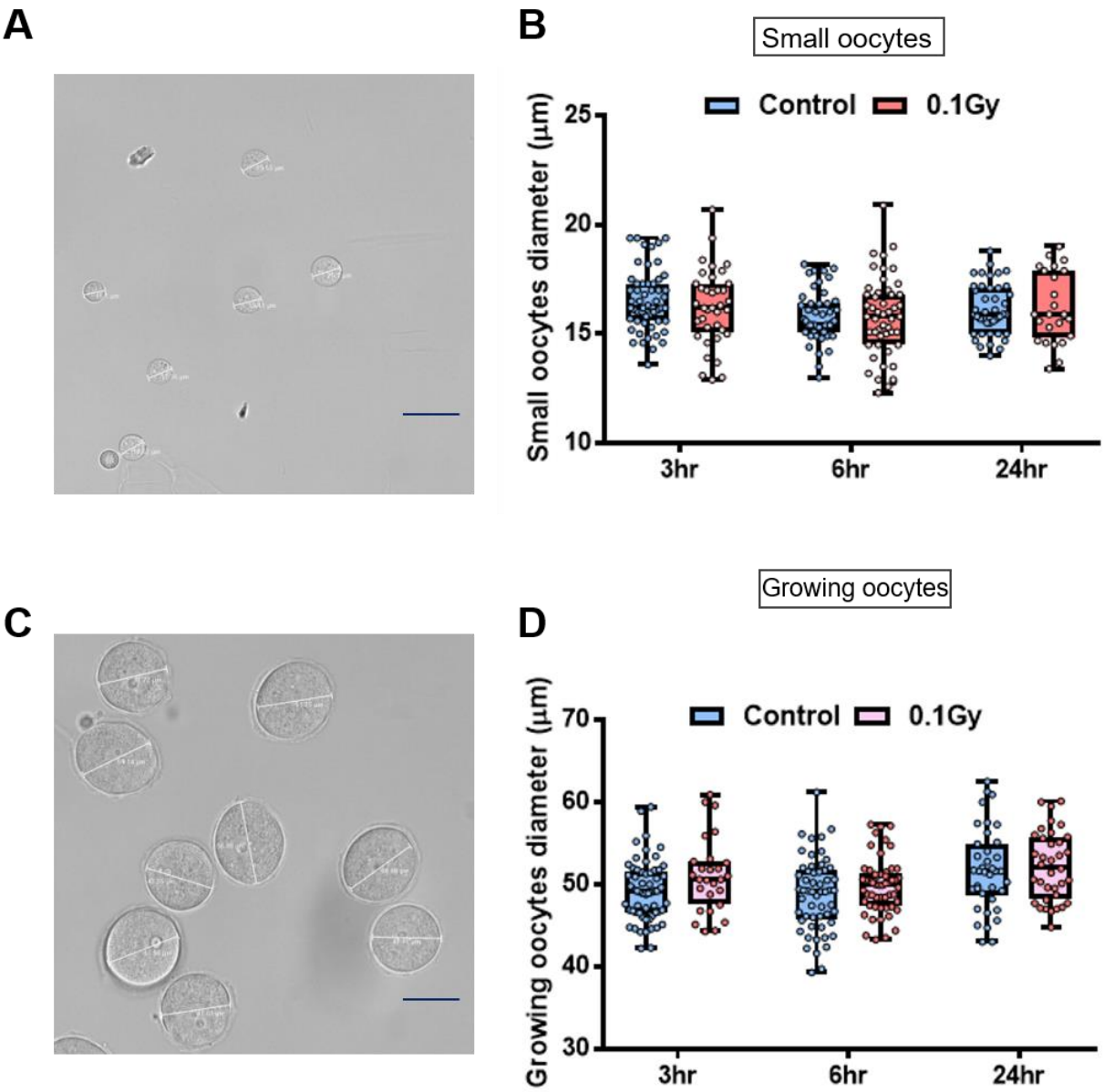

Supplemental Figure 1. Classification of oocytes according to size. A, Small oocytes (diameter ~20µm) were isolated from primordial or primary follicles. Scale bar = 50µm. B, Diameter of individual small oocytes, used for immunofluorescence analysis. Oocyte number at 3 (n=55/37), 6 (n=48/50) and 24 hours (n=42/25) for control and 0.1Gy γ-irradiated, respectively. C, Growing oocytes were isolated from secondary follicles. Scale bar = 50µm. D, Diameter of individual growing oocytes, used for immunofluorescence analysis. Oocyte number at 3 (n=64/61), 6 (n=56/54) and 24 (n=38/36) hours for control and γ-irradiated, respectively. Oocytes were collected from a minimum of 3 separate mice for each group.

Chapter 3. Evaluation of mitochondria in oocytes following cisplatin exposure

Journal of Ovarian Research

RESEARCH Open Access

Evaluation of mitochondria in mouse oocytes following cisplatin exposure

Qiaochu Wang and Karla J. Hutt*

Abstract

Background: Cisplatin is a platinum-based chemotherapeutic that damages genomic DNA leading to cell death. It also damages mitochondrial DNA and induces high levels of mitochondrial reactive oxygen species (mtROS), further sensitising cells to apoptosis. Notably, immature oocytes are particularly vulnerable to cisplatin treatment, a common side effect of which is depletion of the primordial follicle reserve, leading to infertility and early menopause. Cisplatin is known to damage the DNA of oocytes, but the possibility that cisplatin also compromises oocyte survival and quality by damaging mitochondria, has not been investigated. To begin to address this question, neonatal mice were treated with saline or cisplatin (2 mg/kg or 4 mg/kg) and the short and long-term impacts on mitochondria in oocytes were characterised.

Results: At 6 and 24 h after treatment, mitochondrial localisation, mass and ATP content in immature oocytes were similar between groups. However, TMRM staining intensity, a marker of mitochondrial membrane potential, was decreased in immature oocytes from cisplatin treated mice compared to saline treated controls, consistent with the induction of apoptosis. When mice were super ovulated 5 weeks after exposure, the number of mature oocytes harvested from cisplatin treated mice was significantly lower than controls. Mitochondrial localisation, mass, membrane potential and ATP levels showed no differences between groups.

Conclusions: These findings suggest that mitochondrial dysfunction may contribute to the depletion of the ovarian reserve caused by cisplatin, but long-term impacts on mitochondria may be minimal as those immature oocytes that survive cisplatin treatment develop into mature oocytes with normal mitochondrial parameters.

Keywords: Oocyte, Cisplatin, Mitochondria, Fertility, Follicle

Introduction

Within the ovary of mammalian females, the finite supply of immature oocytes are stored in structures called primordial follicles [1]. These primordial follicles represent the stockpile from which all mature hormone producing follicles and ovulatory oocytes are derived, and their gradual depletion throughout reproductive life ultimately leads to infertility and loss of ovarian endocrine function [2–5]. In women, the supply of primordial follicles can be prematurely depleted by exposure to radiotherapy and DNA damaging chemotherapy, causing premature ovarian failure (POF) and permanent loss of fertility [6–8]. Indeed, for reasons unknown, immature oocytes appear to be much more vulnerable to the effects of these treatments than the surrounding granulosa cells, growing oocytes, or other somatic cells in the body [9].

As a member of the platinum-based chemotherapeutic family, cisplatin ([Pt(NH3)2Cl2]) has been widely used since 1970 s for the treatment of testicular cancer, ovarian cancer, breast cancer and other solid tumours [10]. Whilst cisplatin is a valuable anticancer agent, direct damage to ovarian follicles has been reported as a common side-effect [11, 12]. The cytotoxicity of cisplatin is attributed to its ability to bind nuclear DNA to induce

* Correspondence: karla.hutt@monash.edu
Ovarian Biology Laboratory, Biomedicine Discovery Institute, Department of Anatomy and Developmental Biology, Monash University, Melbourne, Australia

apoptosis, necrosis, or both, in cancer and non-cancerous cells [13]. However, mounting evidence demonstrates that the effects of cisplatin extend beyond direct nuclear DNA damage [14, 15]. In particular, the chloride ligands of cisplatin can be replaced by water molecules in the cell, generating positively charged electrophiles that have a high affinity for negatively charged mitochondria [16]. Cisplatin has a much greater propensity (300–500 fold) to form platinum adducts with mitochondrial DNA (mtDNA) than nuclear DNA (nDNA) [17]. Since mtDNA encodes vital mitochondrial proteins, damage to mtDNA can result in mitochondrial malfunction [18]. Furthermore, a recent study has suggested that cisplatin sensitive cancer cells contain higher mitochondrial content and higher levels of mitochondrial reactive oxygen species (mtROS) than those that are resistant to cisplatin induced cell death [19]. This observation indicates that cisplatin directly impacts mitochondrial activity, which in turn influences cell survival/death following exposure to this drug. Indeed, mitochondrial damage may be more important than genomic DNA damage in triggering apoptosis in response to cisplatin exposure, as cisplatin treated cells can activate cell death even in the absence of a nucleus or activation of the nuclear DNA damage response [20, 21].

The primary role of mitochondria is to produce energy, in the form of adenosine triphosphate (ATP), to fuel cellular processes, with approximately 95 % of ATP being generated by the oxidative phosphorylation (OXPHOS) pathway [22]. Of note, mammalian oocytes have limited capacity of glycolysis. Thus, the energy intensive processes of oocyte growth, maturation, fertilization, and early embryo development are all heavily dependent on mitochondrial number and function [23]. In line with this requirement, mitochondrial number increases dramatically throughout oogenesis and folliculogenesis, such that mature oocytes can contain 100,000 mitochondria and 50,000–1,500,000 copies of the mitochondrial genome [24], which is significantly more than somatic cells [23, 25]. Indeed, the importance of maintaining mitochondrial number and function is demonstrated by studies showing that the maturation of oocytes is severely impaired when mitochondrial activities are sub-optimal [26, 27].

Cisplatin is known to damage the DNA of oocytes, but the possibility that cisplatin also compromises oocyte survival and quality by damaging mitochondria, has not been investigated. A better understanding of how oocytes respond to platinum drugs is important for the development of effective strategies to protect the ovarian reserve during cancer treatment. Therefore, to gain insight into the impact of cisplatin on mitochondria within oocytes, postnatal day 10 (PN10) or adult mice were injected with saline, or 2 mg/kg or 4 mg/kg cisplatin. Immature oocytes were collected at 3, 6 and 24 h after treatment to evaluate acute effects on mitochondria, including alterations in mitochondrial localisation, mass, membrane potential and ATP level. Mature oocytes were also collected 5 weeks after treatment to determine if any alterations in these mitochondrial parameters persisted in the long term, and thus had the potential to impair fertility or offspring health.

Materials and methods

Animals, treatments and oocyte collection

C57BL/6J mice were housed in a light and temperature controlled high-barrier facility (Monash University ARL) with free access to food and water. All animal procedures and experiments were performed in accordance with the NHMRC Australian Code of Practice for the Care and Use of Animals and approved by the Monash Animal Research Platform Animal Ethics Committee. PN10 mice were weighed and injected intraperitoneally (i.p.) with 2 mg/kg or 4 mg/kg cisplatin or equivalent saline using 27-gauge needles. This dose was lower than previous reported doses applied in prepubertal mice to increase the possibility that oocytes could be harvested at later time points [11]. At 3, 6, 24 h or 5 weeks after saline or cisplatin injection, ovaries were harvested. Immature oocytes from primordial, primary, secondary and small antral follicles in PN10 mice were obtained by digesting ovaries in 0.25 % trypsin (SM-203-C, Merck) for 13 min with gentle and repeated pipetting and 200 μl 10 % FBS (12,003 C, Sigma-Aldrich) in M2 (M7167; Sigma-Aldrich) was added to stop digestion. Matured oocytes within the cumulus-oocyte complexes from PN50 mice were collected 12–16 h after the sequential i.p. injection of pregnant mare serum gonadotrophin (10 IU PMSG; Intervet) and human chorionic gonadotropin (10 IU hCG; Intervet) at 48 h interval. Denuded mature oocytes were collected after digestion in 0.3 % hyaluronidase (Sigma-Aldrich) in M2 media for 2 min. An additional cohort of adult (PN50) female mice treated with saline or 4 mg/kg cisplatin and mature oocytes harvested after superovulation 3 weeks later, as described above.

Assessment of mitochondrial distribution and mass

Mitochondrial distribution and mitochondrial mass were determined by live cell imaging. Briefly, oocytes were incubated with 200nM MitoTracker Green (M7514, ThermoFisher) diluted in M2 at 37 °C for 30 min. After 3 times washing in warm and fresh M2 medium, oocytes were transferred to a dish with glass bottom covered with mineral oil (M5904, Sigma-Aldrich). Mounted oocytes were immediately observed under the confocal microscope (SP8, Leica) with a 40x water immersion objective (1.1 NA) at 37 °C. The excitation of MitoTracker Green was provided by the 488 nm laser line and the

fluorescence was collected using a 495–523 nm band pass filter. The images were captured for analysis when the plane of focus encompassed the largest oocyte diameter. The fluorescence intensity of each cell was measured by FIJI software. The results were expressed as the ratio of actual intensity of each cell to the mean intensity of control group.

Assessment of mitochondrial membrane potential

Mitochondrial membrane potential was determined by live cell imaging. Briefly, oocytes were incubated with 25nM tetramethyl rhodamine methyl ester perchlorate (TMRM (T668, ThermoFisher)) diluted in M2 medium at 37 °C for 30 min. After 3 times washing in warm and fresh M2 medium, oocytes were transferred to a dish with glass bottom covered with mineral oil. Mounted oocytes were immediately observed under the confocal microscope with a 40x water immersion objective (1.1 NA) at 37 °C. The excitation of TMRM was provided by the 552 nm laser line and the fluorescence was collected using a 563–627 nm band pass filter. The images were captured for analysis when the plane of focus encompassed the largest oocyte diameter. The fluorescence intensity of each cell was measured by FIJI software. The ratio of actual intensity of each cell to the mean intensity of control group was calculated and the results were expressed as the ratio of TMRM intensity to MitoTracker intensity.

ATP quantification

Total ATP content of 10 pooled immature oocytes from PN10 mice or 5 pooled mature oocytes from PN50 mice was measured by a luminometer (BMG, Clariostar, 76G58). The samples were treated using the Adenosine 5'-triphosphate (ATP) bioluminescent somatic cell assay kit (FLASC, Sigma) according to the manufacturer's instructions. A standard curve generated from serial dilution of 10^{-7} M ATP standard stock was prepared for each experiment. The ATP content was calculated according to the linear regression formula obtained from the standard curve. The results were expressed as ATP content per oocyte.

Statistical analysis

Data were presented as mean ± SEM and the analysis were performed by GraphPad Prism Software. Student's t-test was used to compare two groups of data that were normally distributed, and Mann-Whitney test was used to compare two groups of data that were not normally distributed. Ordinary one-way ANOVA with Dunnett's multiple comparisons test was used to compare the differences in mitochondrial localisation. Statistically significant differences were considered when $p < 0.05$.

Results

Cisplatin alters mitochondrial distribution, but not mass, in immature oocytes

Immature oocytes were collected from mice 3, 6 and 24 h after saline or cisplatin (2 mg/kg or 4 mg/kg) treatment and classified as small or growing as previously described [28]. Small oocytes were from primordial and primary follicles, and growing oocytes were from secondary and small antral follicles. Mitochondrial localisation in small immature oocytes was evenly distributed in the cytoplasm around nucleus at all time points after 2 mg/kg cisplatin injection, and at 3 and 6 h after 4 mg/kg cisplatin (Fig. 1A, B, Ea). However, in some oocytes, mitochondria showed restricted cytoplasmic localisation at 24 h after 4 mg/kg cisplatin (Fig. 1B, Eb). In growing immature oocytes, homogenously distributed (Fig. 1E b) and aggregated mitochondria (Fig. 1E c) were observed in both control and cisplatin treated groups (Fig. 1C, D) and no significant differences were found at different time points after 2 mg/kg or 4 mg/kg cisplatin treatment compared to saline treated controls (Fig. 1F, G).

Mitochondrial mass was evaluated by the relative fluorescence intensity of MitoTracker Green. There were no significant differences observed in small or growing immature oocytes at any time points after saline or cisplatin treatment at either dose (Fig. 1H-K).

Cisplatin disrupted mitochondrial membrane potential in immature oocytes

Mitochondrial membrane potential was assessed using TMRM staining and expressed as a ratio relative to MitoTracker intensity. In small immature oocytes, TMRM signal was detectable at all time points after 2 mg/kg cisplatin injection, but mitochondrial membrane potential was significantly lower than controls at 24 h (Fig. 2A, B). Similarly, in the 4 mg/kg group, mitochondrial membrane potential was slightly lower than controls at 6 and 24 h, and 60 % of small immature oocytes lost TMRM signal at the latter time point (Fig. 2C, D, E). Notably, those oocytes had rough edges and abnormal mitochondrial distribution (Fig. 2F).

In growing immature oocytes, TMRM signal was detectable in both 2 mg/kg and 4 mg/kg cisplatin treated groups at all time points (Fig. 3a, d). At 24 h, mitochondrial membrane potential was slightly lower in oocytes from cisplatin (2 and 4 mg/kg) treated mice than controls (Fig. 3a, b, d, e). ATP content was similar in growing oocytes from control and cisplatin treated groups (Fig. 3c, f).

Cisplatin reduced number of mature oocytes without changing mitochondrial distribution, mitochondrial mass and mitochondrial function

To investigate the ability of cisplatin-exposed primordial follicle to develop into mature oocytes, PN10 mice were

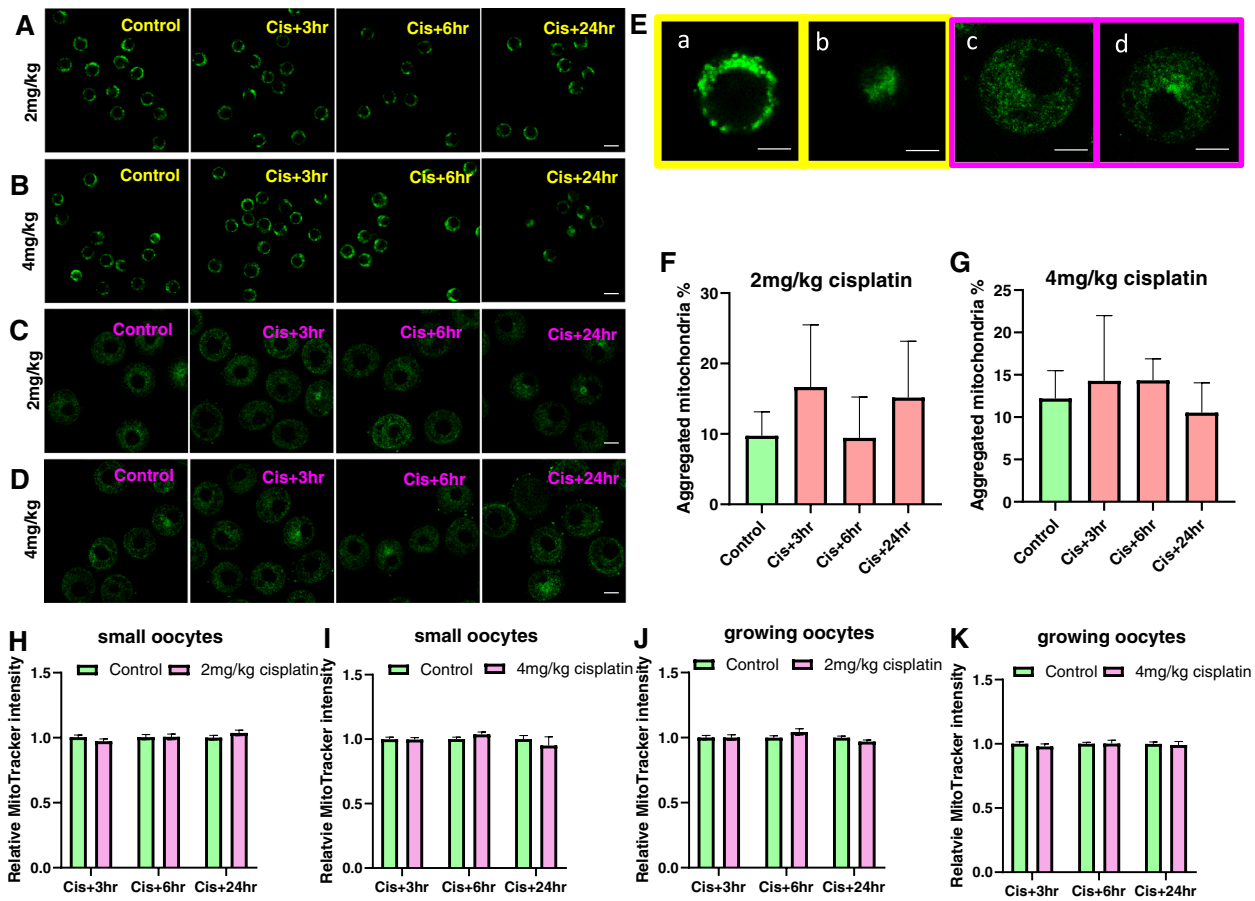

Fig. 1 The distribution of mitochondria in small and growing immature oocytes from saline and cisplatin (2 and 4 mg/kg) treated mice. Immature oocytes were isolated from saline treated control mice, or 3, 6 and 24 h after cisplatin and mitochondrial distribution was assessed using MitoTracker Green (green) ($N = 3$–4 mice per group). Mitochondrial localisation in small oocytes treated with saline or cisplatin 2 mg/kg (**A**) or 4 mg/kg (**B**), and growing oocytes treated with saline or cisplatin 2 mg/kg (**C**) or 4 mg/kg (**D**). Scale bar = 20 μm. **E** Magnification of small (**a**-**b**, scale bar = 10 μm) and growing oocytes (**c**-**d**, scale bar = 20 μm). **F** Percentage of growing oocytes with aggregated mitochondria for controls ($n = 88$) and 3 ($n = 28$), 6 ($n = 32$), 24 ($n = 31$) hours after 2 mg/kg cisplatin and **G** controls ($n = 144$) and 3 ($n = 45$), 6 ($n = 43$), 24 ($n = 60$) hours after 4 mg/kg cisplatin. No significant differences were observed (Kruskal-Wallis test, p-value > 0.05). Relative MitoTracker intensity of small oocytes treated with saline or cisplatin 2 mg/kg (**H**) or 4 mg/kg (**I**), and growing oocytes treated with saline or cisplatin 2 mg/kg (**J**) or 4 mg/kg (**K**). For 2 mg/kg cisplatin, small oocyte number $n = 46/48$ at 3 h, $n = 35/29$ at 6 h and $n = 41/44$ at 24 h after cisplatin treatment; growing oocyte number $n = 35/35$ at 3 h, $n = 31/33$ at 6 h and $n = 37/39$ at 24 h after cisplatin treatment. For 4 mg/kg cisplatin, small oocyte number $n = 45/50$ at 3 h, $n = 72/75$ at 6 h and $n = 35/22$ at 24 h after cisplatin treatment; growing oocyte number $n = 38/41$ at 3 h, $n = 37/41$ at 6 h and $n = 51/45$ at 24 h after cisplatin. t-test for comparison of treated oocytes with relevant controls at each time point

treated with saline or cisplatin (2 mg/kg or 4 mg/kg) and then mature oocytes harvested 5 weeks later. Significantly fewer mature oocytes were obtained from mice treated with 2 mg/kg cisplatin injected mice than controls (Control 25 ± 9 vs. cisplatin 2 mg/kg 9 ± 2, $n = 5/16$ mice, $p < 0.05$) (Fig. 4a). No oocytes were collected from 8/11 mice treatment with 4 mg/kg cisplatin, with only very low number from the remaining 3 animals, meaning there were insufficient oocytes in this group for further analysis (Control 10 ± 2 vs. cisplatin 4 mg/kg 1 ± 1, $n = 3/11$ mice, $p < 0.01$) (Fig. 4b).

Following incubation of ovulated oocytes with MitoTracker Green, mitochondria were found to be homogeneously distributed in the cytoplasm in control and cisplatin (2 mg/kg) treated groups (Fig. 4c). No differences were observed in relative MitoTracker Green intensity, TMRM intensity or ATP content in cisplatin-treated (2 mg/kg) oocytes compared to controls (Fig. 4d-f).

Cisplatin treatment did not alter mitochondrial characteristics in adult mice

In the experiment above, mature oocytes could not be collected from mice exposed at PN10 with 4 mg/kg cisplatin. As other studies have suggested that adult mice treated with similar doses are fertile (albeit less so than saline treated controls) [29], we reasoned that it may be

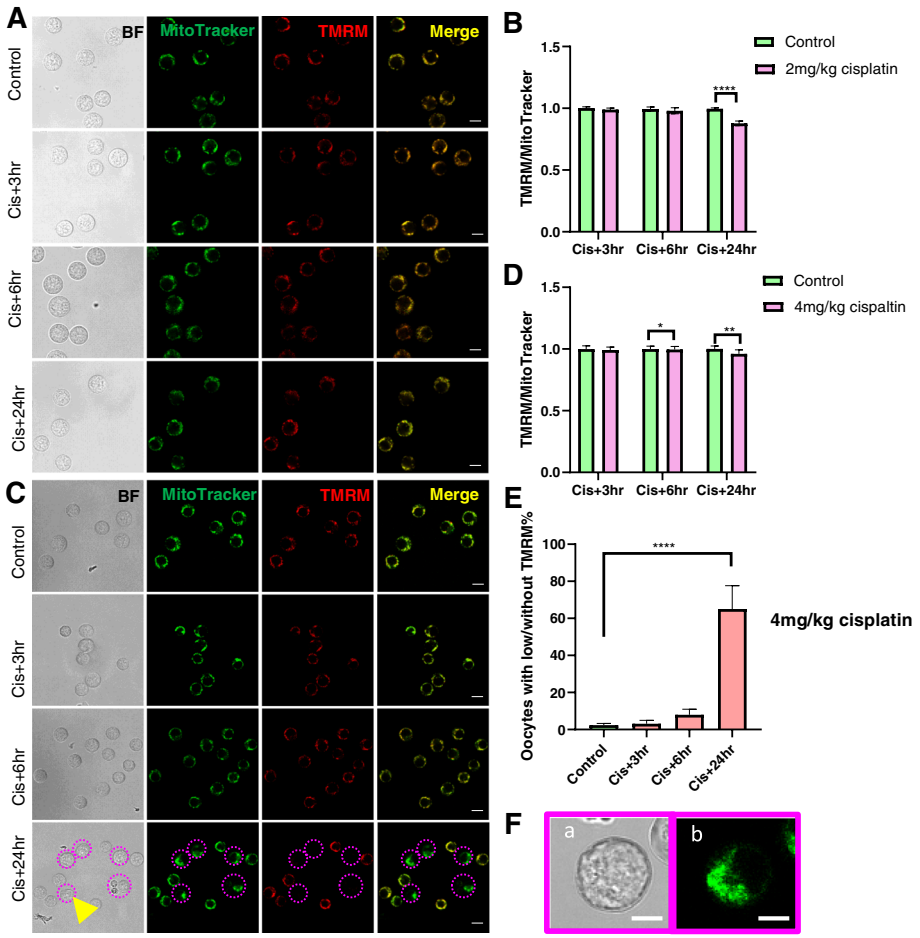

Fig. 2 Membrane potential of mitochondria in small immature oocytes from saline and cisplatin (2 and 4 mg/kg) treated mice. Small oocytes were isolated from saline control mice, or 3, 6 and 24 h after cisplatin treatment and mitochondrial membrane potential was assessed using TMRM. **A** Representative confocal images of small oocytes from controls and 2 mg/kg cisplatin treated mice at 3, 6 and 24 h. Scale bar = 20 μm. **B** Relative TMRM/MitoTracker ratio in small oocytes with TMRM signal at 3 ($n = 46/48$), 6 ($n = 35/29$) and 24 ($n = 41/44$) hours after 2 mg/kg cisplatin. **C** Representative confocal images of small oocytes from saline treated controls and mice at 3, 6 and 24 h after 4 mg/kg cisplatin treatment. Scale bar = 20 μm. **D** Relative TMRM/MitoTracker ratio in small oocytes with TMRM signal at 3 ($n = 45/50$), 6 ($n = 72/75$) and 24 ($n = 35/22$) hours after 4 mg/kg cisplatin. **E** Percentage of small oocytes with low or without TMRM in control ($n = 229$) and 3 ($n = 76$), 6 ($n = 80$) and 24 ($n = 68$) hours after 4 mg/kg cisplatin treatment. **F** Magnification of small oocytes (indicated by the yellow arrow in **C**) without TMRM signal (**a**) and abnormal mitochondrial distribution (**b**). Scale bar = 10 μm. * p-value < 0.05, ** p-value < 0.01, **** p-value < 0.0001

possible to collect mature oocytes for mitochondrial analysis from PN50 mice treated with 4 mg/kg cisplatin. There were no significant differences in the number of oocytes harvested from control and cisplatin (4 mg/kg) treated animal (Control 24 ± 4 vs. cisplatin 4 mg/kg 23 ± 3, $n = 6/12$ mice, $p > 0.05$) (Fig. 5a). In addition, mitochondrial distribution, relative MitoTracker Green intensity and TMRM intensity and ATP content were similar in mature oocytes collected from cisplatin and saline treated animals (Fig. 5b-e).

Discussion

Cisplatin is an effective chemotherapeutic for breast and ovarian tumors, but some cancer survivors will experience acute or permanent ovarian failure due to treatment-induced depletion of the ovarian follicular reserve [30, 31]. To minimize the reproductive and endocrine related side-effects of cisplatin, it is crucial to comprehensively understand the mechanisms by which cisplatin causes ovarian damage. While previous works have focused on the ability of cisplatin to damage the nuclear DNA of immature oocytes [12, 29, 32], in this study we examined the short- and long-term impacts of cisplatin on mitochondria.

Previous studies have suggested that mitochondrial distribution is an important marker of the ability of an oocyte undergo maturation and is essential for ATP delivery [33, 34]. Thus, we employed MitoTracker Green, a fluorescent dye that localises with mitochondria, regardless of mitochondrial membrane potential, to monitor

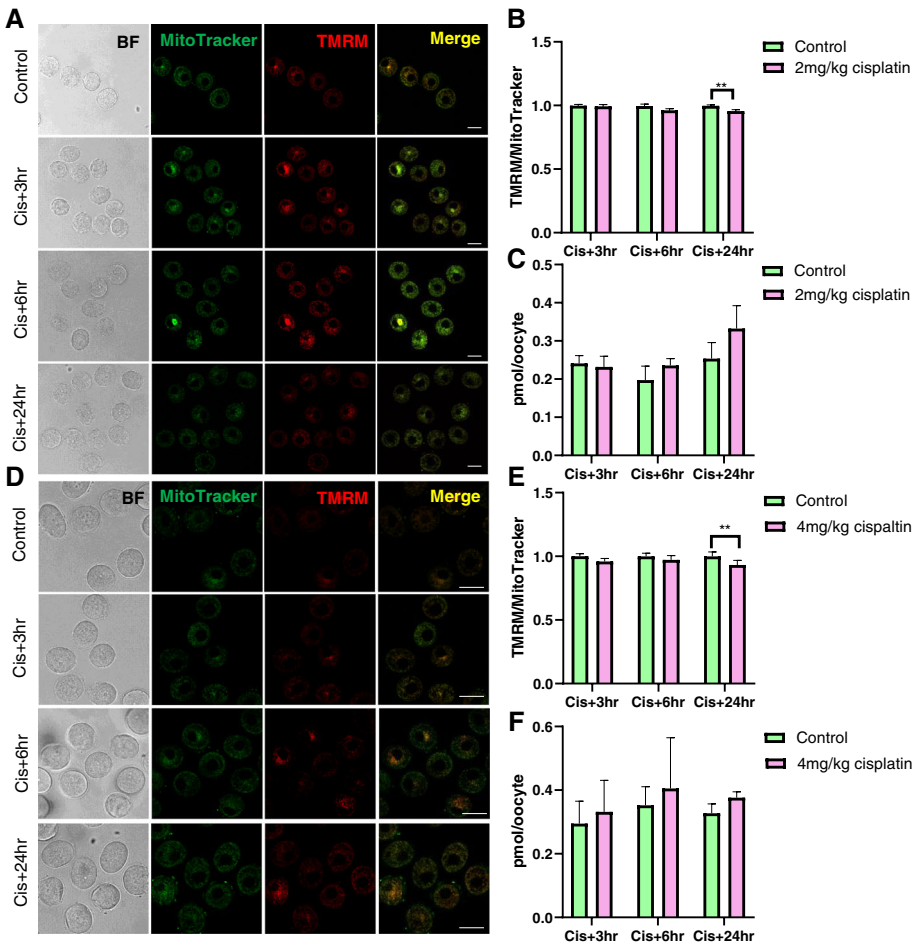

Fig. 3 Membrane potential of mitochondria in growing immature oocytes from saline and cisplatin (2 and 4 mg/kg) treated mice. Growing oocytes were isolated from saline treated control mice, or 3, 6 and 24 h after cisplatin and mitochondrial membrane potential was assessed using TMRM. **a** Representative confocal images of growing oocytes from saline and 2 mg/kg treated cisplatin mice at 3, 6 and 24 h after treatment. Scale bar = 50 μm. **b** Relative TMRM/MitoTracker ratio in growing oocytes at 3 ($n = 35/35$), 6 ($n = 31/33$) and 24 ($n = 37/39$) hours after 2 mg/kg cisplatin. **c** ATP content in growing oocytes 3 ($n = 4/4$), 6 ($n = 3/3$) and 24 ($n = 3/3$) hours after 2 mg/kg cisplatin. **d** Representative confocal images of growing oocytes from saline and 4 mg/kg treated cisplatin mice at 3, 6 and 24 h after treatment. Scale bar = 50 μm. **e** Relative TMRM/MitoTracker ratio in growing oocytes at 3 ($n = 38/41$), 6 ($n = 37/41$) and 24 ($n = 50/44$) hours after 4 mg/kg cisplatin. **f** ATP content in growing oocytes 3 ($n = 5/5$), 6 ($n = 5/5$) and 24 ($n = 5/4$) hours after 4 mg/kg cisplatin. $^{**}p$-value < 0.01

mitochondrial distribution in immature oocytes after treatment with saline or cisplatin. Consistent with other reports [35], we found mitochondria to be distributed throughout the cytoplasm in small immature oocytes from control mice. Similar distributions were observed 3 and 6 h after cisplatin treatment. However, mitochondria were present in only a small part of the cytoplasm of some oocytes at 24 h after 4 mg/kg cisplatin. Interestingly, those oocytes with abnormal mitochondrial distribution also displayed rough edges, suggesting that they were undergoing apoptosis [36, 37]. Indeed, the induction of apoptosis in immature oocytes has been previously shown to occur in oocytes from primordial follicles within 24 h of cisplatin exposure [12]. Cisplatin treatment did not alter mitochondrial distribution in growing oocytes, suggesting that the response to cisplatin is stage dependent, with the impacts more pronounced on oocytes from primordial follicles. Moreover, both homogeneous and aggregated mitochondria were observed in the cohort of growing oocytes, which may represent different stages of development, with aggregated mitochondria found in large preantral follicles [33].

Cisplatin has been reported to have differing effects on mitochondrial mass. In skeletal muscle cells, cisplatin disrupts mitochondrial homeostasis, leading to a reduction of mitochondrial number and the activation of apoptosis [38]. In contrast, an increase of mitochondrial mass and mitochondrial fission protein have been observed after cisplatin treatment in other cells [39, 40]. Ovarian cancer cells, for example, respond to cisplatin

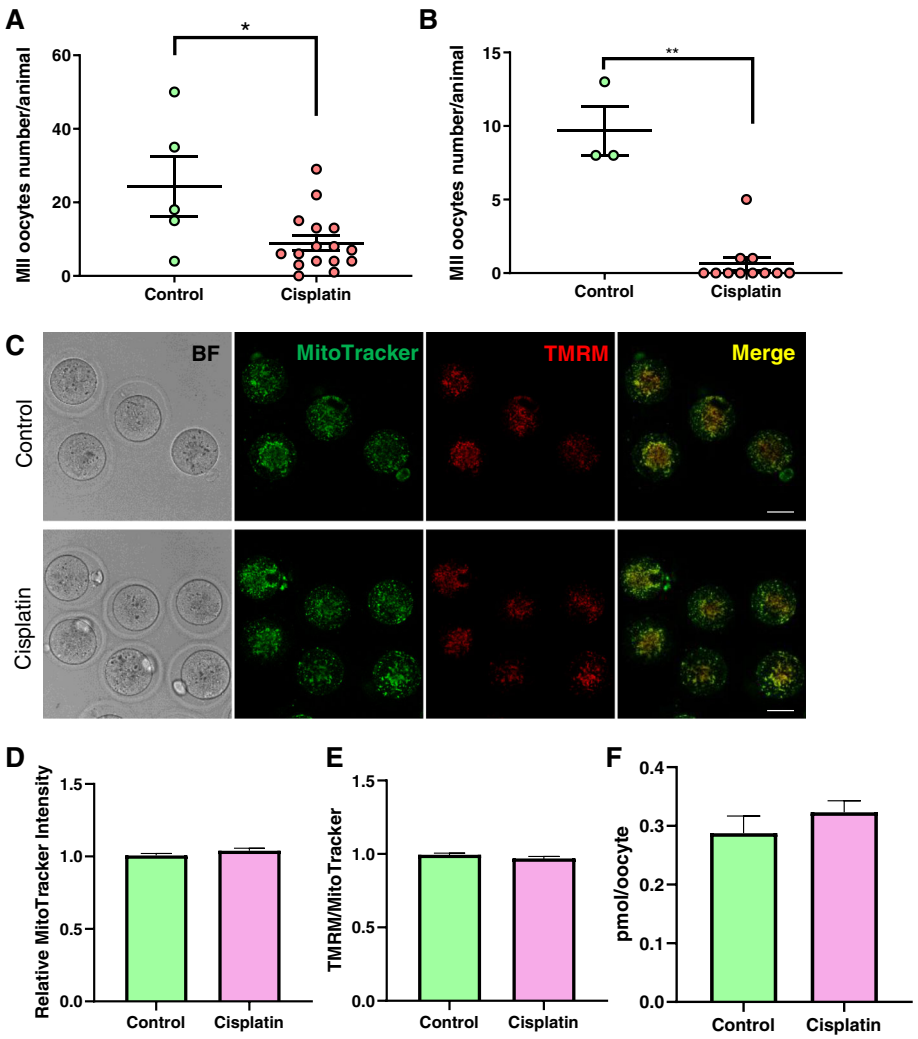

Fig. 4 Mitochondria in mature oocytes (2 mg/kg cisplatin injected at PN10). Mice were untreated (controls) or 2 mg/kg cisplatin at PN9-11 and then allowed to develop to sexual maturity before being super ovulated. **a** Number of oocytes harvested from 2 mg/kg cisplatin treated mice. Each dot represents one animal, animal number $n = 5/16$ control and 2 mg/kg cisplatin treated groups respectively. **b** Number of oocytes harvested from 4 mg/kg cisplatin treated mice. Each dot represents one animal, $N = 3/11$ for control and 4 mg/kg cisplatin treated groups, respectively. **c** Representative confocal images of mature oocytes (BF; bright field) stained with Mitotracker and TMRM. Scale bar = 50 μm. **d** Relative MitoTracker intensity of mature oocytes from control mice ($n = 35$ oocytes) and cisplatin treated mice ($n = 37$ oocytes). **e** TMRM to MitoTracker ratio of mature oocytes from control mice ($n = 35$ oocytes) and cisplatin treated mice ($n = 37$ oocytes). **f** ATP content in mature oocytes. $N = 3/3$ from control and cisplatin treated groups respectively. *t*-test, **p*-value < 0.05, ***p*-value < 0.01

by increasing the cellular amount of mitochondria and this response is associated with increased mtROS and increased likelihood of cell death [19]. In our study, cisplatin treatment did not significantly alter MitoTracker fluorescent intensity in small or growing oocytes at 3, 6 or 24 h, suggesting mitochondrial mass was not affected at these early time points. However, this possibility could be further investigated by analysing the expression of mitochondrial fission related genes or proteins.

Mitochondrial membrane potential is reflective of mitochondrial activity and is crucial for ATP generation [27]. Depleted mitochondrial membrane potential impedes oocyte maturation and embryo development in pig and mouse oocytes [26, 27]. We used TMRM, a low toxicity, cell-permeant dye that accumulates in active mitochondria, to determine if cisplatin impaired mitochondrial membrane potential in immature oocytes. Within 24 h of exposure to 2 mg/kg or 4 mg/kg cisplatin, oocytes showed a small reduction in membrane potential, indicating that there may be at least a partial loss of function. Furthermore, in the 4 mg/kg cisplatin treated group, 60 % of the small immature oocytes lost mitochondrial membrane potential and displayed abnormal morphology, indicating the activation of apoptosis

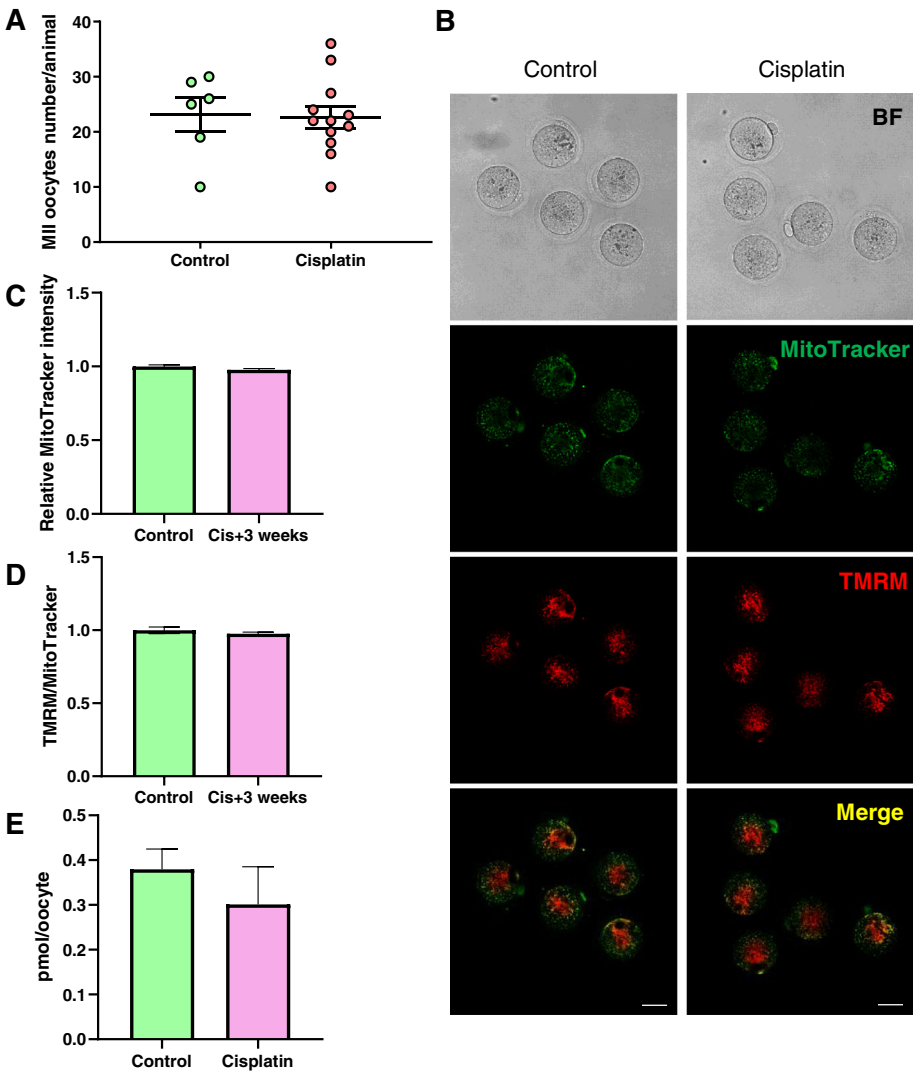

Fig. 5 Mitochondria in mature oocytes (4 mg/kg cisplatin injected at PN50). Mice were treated with saline (controls) or 4 mg/kg cisplatin at PN50 and then super ovulated 3 weeks later. **a** Number of oocytes harvested from mice treated at PN50. Each dot represents one animal, $N = 6/12$ for control and cisplatin groups, respectively. **b** Representative confocal images of mature oocytes stained with Mitotracker and TMRM. Scale bar = 50 μm. **c** Relative MitoTracker intensity of mature oocytes from untreated control mice ($n = 29$ oocytes) and 4 mg/kg cisplatin treated mice ($n = 59$ oocytes). **d** TMRM to MitoTracker ratio in mature oocytes from untreated control mice ($n = 29$ oocytes) and 4 mg/kg cisplatin treated mice ($n = 59$ oocytes). **e** ATP content in mature oocytes. $N = 3/3$ from control and cisplatin treated groups, respectively

[36, 41]. Thus, whilst lower doses of cisplatin may impair mitochondrial activity, higher doses of cisplatin trigger cell death via apoptosis.

Like small immature oocytes, growing immature oocytes showed a slight reduction in mitochondrial membrane potential at 24 h in 2 mg/kg and 4 mg/kg cisplatin injected groups. However, we did not observe any oocytes with no TMRM staining, suggesting that all growing oocytes were still viable. This finding is in accordance with a previous study demonstrating small immature oocytes from dormant follicles are more sensitive to cisplatin than growing immature oocytes from growing follicles [42]. Notably, despite the decrease in mitochondrial membrane potential at 24 h after cisplatin treatment, indicating impaired mitochondrial function, ATP content did not change. Interestingly, oocytes are capable of obtaining ATP from granulosa cells via gap junctions [43]. Thus, it is possible that oocyte are 'charged' by granulosa cells when their mitochondria fail to generate sufficient ATP to support cell growth. Alternatively, reductions in ATP content may not be evident at this relatively early point and may take longer to become apparent.

To examine the persistent effects of cisplatin on mitochondria, cisplatin injected PN10 mice were held for 5 weeks and then super ovulated to harvest mature MII

oocytes. Even though we collected a small number of mature oocytes from 2 mg/kg cisplatin treated mice, we failed to collect mature oocytes from 4 mg/kg cisplatin treated mice. This finding suggested that cisplatin depleted the ovarian reserve in a dose dependent manner. Interestingly, however, although adult mice treated with a similar dose of cisplatin (i.e. 5 mg/kg) have reduced number of follicles, they were able to bear litters from natural mating, suggesting oocytes were capable of maturation and ovulation [29]. This discrepancy may be related to age-associated differences in oocyte sensitivity to cisplatin (i.e. the PN10 mice were more sensitive to cisplatin than adults, and the ovarian reserve was exhausted). It is also possible that cisplatin impairs the ability of mice to respond to exogenous hormonal stimulation. Importantly, in those mature oocytes collected after 2 mg/kg cisplatin treatment, mitochondrial localisation, mass, membrane potential and ATP content were similar to controls. Thus, our results suggested that cisplatin treated mice contained healthy mitochondria in mature oocytes. In additional, the oocytes from adult mice treated with the higher 4 mg/kg dose of cisplatin had normal mitochondrial parameters and this observation is supported by reports of cisplatin treated mice producing apparently healthy offspring [29]. Additional analyses that could be undertaken in the future to further verify mitochondria health in this model include an evaluation of cytochrome C content or cytochrome C oxidase activity.

One limitation of our study is that a single dose regimen was used, whereas clinically, patients receive multiple doses. Whist the model we used is best for analysing the immediate impacts of cisplatin on mitochondria (i.e. in the hours following exposure), it is possible that repeated doses of cisplatin could result in cumulative effects that might persist in the long term and compromise oocyte survival and quality. Therefore, future studies could employ a lower dose of cisplatin (> 2 mg/kg) that would permit daily treatments, whilst allowing for sufficient numbers of oocytes to survive for analysis after the last dose (with the caveat that low doses might also not be reflective of clinical regimens).

Conclusions

The present study demonstrated that mitochondrial dysfunction may be involved in cisplatin cytotoxicity in immature oocytes from pre-pubertal mice. Additional studies are required to further address this issue, such as an evaluation of mtDNA copy number, mitochondrial gene expression, and mtROS production. Importantly, mature oocytes harvested from cisplatin treated prepubertal mice and adult mice contained healthy mitochondria. Our findings highlight the need for a better understanding of the mechanisms underlying cisplatin induced oocyte depletion, in order to better preserve fertility in female cancer patients treated with cisplatin.

Acknowledgements

This work was made possible through Victorian State Government Operational Infrastructure Support and Australian Government NHMRC IRIISS. The authors would like to acknowledge the technical support of the Monash Animal Research Platform, Monash Histology Platform and Monash Micro Imaging facility, Monash University.

Authors' contributions

QW performed experiments. QW, KH analysed data, designed the study and wrote the manuscript. The author(s) read and approved the final manuscript.

Authors' information

Not applicable.

Funding

Australian Research Council (KJH #FT190100265).

Availability of data and materials

The datasets used and/or analysed during the current study are available from the corresponding author on reasonable request.

Declarations

Ethics approval and consent to participate

All animal procedures and experiments were performed in accordance with the NHMRC Australian Code of Practice for the Care and Use of Animals and approved by the Monash Animal Research Platform Animal Ethics Committee.

Consent for publication

Not applicable.

Competing interests

The authors declare that they have no competing interests.

Received: 2 December 2020 Accepted: 28 April 2021
Published online: 10 May 2021

References

1. Findlay JK, Hutt KJ, Hickey M, Anderson RA. How is the number of primordial follicles in the ovarian reserve established? Biol Reprod. 2015; 93(5):111.
2. Hsueh AJ, Billig H, Tsafriri A. Ovarian follicle atresia: a hormonally controlled apoptotic process. Endocr Rev. 1994;15(6):707–24.
3. Kerr JB, Myers M, Anderson RA. The dynamics of the primordial follicle reserve. Reproduction. 2013;146(6):R205-15.
4. Faddy MJ, Gosden RG, Gougeon A, Richardson SJ, Nelson JF. Accelerated disappearance of ovarian follicles in mid-life: implications for forecasting menopause. Hum Reprod. 1992;7(10):1342–6.
5. McGee EA, Hsueh AJ. Initial and cyclic recruitment of ovarian follicles. Endocr Rev. 2000;21(2):200–14.
6. Sarma UC, Findlay JK, Hutt KJ. Oocytes from stem cells. Best Pract Res Clin Obstet Gynaecol. 2019;55:14–22.
7. Somigliana E, Terenziani M, Filippi F, Bergamini A, Martinelli F, Mangili G, et al. Chemotherapy-related damage to ovarian reserve in childhood cancer survivors: interpreting the evidence. J Assist Reprod Genet. 2019;36(2):341–8.
8. Ebrahimi M, Akbari Asbagh F. Pathogenesis and causes of premature ovarian failure: an update. Int J Fertil Steril. 2011;5(2):54–65.
9. Kerr JB, Brogan L, Myers M, Hutt KJ, Mladenovska T, Ricardo S, et al. The primordial follicle reserve is not renewed after chemical or gamma-irradiation mediated depletion. Reproduction. 2012;143(4):469–76.
10. Dasari S, Tchounwou PB. Cisplatin in cancer therapy: molecular mechanisms of action. Eur J Pharmacol. 2014;740:364–78.
11. Kerr JB, Hutt KJ, Cook M, Speed TP, Strasser A, Findlay JK, et al. Cisplatin-induced primordial follicle oocyte killing and loss of fertility are not prevented by imatinib. Nat Med. 2012;18(8):1170–2. author reply 2–4.

12. Nguyen QN, Zerafa N, Liew SH, Findlay JK, Hickey M, Hutt KJ. Cisplatin- and cyclophosphamide-induced primordial follicle depletion is caused by direct damage to oocytes. Mol Hum Reprod. 2019;25(8):433–44.
13. Cepeda V, Fuertes MA, Castilla J, Alonso C, Quevedo C, Perez JM. Biochemical mechanisms of cisplatin cytotoxicity. Anticancer Agents Med Chem. 2007;7(1):3–18.
14. Marullo R, Werner E, Degtyareva N, Moore B, Altavilla G, Ramalingam SS, et al. Cisplatin induces a mitochondrial-ROS response that contributes to cytotoxicity depending on mitochondrial redox status and bioenergetic functions. PLoS One. 2013;8(11):e81162.
15. Wisnovsky SP, Wilson JJ, Radford RJ, Pereira MP, Chan MR, Laposa RR, et al. Targeting mitochondrial DNA with a platinum-based anticancer agent. Chem Biol. 2013;20(11):1323–8.
16. Meirow D, Biederman H, Anderson RA, Wallace WH. Toxicity of chemotherapy and radiation on female reproduction. Clin Obstet Gynecol. 2010;53(4):727–39.
17. Yang Z, Schumaker LM, Egorin MJ, Zuhowski EG, Guo Z, Cullen KJ. Cisplatin preferentially binds mitochondrial DNA and voltage-dependent anion channel protein in the mitochondrial membrane of head and neck squamous cell carcinoma: possible role in apoptosis. Clin Cancer Res. 2006; 12(19):5817–25.
18. Nunnari J, Suomalainen A. Mitochondria: in sickness and in health. Cell. 2012;148(6):1145–59.
19. Kleih M, Bopple K, Dong M, Gaissler A, Heine S, Olayioye MA, et al. Direct impact of cisplatin on mitochondria induces ROS production that dictates cell fate of ovarian cancer cells. Cell Death Dis. 2019;10(11):851.
20. Gutekunst M, Oren M, Weilbacher A, Dengler MA, Markwardt C, Thomale J, et al. p53 hypersensitivity is the predominant mechanism of the unique responsiveness of testicular germ cell tumor (TGCT) cells to cisplatin. PLoS One. 2011;6(4):e19198.
21. Berndtsson M, Hagg M, Panaretakis T, Havelka AM, Shoshan MC, Linder S. Acute apoptosis by cisplatin requires induction of reactive oxygen species but is not associated with damage to nuclear DNA. Int J Cancer. 2007; 120(1):175–80.
22. Sirey TM, Ponting CP. Insights into the post-transcriptional regulation of the mitochondrial electron transport chain. Biochem Soc Trans. 2016; 44(5):1491–8.
23. Babayev E, Seli E. Oocyte mitochondrial function and reproduction. Curr Opin Obstet Gynecol. 2015;27(3):175–81.
24. Monnot S, Samuels DC, Hesters L, Frydman N, Gigarel N, Burlet P, et al. Mutation dependance of the mitochondrial DNA copy number in the first stages of human embryogenesis. Hum Mol Genet. 2013;22(9):1867–72.
25. May-Panloup P, Boucret L, Chao de la Barca JM, Desquiret-Dumas V, Ferre-L'Hotellier V, Moriniere C, et al. Ovarian ageing: the role of mitochondria in oocytes and follicles. Hum Reprod Update. 2016;22(6):725–43.
26. Ge H, Tollner TL, Hu Z, Dai M, Li X, Guan H, et al. The importance of mitochondrial metabolic activity and mitochondrial DNA replication during oocyte maturation in vitro on oocyte quality and subsequent embryo developmental competence. Mol Reprod Dev. 2012;79(6):392–401.
27. Lee SK, Zhao MH, Kwon JW, Li YH, Lin ZL, Jin YX, et al. The association of mitochondrial potential and copy number with pig oocyte maturation and developmental potential. J Reprod Dev. 2014;60(2):128–35.
28. Wang Q, Stringer JM, Liu J, Hutt KJ. Evaluation of mitochondria in oocytes following gamma-irradiation. Sci Rep. 2019;9(1):19941.
29. Nguyen QN, Zerafa N, Liew SH, Morgan FH, Strasser A, Scott CL, et al. Loss of PUMA protects the ovarian reserve during DNA-damaging chemotherapy and preserves fertility. Cell Death Dis. 2018;9(6):618.
30. Sklar C. Maintenance of ovarian function and risk of premature menopause related to cancer treatment. J Natl Cancer Inst Monogr. 2005;2005(34):25–7.
31. Ruddy KJ, Gelber SI, Tamimi RM, Ginsburg ES, Schapira L, Come SE, et al. Prospective study of fertility concerns and preservation strategies in young women with breast cancer. J Clin Oncol. 2014;32(11):1151–6.
32. Kim SY, Cordeiro MH, Serna VA, Ebbert K, Butler LM, Sinha S, et al. Rescue of platinum-damaged oocytes from programmed cell death through inactivation of the p53 family signaling network. Cell Death Differ. 2013; 20(8):987–97.
33. Wang LY, Wang DH, Zou XY, Xu CM. Mitochondrial functions on oocytes and preimplantation embryos. J Zhejiang Univ Sci B. 2009;10(7):483–92.
34. Frazier AE, Kiu C, Stojanovski D, Hoogenraad NJ, Ryan MT. Mitochondrial morphology and distribution in mammalian cells. Biol Chem. 2006;387(12): 1551–8.
35. Pepling ME, Wilhelm JE, O'Hara AL, Gephardt GW, Spradling AC. Mouse oocytes within germ cell cysts and primordial follicles contain a Balbiani body. Proc Natl Acad Sci U S A. 2007;104(1):187–92.
36. Hacker G. The morphology of apoptosis. Cell Tissue Res. 2000;301(1):5–17.
37. Chaube SK, Prasad PV, Thakur SC, Shrivastav TG. Hydrogen peroxide modulates meiotic cell cycle and induces morphological features characteristic of apoptosis in rat oocytes cultured in vitro. Apoptosis. 2005; 10(4):863–74.
38. Sirago G, Conte E, Fracasso F, Cormio A, Fehrentz JA, Martinez J, et al. Growth hormone secretagogues hexarelin and JMV2894 protect skeletal muscle from mitochondrial damages in a rat model of cisplatin-induced cachexia. Sci Rep. 2017;7(1):13017.
39. Sheng J, Shen L, Sun L, Zhang X, Cui R, Wang L. Inhibition of PI3K/mTOR increased the sensitivity of hepatocellular carcinoma cells to cisplatin via interference with mitochondrial-lysosomal crosstalk. Cell Prolif. 2019;52(3): e12609.
40. Pons DG, Torrens-Mas M, Nadal-Serrano M, Sastre-Serra J, Roca P, Oliver J. The presence of estrogen receptor beta modulates the response of breast cancer cells to therapeutic agents. Int J Biochem Cell Biol. 2015;66:85–94.
41. Ly JD, Grubb DR, Lawen A. The mitochondrial membrane potential (deltapsi(m)) in apoptosis; an update. Apoptosis. 2003;8(2):115–28.
42. Rossi V, Lispi M, Longobardi S, Mattei M, Di Rella F, Salustri A, et al. LH prevents cisplatin-induced apoptosis in oocytes and preserves female fertility in mouse. Cell Death Differ. 2017;24(1):72–82.
43. Dalton CM, Szabadkai G, Carroll J. Measurement of ATP in single oocytes: impact of maturation and cumulus cells on levels and consumption. J Cell Physiol. 2014;229(3):353–61.

Publisher's Note

Chapter 4. Investigation of the potential of MitoQ to protect against ovarian damage caused by ionising radiation

4.1 Introduction

Reactive oxygen species (ROS) are highly reactive molecules that must be well balanced in the cell in order for optimal function to occur [166]. ROS function as important intracellular signaling molecules, and moderate levels are beneficial for the regulation of cell proliferation and cell death [194]. However, excessive ROS levels can lead to DNA, lipid and protein damage (discussed in Chapter 1) and are associated with cancer, inflammatory diseases, neurodegeneration and other pathological conditions [145, 195]. The primary site of ROS generation is the electron transport chain (ETC, also called the respiratory chain), located at the inner membrane of mitochondria [144]. The ETC comprises five complexes that are encoded by nuclear and mitochondrial DNA [196]. Notably, insults to DNA or mitochondria can result in elevated ROS production and oxidative damage within the cell, which if severe enough, can compromise cellular function or trigger cell death.

Although there are a variety of complex and efficient mechanisms existing in cells to protect against the damaging effects of ROS production [160], the excessive ROS caused by cancer treatments, including radiotherapy and some chemotherapies, cannot be effectively neutralised, eventually resulting in loss of cell function and/or cell death [197, 198] [140]. Over half of all cancers are treated with radiotherapy [199]. Exposure to penetrating radiation, like γ-radiation, increases extracellular ROS levels through direct water radiolysis to form superoxide anion ($O2^{-}$), hydroxyl radicals (OH^{-}) and hydrogen peroxide (H_2O_2) [140]. It also compromises mitochondrial membrane integrity, which stimulates ROS production [200], and further increases the generation of endogenous ROS by affecting mitochondrial OXPHOS[160]. The accumulation of ROS in turn attacks mtDNA, reduces the efficiency of electron transport chain and produces more ROS [140, 160]. In particular, γ-radiation is well known to directly induce large scale deletions in human mitochondrial DNA (also called common deletions), including genes encoding ETC complex proteins that are essential to maintain normal mitochondrial functions [201, 202]. Since γ-radiation can damage mitochondria and elevate intracellular ROS levels, protecting mitochondria by supplying exogenous antioxidants might be a novel strategy to avoid the off-target toxicity of cancer treatments, including the damaging effects of these treatments on the ovary.

Coenzyme Q10 (CoQ10 or Ubiquinone) is a co-factor in the electron transport chain that plays vital roles in ATP generation [177]. It is also a powerful free radical scavenger and antioxidant, acting to reduce oxidative damage to proteins, lipids, and DNA. A wide range of CoQ10 derivatives have been developed by replacing the hydrophobic isoprenoid chain with a hydrosoluble motif in order to preferentially deliver CoQ to mitochondria [177]. Among them, MitoQ (mitoquinone mesylate: (10-(4,5-Dimethoxy-2-methyl-3,6-dioxo-1,4-cyclohexadien-1-yl)decyl)(triphenyl)phosphonium methanesulfonate) is the most efficient antioxidant that specifically accumulates in the inner membrane of mitochondria [181]. MitoQ is synthesised by linking the ubiquinone to the lipophilic triphenylphosphonium cation (TPP^+) via a carbon alkyl chain [177]. The ability of MitoQ to penetrate the phospholipid bilayer increases with the extension of the carbon bridge [178]. To date, MitoQ (which contains a 10-carbon alkyl chain) has been commercially produced and widely used in different experimental situations [203].

MitoQ is a safe drug that can be administrated by oral uptake, intravenous (iv) injection and intraperitoneal (ip) injection [178, 190]. No toxicity was observed in mice after supplementation of 500 μM in drinking water for 28 weeks or 20 mg/kg iv injection or 5mg/kg ip injection twice a week for 12 weeks [179, 190]. In mice, MitoQ exerted excellent ROS scavenging ability in a variety of disease models associated with mitochondrial damage, such as diabetic kidney disease and cardiovascular diseases [187, 190]. In human trials, MitoQ has been proven to be a powerful protective antioxidant during chronic hepatitis C virus infection, which is characterised by elevated ROS levels and mitochondrial damage [190]. Of note, the findings from Chapter 2 and 3 indicated that mitochondrial damage might be involved in cancer treatment induced depletion of the ovarian reserve. Thus, it is possible that supplementation of MitoQ during cytotoxic cancer treatment can preserve the ovarian reserve by protecting mitochondria and eliminating cellular oxidative damage in mice.

Thus, this chapter aimed to address the following two related hypotheses:

1. MitoQ can reduce follicle depletion caused by radiation exposure.
2. Radiation induces oxidative damage to lipids, proteins and nucleic acids to cells within the ovary, and this damage can be mitigated by MitoQ treatment.

To determine the potential for MitoQ to protect the ovarian reserve against cancer treatment, mice received MitoQ ip for 3 days before exposure to 0.45Gy whole body γ-irradiation. The number of follicles comprising the ovarian reserve was determined 3 hours or 5 days later. Since mitochondria are the main source of ROS, and excessive ROS results in oxidative stress, the role of MitoQ in protecting DNA, lipid, and protein from peroxidative damage was also evaluated at both time points.

4.2 Materials and Methods

4.2.1 Mice and treatments

Two-month-old female C57BL/6 mice were used in this study. Mice were housed in a high-barrier, light, and temperature-controlled facility (Monash University ARL) with free access to food and water. All animal experiments and procedures were performed in accordance with the NHMRC Australian Code of Practice for the Care and Use of Animals and approved by the Monash Animal Research Platform Animal Ethics Committee.

Study 1: Pilot. For an initial tolerance pilot study, 12 mice were allocated into 2 groups; 1) saline or 2) 5mg/kg MitoQ. MitoQ (5mg/kg), or an equivalent volume of saline (1% DMSO), was administered to mice by intraperitoneal injection each day for 4 days and mice were then sacrificed 5 days later. For the second pilot study, 8 mice were allocated into 2 groups; 1) saline or 2) 2mg/kg MitoQ. The treatment protocol was as the same as the first pilot study.

Study 2: Irradiation. Twenty-four mice were randomly allocated into to the following 4 treatments groups (N=6/group): 1) saline + no irradiation, 2) saline + 0.45Gy whole body γ-irradiation, 3) 2 mg/kg MitoQ + no irradiation and 4) 2 mg/kg MitoQ + 0.45Gy whole body γ-irradiation. MitoQ (2mg/kg), or an equivalent volume of saline (1% DMSO), was administered to mice by intraperitoneal injection each day for 3 days before irradiation, with the third dose given 2 hours before irradiation. Three mice from each group were sacrificed 3 hours after irradiation and the other three mice from each group were sacrificed 5 days after irradiation. Mice in the 5-day time point received a fourth dose of 2mg/kg MitoQ or saline 20 hours after irradiation (Fig. S1). Both ovaries were harvested at each time point and one

was fixed in Bouins' solution, the other one was fixed in formalin at 4 ℃ overnight. After fixation, ovaries were transferred into 70% ethanol for future use.

The two time points that represented the induction and completion of apoptosis were chosen based on the known knowledge that mitochondrial dysfunction and DNA double strain breaks occurred 3 hours after irradiation and no mitochondrial or DNA damage were detected at later time point [3, 51, 204].

4.2.2 Chemicals

MitoQ was a gift from MitoQ company (New Zealand). Pure MitoQ powder was diluted in Dimethyl sulfoxide (DMSO) (D2650, sigma-aldrich) to a final concentration of 30mg/ml. MitoQ (1 in 100 diluted in saline to keep DMSO concentration at 1%) was prepared daily before use. Whole body γ-irradiation at 0.45Gy was performed by technicians from Monash Animal Research Platform in a Gammacell40 Exactor Irradiator.

4.2.2 Histology

Ovaries fixed in Bouin's solution were embedded in glycol-methacrylate resin and serially sectioned at 20 μm and every third section were collected by technicians at Monash Histology Platform. The resin sections were stained with periodic acid-Schiff (PAS) and counterstained with heamatoxylin. Formalin fixed ovaries were embedded in paraffin and serially sectioned at 5 μm and every section was collected.

4.2.3 Quantification of primordial and primary follicles

Direct follicle counts was used to access primordial and primary follicles in Bouin's fixed resin embedded sections using methods described in detail in [205, 206]. The characteristics of each follicular stage were described in Chapter 1.

For stereology, the Olympus BX50 microscope (Tokyo, Japan) equipped with a 100x oil immersion objective and an Autoscan stage (Autoscan Systems Pty Ltd, Melbourne, VIC, Australia) controlled by the StereoInvestigator stereological system (Version 11.06.02, MBF Bioscience 2015, MicroBrightField, Inc., Williston, VT, USA). Follicles with a visible nucleus were counted. Total follicle numbers were

obtained by applying the formula described in [26] to the raw counts. For direct follicle counts, the Olympus BX51 dotslide scanner (Tokyo, Japan) at Monash Micro Imaging (MMI) (Clayton, Australia) was used. Entire sections were captured using a 20x objective and follicles were counted in digitised images using ImageJ (NIH) open-source software. Total follicle numbers were determined by multiplying the raw counts by 3 (to account for every 3rd section being counted).

4.2.4 Quantification of secondary follicles, antral follicles, atretic follicles and corpora lutea

Secondary, antral, atretic follicles and corpora lutea were counted under the light microscope as previously described [205, 206]. The characteristics of each follicular stage were described in Chapter 1. Every 9th section was evaluated to quantify the secondary and antral follicles. Follicles with an obvious nucleus were counted. Secondary and antral follicles with more than 10% pyknotic nuclei in their granulosa cells were defined as atretic follicles. The total follicle number was determined by multiplying the raw counts by 9. The number of corpora lutea was determined by tracing each section to avoid double counting, as corpora lutea are large and span several slides.

4.2.5 Immunofluorescence

Immunofluorescence was performed on formalin fixed ovarian sections. Three sections were chosen to quantify the DNA oxidative damage marker, lipid oxidative damage marker and protein oxidative damage marker. The sections were dewaxed in histolene and rehydrated, then subjected to heat-mediated antigen retrieval in sodium citrate buffer (pH 6.0). After cooling down to room temperature, sections were blocked with 10% goat serum (Sigma Aldrich, G9023) in Tris-sodium chloride (TN) buffer in 3% Bovine Serum Albumin (BSA) (Sigma Aldrich, A9418). Following incubation with blocking buffer at room temperature for 1 hour, sections were then incubated with primary antibodies at 4 ℃ overnight. All the primary antibodies were diluted with 10% goat serum in TN buffer. Anti-DNA/RNA damage (1:100, Abcam, ab62623), anti-Nitro tyrosine (1:50, Abcam, ab7048) and anti-4 hydroxynonenal (1:500, Abcam, ab48506) antibodies were used to detect DNA/RNA, protein, and lipid oxidative damage, respectively. After incubation, sections were washed with Tris-NaCl-Tween (TNT) buffer 3 times and then incubated with goat anti mouse 568 secondary antibody at room temperature for

1 hour. The secondary antibody was diluted 1:500 in TN buffer. After secondary antibody incubation, sections were washed with TNT buffer 3 times and then incubated with DAPI (ThermoFisher Scientific, MA, USA, P36931) at room temperature for 10 minutes. Slides were mounted with FluorSave Reagent (345789, EMD Millipore Corp, Burlington, MA, USA) and visualised with the laser-scanning confocal microscope (SP8, Leica) or the fluorescent microscope (Zeiss Axio Imager, Germany). Every follicle in each section was analysed for positive or negative staining. The percentage of follicles for each ovary exhibiting positive staining was then calculated.

4.2.6 Statistical analysis

Data were analysed using GraphPad Prism version 9 (GraphPad Software, CA, USA) and expressed as mean ± SEM. Data were analysed using one-way ANOVA followed by Tukey's multiple comparison test. Pairwise comparisons were analysed using Students t-test. Differences were considered significant when $p<0.05$.

4.3 Results

4.3.1 5 mg/kg MitoQ supplementation caused swollen intestines and suppressed ovulation, but these impacts were not observed when 2 mg/kg was used

A previous study demonstrated that 5mg/kg MitoQ administered via intraperitoneal injection twice a week for 12 weeks protected mitochondria in a mouse model of diabetic kidney disease and no adverse effects were noted [190]. To test the tolerance of mice in our study to a similar MitoQ regimen, adult females were injected with saline or 5mg/kg MitoQ, via intraperitoneal injection, once a day for 4 days and ovaries were harvested 5 days later. Unexpectedly, of the 6 mice treated with MitoQ, 4 were found to have extremely swollen intestines at the study endpoint, whereas none of the saline injected mice (total animal number =6) displayed the same phenotype (Fig. 1A, B). No other gross abnormalities were observed. The reason for the effects of MitoQ on the intestine was not clear.

An analysis of the overall ovarian and follicular morphology in histological tissue sections revealed no obvious differences between groups (Fig. 1C). In addition, primordial, primary, secondary and antral follicle numbers were similar in saline and 5 mg/kg MitoQ treated groups (Fig. 1D). Notably, however,

corpora lutea numbers were significantly reduced in the ovary of 5 mg/kg MitoQ treated mice compared to controls, which could indicate the suppression of ovulation (Fig. 1E). Atretic secondary and antral follicle number showed an upwards trend in 5mg/kg MitoQ treated mice (saline 9 ± 3.674 vs. MitoQ 14.4 ± 4.589, $P>0.05$), but there was no statistically significant difference between groups (Fig. 1F).

To avoid the intestinal and ovulatory side-effects observed in animals treated with 5mg/kg MitoQ, the dose was decreased to 2mg/kg in the second pilot study. This reduced dose administrated by intraperitoneal injection had previously been shown to protect acute lung injury in rats [207]. Mice treated with 2mg/kg MitoQ exhibited normal intestines (data not shown) and ovarian morphology when compared to untreated mice (Fig. 2A). Notably, MitoQ supplementation had no impact on the number of healthy follicles (Fig. 2B), corpora lutea (Fig. 2C) or atretic follicles (Fig. 2D) compared to saline treated group. This observation indicated that 2mg/kg MitoQ did not produce the unwanted side effects of swollen intestines or reduced number of corpora lutea observed in the previous experiment with 5 mg/kg MitoQ. Therefore, 2 mg/kg MitoQ was used in the following experiments.

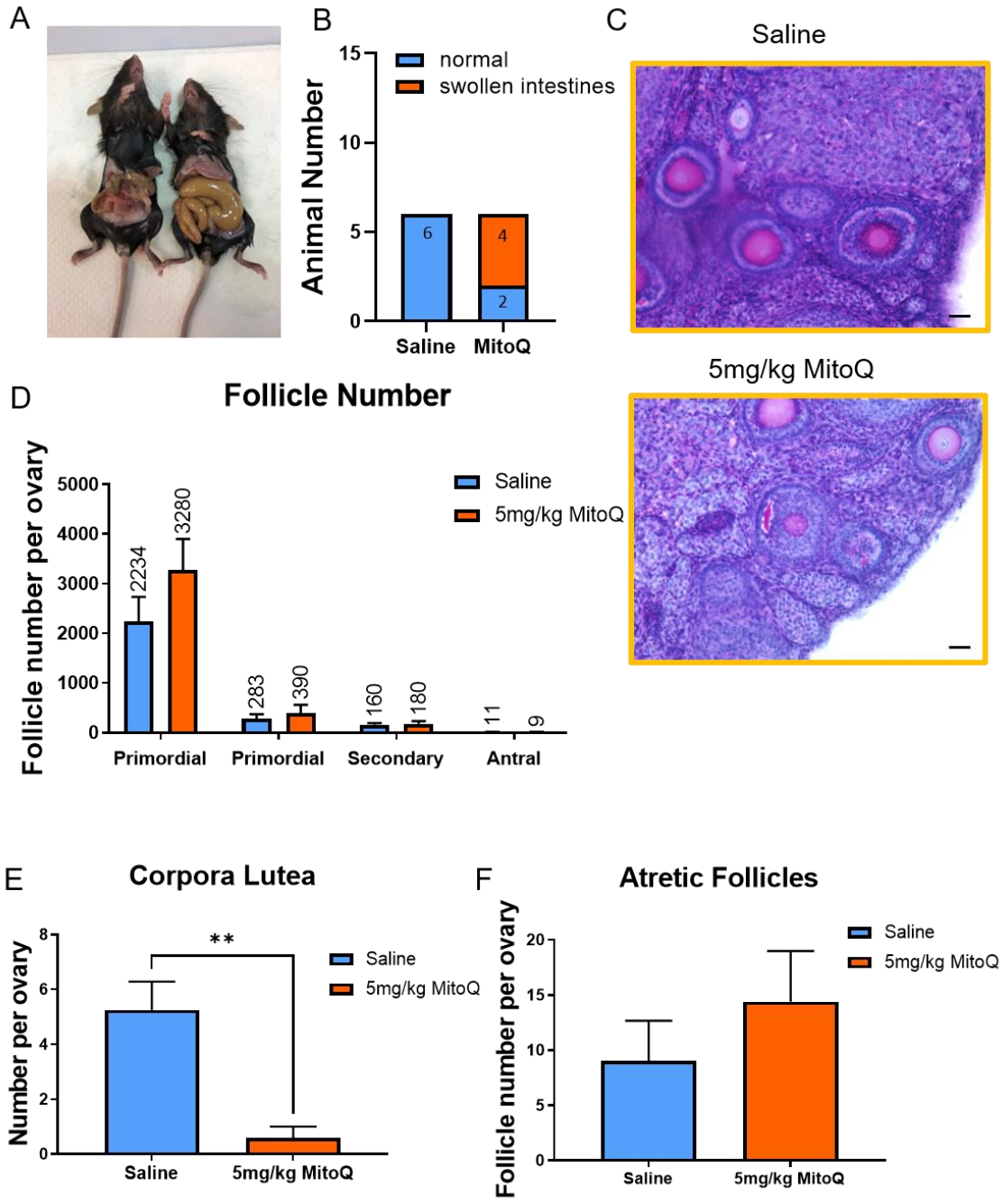

Figure 1. Effects of 5mg/kg/day MitoQ on the intestine and ovaries of mice. Mice were treated with 5mg/kg MitoQ for 4 days and ovaries were collected 5 days later (n=6/group). Saline (left) or 5mg/kg MitoQ (right) injected mice (A). Animal number with normal and swollen intestines (B). Representative ovarian histology (PAS stained) from mice received saline or 5mg/kg MitoQ injection, scale bar=50μm (C). The number of primordial, primary, secondary and antral follicles (D), corpora lutea (E) and atretic follicles (F) after 5mg/kg MitoQ injection, n=3-5 ovaries counted per group. Data are shown as mean ± s.e.m. Data for each follicle stage/structure were compared between groups using unpaired t-test, **p<0.01.

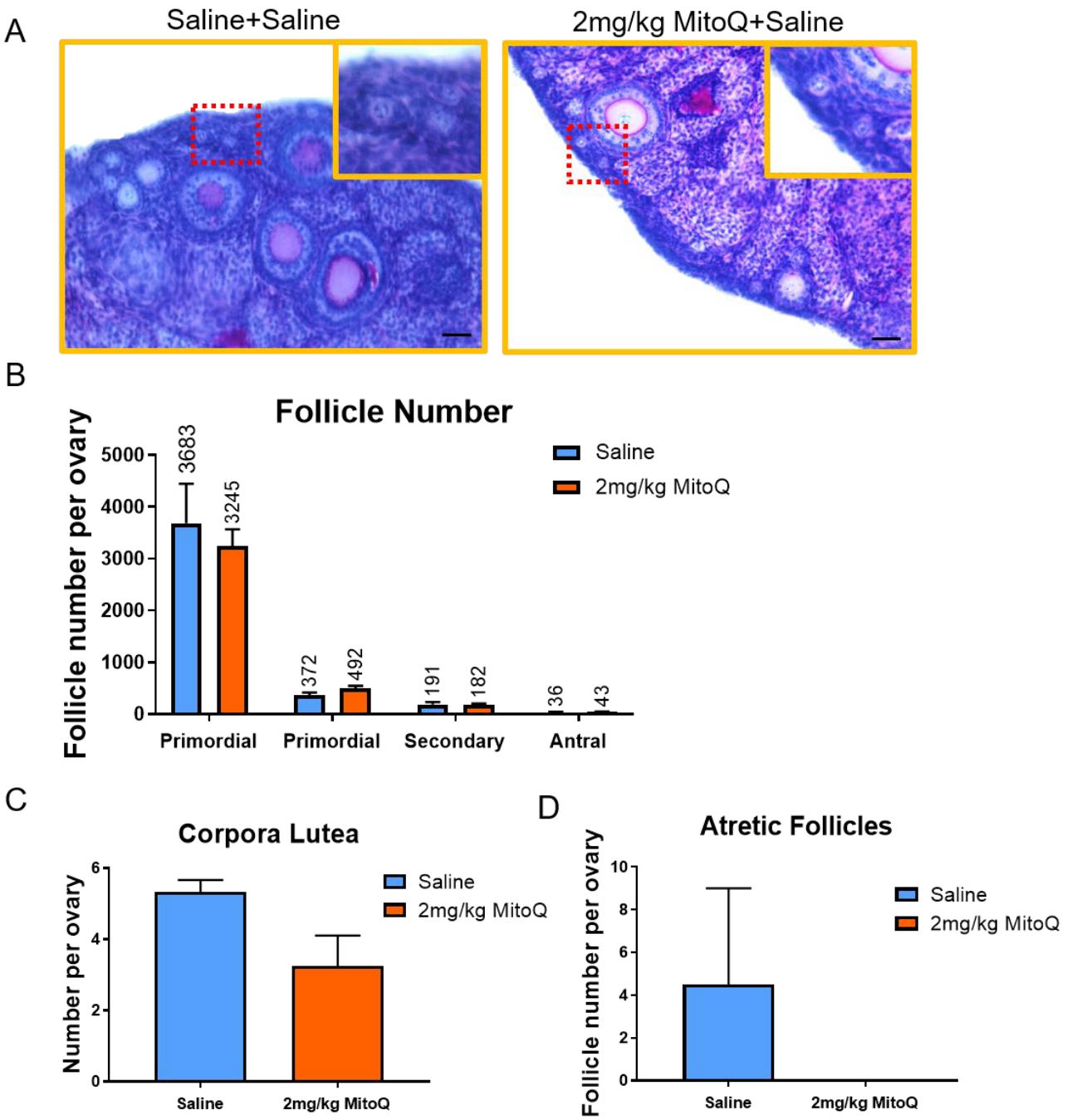

Figure 2. Effects of 2mg/kg/day MitoQ on the intestine and ovaries of mice. Mice were treated with 2mg/kg MitoQ for 4 days and ovaries were collected 5 days later (n=4/group). Representative ovarian histology (PAS stained) from mice received saline or 2mg/kg MitoQ injection, scale bar=50μm (A). The number of primordial, primary, secondary and antral follicles (B), corpora lutea (C) and atretic follicles (D) after 2mg/kg MitoQ injection, n=3-4 ovaries were counted per group. Data are shown as mean ± s.e.m. Data for each follicle stage/structure were compared between groups using unpaired t-test.

4.3.3 MitoQ protected primary follicle loss 3 hours after 0.45Gy whole body γ-irradiation

To determine if MitoQ could prevent follicle loss caused by γ-irradiation, mice were injected with saline or 2mg/kg MitoQ for 3 days and whole body γ-irradiation (0.45Gy) was performed 2 hours after the third dose, or mice remained unexposed. Ovaries were collected for assessment 3 hours after γ-irradiation treatment to analyse early impacts. Ovarian and follicular morphology were similar in unexposed and 0.45Gy groups treated with MitoQ or saline (Fig. 3A). At this early time point, primordial follicle numbers were similar among groups (Fig. 3B). However, primary follicles were significantly decreased after exposure to γ-irradiation compared to controls (no γ-irradiation + saline 138 ± 42 vs. γ-irradiation + saline 70 ± 19, $p<0.05$). Notably, significantly more primary follicles were observed in γ-irradiated mice supplemented with MitoQ compared to saline controls (γ-irradiation + saline 70 ± 19 vs. γ-irradiation + MitoQ 143 ± 42, $p<0.05$) (Fig. 3C). This finding suggests that γ-irradiation rapidly induces primary follicles atresia, and that MitoQ mitigates this effect. In contrast, growing follicle numbers, corpora lutea numbers and atretic follicle numbers were not affected by γ-irradiation or MitoQ (Fig. 3D-G).

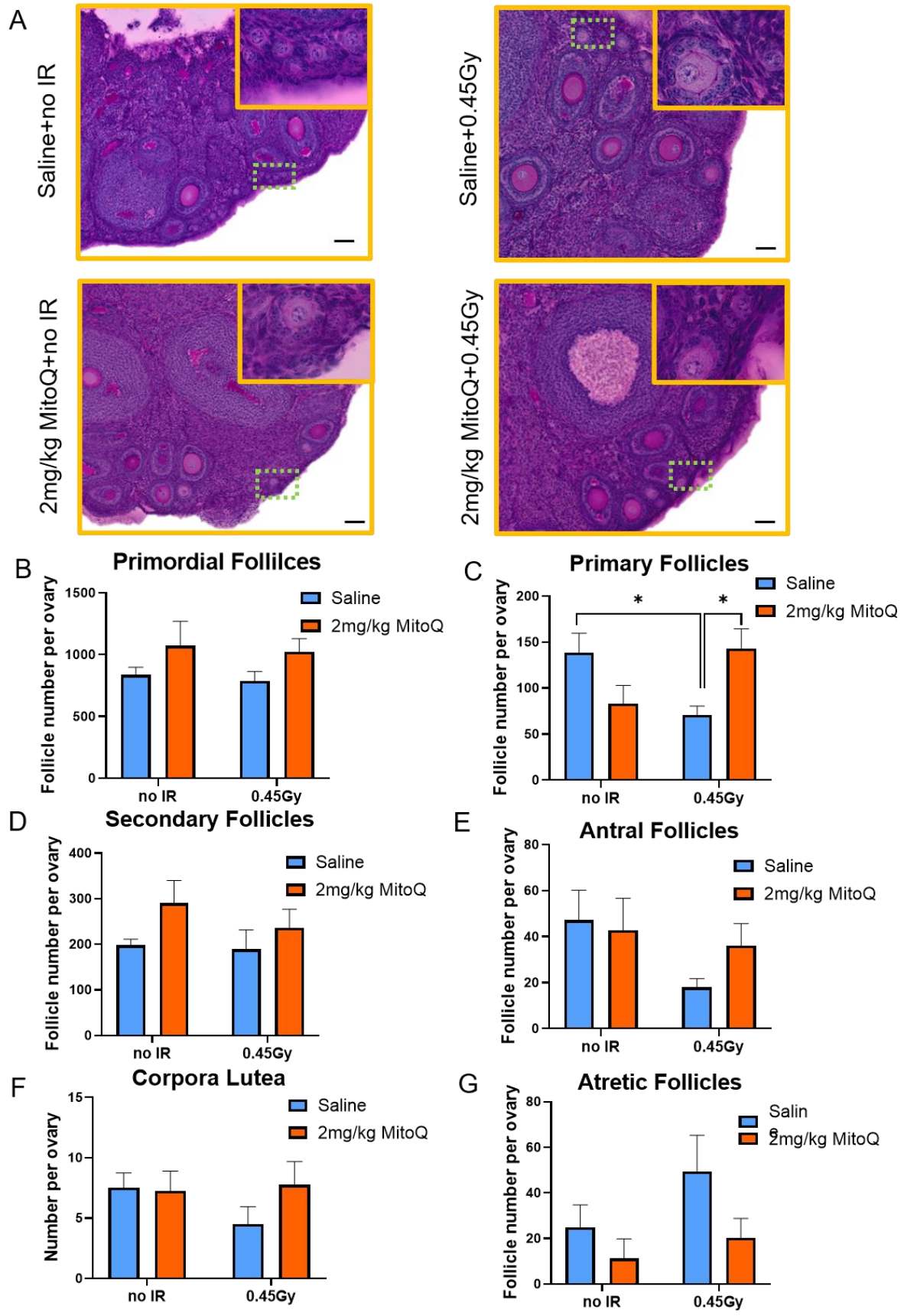

Figure 3. Ovarian morphology and follicle numbers in mice supplemented with MitoQ (2mg/kg/day) and exposed to whole-body γ-irradiation (0.45Gy) at the 3-hour collection time point. MitoQ were

administered daily for 3 days, the third dose was administered 2 hours before γ-irradiation; ovaries were harvested 3 hours later (n=4/group). Ovarian and follicular morphology of mice received different treatments, scale bar= 50μm (A). Primordial (B), primary (C), secondary (D), antral (E) follicle number, corpora lutea(F) and atretic follicle (G) numbers were determined 3 hours later, n=4 ovaries counted per group. Data are shown as mean ± s.e.m. Data was compared using one-way ANOVA followed by Tukey's multiple comparison test. Comparisons of follicle numbers between two groups were made using unpaired t-test, *$p<0.05$.

4.3.4 MitoQ did not prevent the depletion of primordial and primary follicles 5 days after 0.45Gy whole body γ-irradiation

To investigate if MitoQ could prevent follicle loss caused by γ-irradiation (0.45 Gy), mice were injected with 2mg/kg MitoQ for 4 days; the third dose was administered 2 hours before and the fourth dose was administered 20 hours after γ-irradiation exposure (Fig. S1). The ovaries were collected 5 days after the treatment.

The overall ovarian morphology was similar among groups, however, primordial and primary follicle remnants that lacked visible oocytes were evident in ovaries from γ-irradiated mice (Fig. 4A). In keeping with previous findings [1], the elimination of primordial and primary follicles was observed 5 days after exposure to 0.45Gy γ-irradiation (Fig 4B and C). MitoQ treatment did not confer any protection against the depletion of these follicles (Fig 4B and C). There was no difference in the number of secondary, antral or atretic follicles between groups, no differences in corpora lutea number observed (Fig. 4D-G).

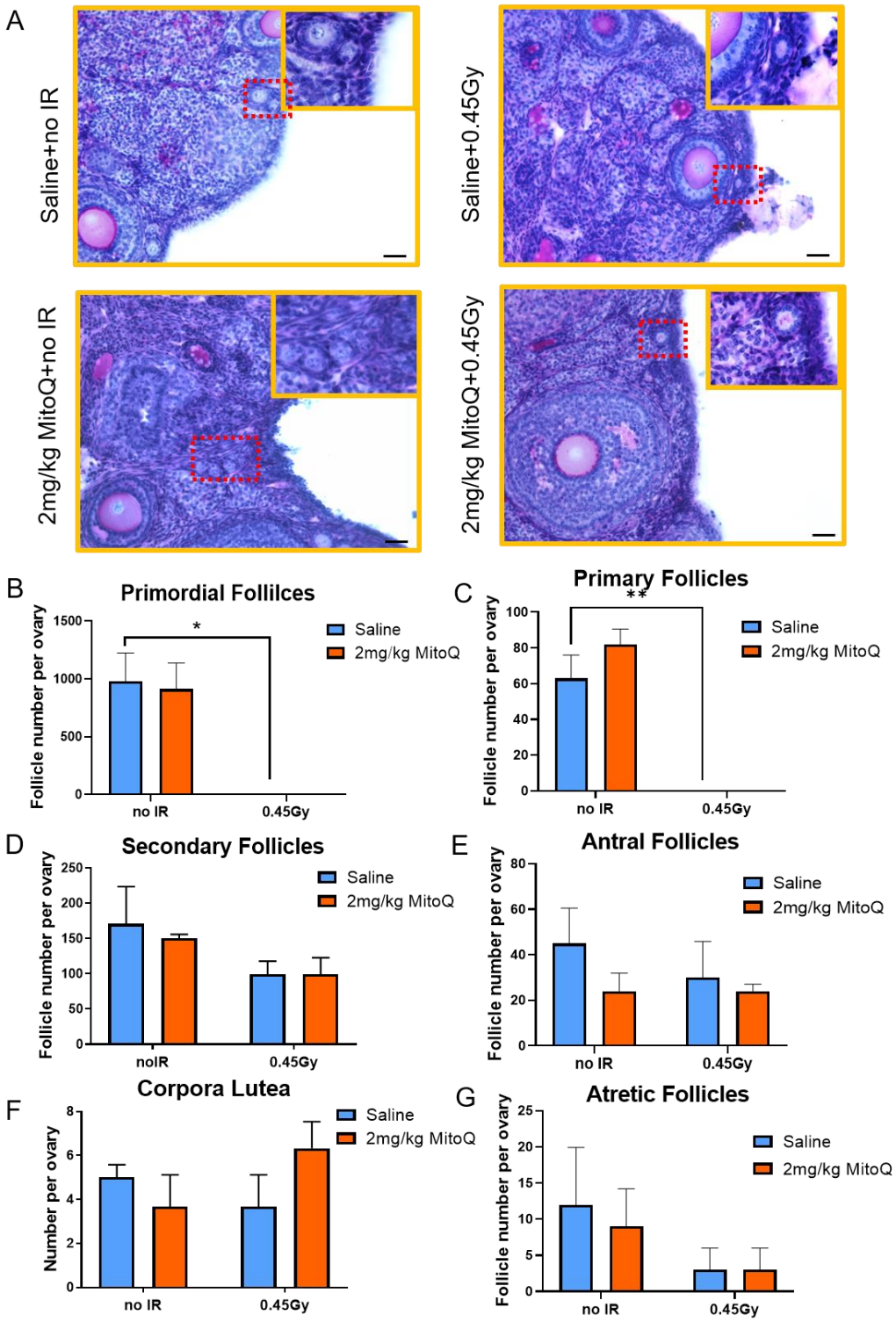

Figure 4. Ovarian morphology and follicle numbers of mice supplemented with MitoQ (2mg/kg/day) and exposure to whole-body γ-irradiation (0.45Gy) at the 5-day collection time point. MitoQ was administered daily for 4 days, the third dose was administered 2 hours before and the fourth dose was administered 20 hours after γ-irradiation; ovaries were harvested 5 days later (n=3/group). Representative ovarian and follicular morphology in mice receiving different treatments, scale bar=

50μm (A). Primordial (B), primary (C), secondary (D), antral (E) follicle number, corpora lutea (F) and atretic follicle (G) numbers were determined 5 days later, n=3 ovaries counted per group. Data are shown as mean ± s.e.m. Data was compared using one-way ANOVA followed by Tukey's multiple comparison test, *p<0.05, **p<0.01.

4.3.5 γ-Irradiation did not enhance DNA/RNA oxidative damage to the ovary

Oxidative damage to cellular structures within the ovary has been shown to increase with age and is proposed to contribute to loss of oocyte/follicle number and quality [208]. However, oxidative damage to the ovary following γ-irradiation had not been previously investigated. Therefore, oxidative damage was examined in tissue sections from ovaries 3 hours and 5 days after γ-irradiation (0.45Gy) and compared with non-irradiated controls. In addition, ovarian tissue sections from untreated and irradiated mice treated with 2mg/kg MitoQ, as described above, were examined to determine if the MitoQ regimen administered in this study could reduce irradiation-induced oxidative damage. Oxidative damage to nucleic acids was detected using the anti-DNA/RNA damage primary antibody that targeted Oxo-8-dG (8-Oxo-7,8-dihydro-2'-deoxyguanosine, a DNA peroxidative damage marker) and Oxo-8-G (8-Oxo-7,8-dihydroguanosine, an RNA peroxidative damage marker).

Using this antibody, labelling was detected in the cytoplasm of oocytes in primordial and primary follicles, and granulosa cells in primary, secondary and antral follicles (Fig. 5A(i)), indicative of oxidative damage to mitochondrial DNA (and possibly RNA) and consistent with previous studies utilising this antibody [209]. Somatic cells in the stroma also showed positive staining. Staining was detected in ovaries from both untreated and γ-irradiated mice, supplemented with saline or MitoQ, at both time points. Nuclear staining was not detected. Negative control sections, in which the primary antibody was omitted, did not show any staining (Fig. S2).

The percentage of follicles at each stage of development exhibiting positive staining was determined. At 3 hours, there was no significant difference among groups in the percentage of follicles at each stage of development with staining for the DNA/RNA oxidative damage marker (Fig. 5B). However, a slight trend towards an increased percentage of primordial and primary follicles with evidence of DNA/RNA

oxidative damage was observed after 0.45Gy γ-irradiation compared to non-irradiated mice (Fig. 5B, the blue columns of each histogram). Interestingly, the percentage of DNA/RNA damage positive primordial and primary follicles showed a subtle, but non-significant, decrease in MitoQ treated irradiated mice compared to saline treated irradiated mice (Fig. 5B, the right two columns of each histogram).

As expected, at 5 days, no primordial or primary follicles were observed in the ovaries from mice exposed to 0.45Gy γ-irradiation pre-treated with saline or MitoQ (Fig. 5B, C, ND). In non-irradiated mice, the percentage of positively stained primordial and primary follicles was slightly reduced in the MitoQ treated group compared to the saline treated group, but this was not statistically significant (Fig. 5C). There appeared to be a large increase in the percentage of antral follicles with positive staining after 0.45Gy γ-irradiation, though these differences were not statistically significant, and were likely due to a large amount of inter-animal variation in the data. This possible increase did not appear to be mitigated by MitoQ treatment (Fig. 5C, the right two columns of each histogram).

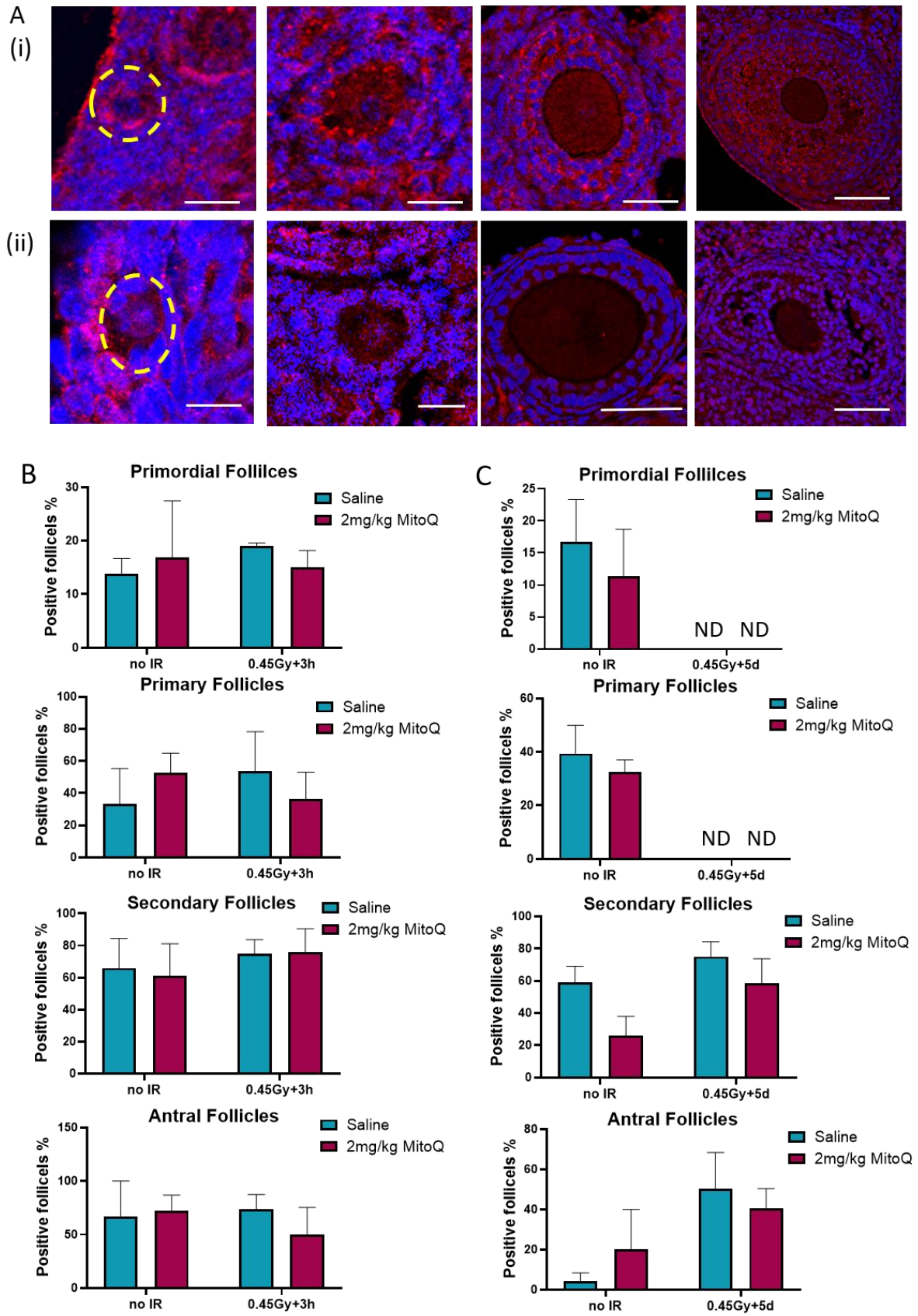

Figure 5. DNA/RNA oxidative damage of ovarian follicles after 0.45Gy γ-irradiation. Representative images of primordial, primary, secondary and antral follicles from different treatments and stained

positively (A (i)) or negatively (A (ii)) with DNA/RNA peroxidative marker. Scale bar=20μm. The percentage of positive follicles 3 hours (B) or 5 days (C) after irradiation. ND =Not Determined (no follicles present). Follicle numbers assessed at the 3-hour time point: primordial follicles =201, primary follicles =67, secondary follicles =184 and antral follicles =40; at the 5-day time point, primordial follicles =82, primary follicles =30, secondary follicles =182 and antral follicles =67. Animal number n=3/group. Data are shown as mean ± s.e.m. Data was compared using one-way ANOVA followed by Tukey's multiple comparison test. No significant differences observed.

4.3.6 γ-Irradiation did not enhance lipid oxidative damage to the ovary

Membranes comprise a high content of polyunsaturated fatty acids (PUFAs), and elevated lipid peroxidation caused by oxidative damage has been previously reported in the ovary, brain and muscles in different contexts [210-212]. Mammalian oocytes also contains large amounts of fatty acids, the peroxidation of which is considered to compromise oocyte quality [213, 214]. Indeed, the products of lipid peroxidation have been shown to damage oocyte structure and activate the intrinsic apoptosis pathway [152, 156]. In this study, oxidative lipid damage was detected using an anti-4 Hydroxynonenal (4-HNE, a stable lipid peroxidative product) antibody. Anti-4-HNE antibody was localised to the cytoplasm of oocytes in follicles across all the stages (Fig. 6A). The cytoplasm of granulosa cells and other somatic cells within the ovary also showed positive staining. Negative control sections, in which the primary antibody was omitted, did not show any staining (Fig. S2).

At 3 hours, there was no significant difference among groups in the percentage of follicles at each stage of development staining with the lipid oxidative damage marker (Fig. 6B). A possible increase of 4-HNE level was only observed in secondary follicles after 0.45Gy γ-irradiation compared to non-irradiated mice, though it did not reach statistical significance (Fig. 6B, the blue columns of each histogram). MitoQ treatment had no obvious impact on the percentage of positively stained follicles (Fig 6B).

At 5 days, no primordial or primary follicles were observed in the ovaries from mice exposed to 0.45Gy γ-irradiation pre-treated with saline or MitoQ. The percentage of follicles staining positively for 4-HNE

was not significantly different among groups, regardless of irradiation exposure or MitoQ treatment (Fig. 6C).

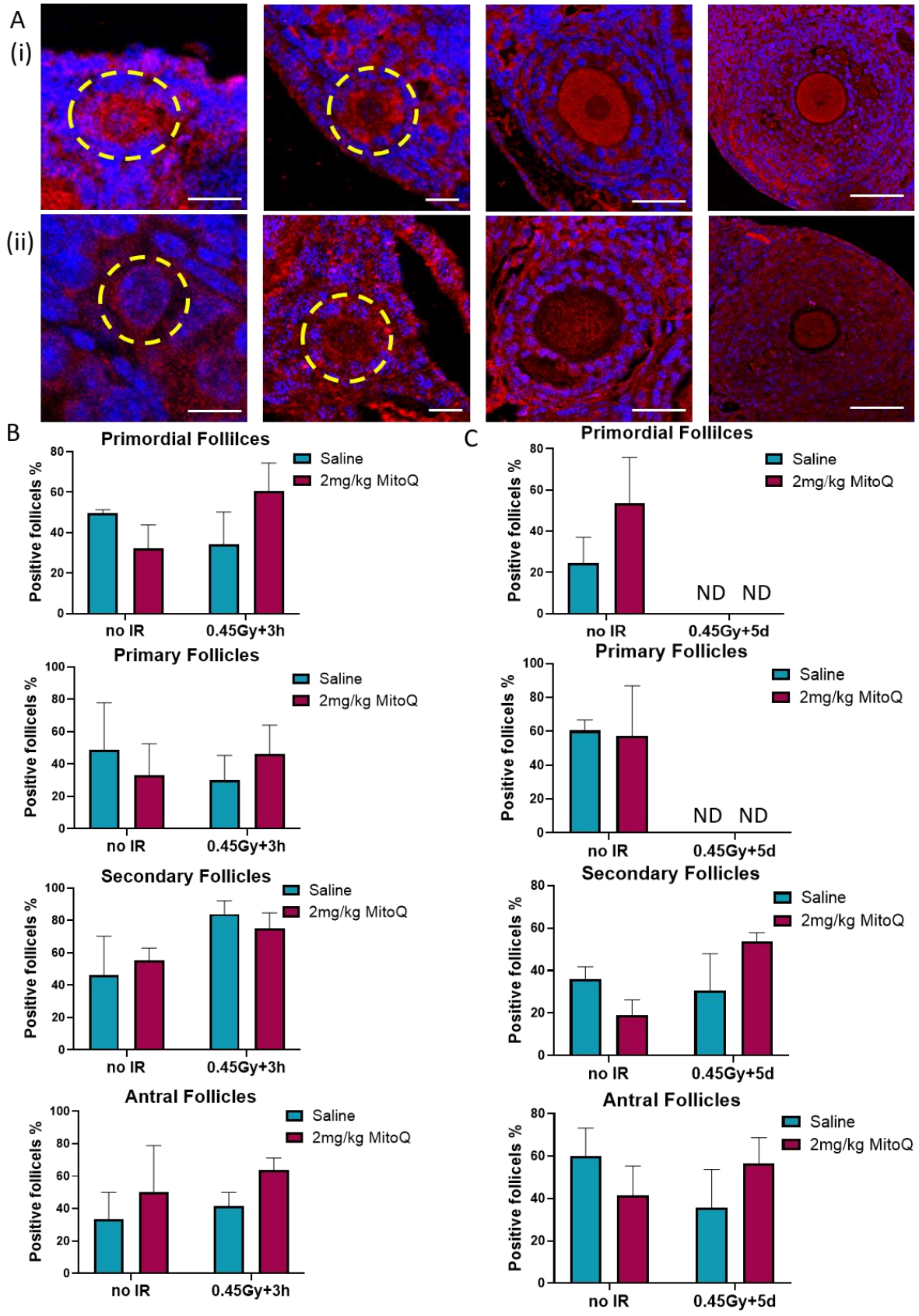

Figure 6. Lipid oxidative damage of ovarian follicles after 0.45Gy γ-irradiation. Representative images of primordial, primary, secondary and antral follicles stained positively (A (i)) or with limited to no staining (A (ii)) with 4-HNE. Scale bar=20μm. The percentage of positive follicles 3 hours (B) or 5 days (C) after irradiation. ND =Not Determined (no follicles present). Number of follicles assessed at the 3-hour time point: primordial follicles =178, primary follicles =68, secondary follicles =177 and antral follicles =38; at the 5-day time point, primordial follicles =85, primary follicles =35, secondary follicles =176 and antral follicles =61. Animal number n=3/group. Data are shown as mean ± s.e.m. Data was compared using one-way ANOVA followed by Tukey's multiple comparison test. No significant differences observed.

4.3.7 γ-Irradiation did not enhance protein oxidative damage to the ovary

In addition to damage DNA and lipid, excessive ROS caused by radiation directly attacks proteins by modifying protein structures and protein peroxidation can be detected in mice 2 years after irradiation [215, 216]. Therefore, in this study, oxidative protein damage was analysed using the anti-nitrotyrosine (NTY) antibody, an indicator of protein oxidation. Anti-NTY was localised to the oocytes within primordial follicles and shifted to somatic cells in primary follicles. In growing follicles, anti-NTY staining was found in both oocytes and somatic cells (Fig. 7A). Negative control sections, in which the primary antibody was omitted, did not show any staining (Fig. S2). Overall, staining patterns were similar to that previously observed in mouse ovaries [217].

At 3 hours and 5 days, there was no significant difference among groups in the percentage of follicles at each stage of development staining with protein oxidative damage marker, regardless of γ-irradiation exposure or MitoQ treatment (Fig. 7B). Notably, while only ~20% of the primordial follicles were NTY positive, ~100% of primary, secondary and antral follicles were positive. Thus, under normal conditions, protein oxidation appears to be heavily related to follicle stage.

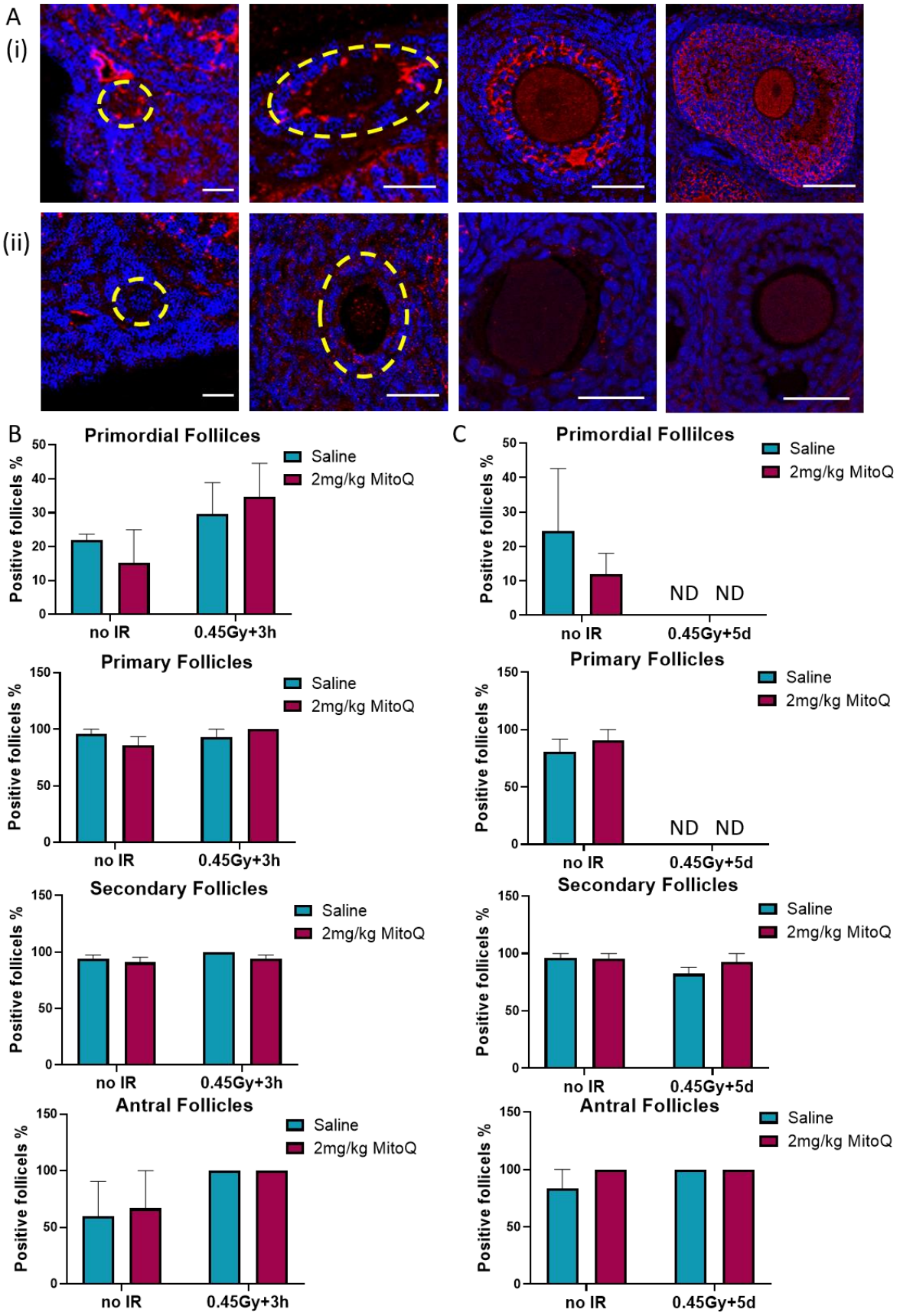

Figure 7. Protein oxidative damage of ovarian follicles after 0.45Gy γ-irradiation. Representative images of primordial, primary, secondary and antral follicles stained positively (A (i)) or negatively (A

(ii)) with NTY. Scale bar=20μm. The percentage of positive follicles 3 hours (B) or 5 days (C) after irradiation. ND =Not Determined (no follicles present). Follicle numbers assessed at the 3-hour time point: primordial follicles =195, primary follicles =67, secondary follicles =175 and antral follicles =44; at the 5-day time point, primordial follicles =86, primary follicles =33, secondary follicles =169 and antral follicles =61. Animal number n=3/group. Data are shown as mean ± s.e.m. Data was compared using one-way ANOVA followed by Tukey's multiple comparison test. No significant differences observed.

4.4 Discussion

It is well-established that DNA damage-induced apoptosis is a primary mechanism underlying the depletion of primordial follicles by cancer treatments, such as radiotherapy and chemotherapy [3, 218] [219]. The findings represented in this thesis, suggest that mitochondrial dysfunction may also contribute to the loss of ovarian reserve after cancer treatments [204, 220]. Within cells, mitochondria are the main source of ROS, which can damage proteins, lipids and DNA, and mitochondria themselves are sensitive to ROS-induced damage [221]. Indeed, the literature demonstrates that one mechanism by which radiation and cisplatin kill cancer cells is through the induction of oxidative stress, leading to apoptosis [222]. Thus, it was hypothesised in this Chapter, that supplementation with the mitochondrial targeted antioxidant MitoQ during cancer treatments could represent a novel method by which to reduce primordial follicle depletion.

MitoQ has been shown to be a safe drug that can be administrated long term to rodents and humans [179, 223], with doses of 5mg/kg MitoQ being protective against diabetic kidney disease in mice and against doxorubicin-induced cardiac damage in rats when administered by intraperitoneal injection twice a week for 12 weeks [190, 224]. However, in the first pilot study reported in this Chapter, mice receiving 5mg/kg/day MitoQ for 4 days had severely swollen intestines at the 5-day collection time point. This phenotype has not been previously reported, and given that MitoQ functions as an antioxidant, the underlying mechanism leading to swollen intestines is unclear. In addition, analyses of ovarian sections revealed no change in follicle numbers, but a significant reduction in the number of corpora lutea in mice MitoQ treated mice, suggesting that ovulation was suppressed. Whether reduced

corpora lutea number was a consequence of the altered intestinal function, or direct impacts on the ovary or endocrine signaling, is not known. These side effects were not expected; the cumulative dose of MitoQ in this study was 20mg/kg over 4 days, which was lower than previously reported cumulative doses of 120mg/kg over 12 weeks with no adverse effects described [190]. MitoQ can be detected in liver and kidney 5 minutes after intravenous injection [225], and has a half-life of 2 hours and 4 hours in liver and kidney, respectively, suggesting rapid accumulation and subsequent clearance, at least in these tissues [225]. Although similar data are not available for intestines or ovaries, MitoQ may be quickly absorbed by the intestines (and ovaries) at high levels, possibly leading to mitochondrial dysfunction and intestinal swelling. Indeed, somewhat counterintuitively, recent studies found high a concentration of MitoQ induced ROS production, autophagy, mitochondrial swelling and depolarization [226-228]. Thus, given the results of the first pilot study, the MitoQ dose was reduced to 2mg/kg in the second pilot study. This dose was selected because it had previously been shown to protect against acute lung injury, with no reported side-effects in rats [207]. Consistent with this prior report, in the studies conducted for this Chapter, 4 daily doses of 2mg/kg MitoQ did not induce any gross changes in intestinal morphology or corpora lutea number, nor did it impact follicle numbers.

The first aim of this Chapter was to determine if MitoQ could prevent follicle depletion cause by radiation exposure. One previous study has shown that irradiation causes lipid and protein oxidative damage in the small intestines of rats, and that this can be prevented by antioxidants, such as melatonin [216]. Consistent with previously reported data [206], in this study, primordial and primary follicles were significantly depleted 5 days following exposure to 0.45Gy γ-irradiation. However, MitoQ treatment, under the conditions employed, did not prevent or reduce this depletion when follicle numbers were analysed at 5 days. There are a number of possible explanations for this finding. It could be that ROS is not elevated in oocyte mitochondria, or ovarian somatic cells, following radiation exposure (discussed in more detail in later sections). Future studies measuring mitochondrial ROS level in oocytes could include the incubation of isolated oocytes with Mitosox Red, as reported [229]. An alternative explanation is that elevated ROS is only a minor contributor to follicle depletion, and that direct DNA damage is the predominant mechanism. It is also possible that the MitoQ regimen used, in terms of the timing and frequency of dosing, was inadequate to combat radiation induced ROS in the ovary. This dose (2mg/kg MitoQ) and administration route (intraperitoneal injection) was chosen as it

had been previously shown to protect against acute lung injury in rats, but it failed to protect neuro functions after traumatic brain injury [207, 230]. In addition, a study in rats showed that this dose of MitoQ prevents radiation-induced damage to the testis [193]. But, the ovary may exhibit different requirements, and additional studies could be undertaken to measure MitoQ accumulation and half-life in the ovary. For example, future studies could use [^{3}H] MitoQ to determine the amount of MitoQ delivered to the ovary using methods established for other tissues [225]. This information could then be used to design an improved treatment regimen so that firmer conclusions could be drawn regarding the ovo-protectant capacity of MitoQ.

One of the interesting observations made in this study was that primary follicle depletion was detected 3 hours after 0.45Gy γ-irradiation, while primordial follicle numbers were unchanged. Strikingly, MitoQ treatment prevented this early depletion of primary follicles. These findings indicate that mitochondrial ROS levels may increase rapidly in primary follicles following radiation treatment, triggering atresia, and that this can be mitigated using a mitochondrial specific antioxidant. However, the protective effect appeared to be transient, as dramatic primary follicle depletion was evident at the 5 days in MitoQ treated radiation exposed mice, just like in saline treated irradiated mice. As described above, it is possible that modification of the MitoQ regimen could lead to long-term primary follicle preservation (for example, dosing more frequently, or continuing to dose for a number of days after radiation exposure).

In contrast to primordial and primary follicles, secondary and antral follicles were more tolerant to irradiation damage than primordial and primary follicles, and this observation is consistent with prior literature [51]. Even though growing follicles were not depleted by radiation, it is possible that exposure reduces the quality of those oocytes/follicle that remain. Indeed, oocytes released by spontaneous ovulation were found to be arrested at metaphase I in irradiated mice, suggesting impaired ability to undergo meiotic maturation [231]. Furthermore, recent *in vitro* studies have shown that MitoQ treatment improves oocyte quality and fertilization rate by reserving spindle defects and decreasing intracellular ROS level [229, 232]. Thus, it would be worthwhile performing follow-up studies to investigate the ability of MitoQ to improve oocyte quality after radiation. This could be done by culturing super ovulated oocytes from irradiated mice with MitoQ, followed by the evaluation of chromatin, spindle

and mitochondria; alternatively, *in vitro* fertilization (IVF) could be performed to assess fertilization and embryo developmental rates.

Elevated ROS levels caused by radiotherapy via radiolysis of water and damage to DNA and mitochondria can activate apoptosis as a result of damage to cellular components, including DNA, lipids, and proteins, beyond the mitochondria [197, 221]. Therefore, this Chapter also aimed to determine if radiation-associated oxidative damage to DNA/RNA, lipids or proteins could be detected in ovarian tissues [233, 234].

ROS can directly attack DNA and affect genome stability, resulting in loss of oocyte/follicle number and quality [235]. In the present study, a DNA/RNA oxidative damage marker was observed in the cytoplasm of oocytes and granulosa cells, which is consistent with previous findings in ovaries of aging mice [233, 234]. Mitochondrial DNA has a similar structure to nuclear DNA, and a previous study has found that 8-oxoG accumulates in mtDNA under conditions of oxidative stress [209]. Thus, cytoplasmic staining may indicate mtDNA oxidative damage. Further analysis by co-staining the DNA/RNA damage marker with a mitochondrial marker, such as TOM20 (outer mitochondrial membrane protein), is required to confirm the precise localisation of damage. Although trends toward an increase in the percentage of follicles showing evidence of DNA/RNA oxidative damage was observed in ovaries from irradiated mice, the data did not reach statistical significance.

Due to their high content of polyunsaturated fatty acids (PUFAs), bio-membranes are sensitive to modification by ROS [152]. In particular, destruction of the mitochondrial membrane can lead to release of cytochrome c and activation of apoptotic pathways [140]. In addition, lipids accumulate in oocytes during follicle growth [236]. In the present study, 4-HNE, a maker of lipid peroxidation was observed in the cytoplasm of oocytes and somatic cells, which was consistent with previous findings [233, 234, 237]. There was no difference in the percentage of follicles positive for this marker in control and irradiated groups, suggesting that lipid peroxidation may not be increased following this treatment. There was also no difference between saline and MitoQ treated animals. However, there was lot of inter-animal variation within groups, making the results inconclusive and highlighting the need for further studies.

Excessive ROS, caused by radiation, has been shown to attack a variety of enzymatic proteins and impair important signaling events, such as those mediated by protein phosphorylation [215, 216]. Thus, the protein oxidative damage marker NTY was used to detect protein oxidative damage after irradiation. In the present study, NTY was detected in the oocytes within primordial follicles and in somatic cells within primary follicles. In secondary and antral follicles, NTY was found in both oocytes and somatic cells. No significant difference among groups in the percentage of follicles stained with NTY was observed, however, it was worth noting that the percentage of NTY positive primordial follicles were less than the positive primary or growing follicles. Since primordial follicles are dormant with low metabolic activity, it is possible that they were more resistant to protein oxidative damage than activated follicles, in which metabolic activities, like protein synthesis, are more active to meet the demands of follicle development. These results are similar to a previous paper reporting that in the mouse ovary, 18% of the oocytes from primordial follicles were NTY positive, whereas 45% of oocytes from antral follicles were NTY positive [238].

A major limitation of this study was the considerable inter-animal variation. To fully understand if MitoQ could have subtle, but important, impacts on preserving ovarian follicle number and protecting DNA, lipid and proteins against irradiation, sample size should be increased to account for this variability. Other techniques, such as Western blot and ELISA could also be included to further analyse oxidative damage within ovaries. Alternatively, the overall ROS level in the ovary could be determined using the sensitive fluorescent dye, 2',7'-dichlorofluorescin diacetate (DCFDA), as described [239]. In addition, to develop a comprehensive understanding of the extent of oxidative damage to DNA, lipid and protein, the immunofluorescent intensity of those markers in isolated oocytes could provide valuable information. Another limitation of the protein, lipid and DNA/RNA damage analysis is that only two time points were analysed; levels may have changed after irradiation, but the correct time point was not analysed. Finally, it is not clear if MitoQ, under the regimen and conditions employed by this

study, reached the ovary in sufficient levels and for a sufficient period of time to reduce oxidative stress and prevent follicle loss. A recent study demonstrated that the combination of MitoQ and vitamin D3 significantly reduced the ovarian oxidative stress and increased follicle numbers in a mouse model of PCOS [191]. Thus, further studies could also determine if MitoQ acting as a co-adjuvant with vitamin D3 (or other inhibitors of apoptosis) protects oocytes and follicles from irradiation damage.

4.5 Conclusion

The results presented in this chapter demonstrated that 0.45Gy γ-irradiation depletes the ovarian reserve 5 days after exposure, however, under the conditions used in this study, MitoQ did not prevent follicle loss. Evidence of DNA/RNA, protein and lipid oxidation could be detected in follicles in normal ovaries, and this did not appear to change with irradiation or MitoQ treatment. Thus, this Chapter reports important in interesting data that provide an essential foundation from which studies could be extended in the future.

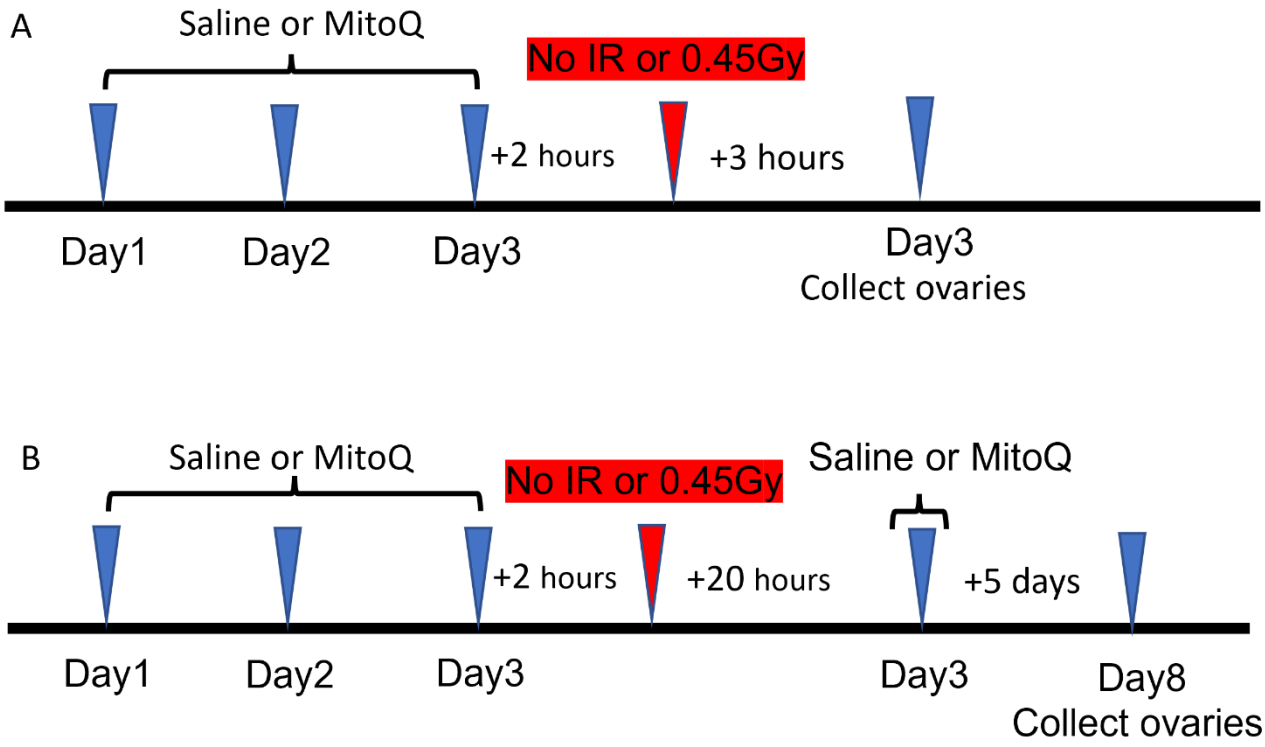

Supplemental Figure 1. Diagram of MitoQ and γ-irradiation treatments. A. Mice received MitoQ (2mg/kg), or an equivalent volume of saline (1% DMSO) by ip injection each day for 3 days before irradiation, with the third dose given 2 hours before irradiation. Mice were sacrificed 3 hours after irradiation to harvest ovaries. B. Mice receive MitoQ (2mg/kg), or an equivalent volume of saline (1% DMSO) by ip injection each day for 3 days before irradiation. Irradiation was performed 2 hours after the third dose and 20 hours before the fourth dose of MitoQ or saline. Mice were sacrificed 5 days after irradiation to harvest ovaries.

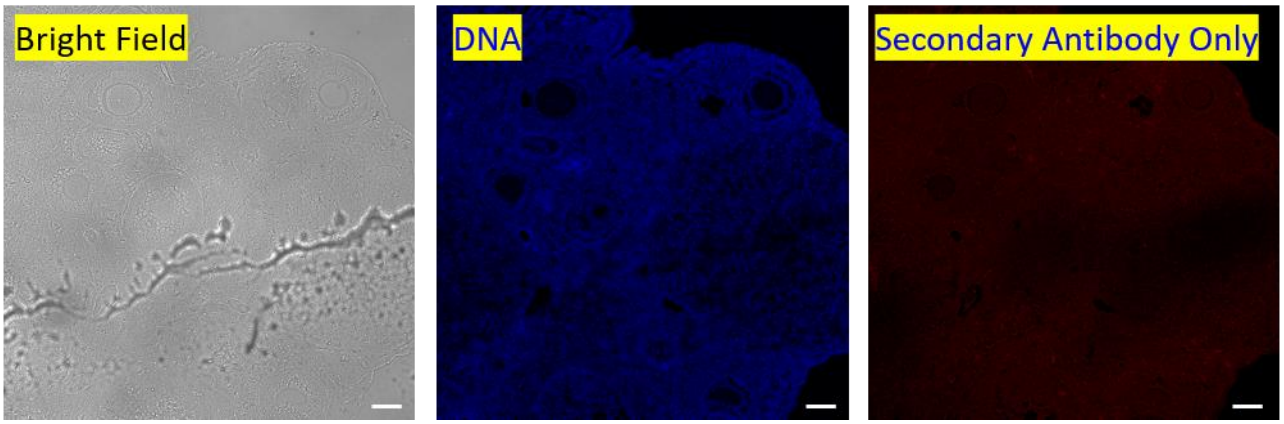

Supplemental Figure 2. Representative images of negative controls for the oxidative damage markers. Immunofluorescent staining was performed as described before, except the primary antibody was omitted. Scale bar= 50µm.

Chapter 5. General discussion

Radiotherapy and certain chemotherapies are well-known to compromise female fertility and induce premature menopause by damaging nuclear DNA and activating apoptosis in oocytes and granulosa cells [3, 116, 132, 240, 241] . However, studies in somatic cells reveal that radiation and chemotherapy also damage intracellular organelles, with the impairment of mitochondria emerging as a key mediator of cell dysfunction and cell death [97, 242]. Indeed, mitochondria are the major source and target of ROS, and are an essential component of the intrinsic apoptosis pathway [243]. These observations raise the possibility that, in addition to causing genomic DNA damage, radiation and chemotherapy could cause mitochondrial damage in oocytes, leading to oocyte death or compromised oocyte quality. The latter is especially important to consider in the context of fertility preservation for female cancer patients, as these organelles are maternally inherited [5]. In addition, a comprehensive understanding of the mechanisms by which cancer treatments deplete follicles may lead to new opportunities for fertility preservation in women and girls being treated for cancer. Thus, this thesis aimed to characterize the short and long-term impacts of γ-irradiation and cisplatin, a widely used platinum containing chemotherapy drug, on mitochondria in oocytes, and to determine if protecting mitochondria using the mitochondria-targeted antioxidant, MitoQ, could prevent or reduce primordial follicle depletion caused by radiation.

Mitochondria are highly dynamic organelles that relocate in the cytoplasm during oocyte and embryo development [244]. Although the redistribution patterns vary in different species, localisation is an important marker of oocyte and embryo quality [244, 245]. Thus, MitoTracker green, a fluorescent dye that localizes with functional and dysfunctional mitochondria, was used to determine if mitochondrial distribution was affected by γ-irradiation (Chapter 2) or cisplatin (Chapter 3). In the irradiation study, mitochondrial distribution was not affected in small immature oocytes from primordial or primary

follicles, or in growing immature oocytes from secondary or early antral follicles. In contrast, cisplatin treatment affected mitochondrial localization in a dose and time dependent manner, with aberrant restricted cytoplasmic localization observed only in small immature oocytes at 24 hours after injection with the higher dose of cisplatin (4mg/kg). Those oocytes also displayed rough edges, suggesting that they were undergoing apoptosis. Notably, both homogeneous and aggregated mitochondrial localization were found in growing oocytes in irradiation and cisplatin studies. Although the functions of the two patterns were not determined in the current study, it could possibly represent the different developmental stages, with aggregated mitochondria found in large preantral follicles [246].

Mitochondria undergo frequent fusion and fission to balance the population and maintain normal functions [247]. In somatic cells, an increase of mitochondrial mass has been commonly detected after exposure to γ-irradiation, and it was proposed to be a compensatory reaction to the oxidative damage [99, 100]. But, both an increase and decrease of mitochondrial mass has been reported in different cells after cisplatin treatment [248, 249]. Notably, however, results from the present study showed mitochondrial mass in small and growing oocytes was not affected by γ-irradiation or cisplatin treatment. It is possible that the timeframe chosen in the studies conducted for this thesis was too late for the detection of changes in mitochondrial mass, as other studies in somatic cells have looked in the hours following treatment. Thus, additional earlier time points could be investigated in future experiments, along with an analysis of mitochondrial fission related genes, such as dynamin-related protein (Drp-1).

Mitochondrial membrane potential, generated by the process of proton pumping, is required for ATP generation and is an indicator of mitochondrial function [250]. Decreased mitochondrial membrane potential is associated with mitochondrial dysfunction and the induction of apoptosis [251-254]. To

assess mitochondrial membrane potential in oocytes after irradiation and cisplatin, TMRM, a low toxicity, cell-permeant dye, that accumulates only in active mitochondria, was used and the fluorescent intensity of TMRM was quantified to evaluate mitochondrial activity. It was found that both irradiation (Chapter 2) and cisplatin (Chapter 3) induced acute mitochondrial damage in a cohort of small immature oocytes (primordial and primary follicles) 24 hours after treatment. This was characterised by the partial or complete loss of mitochondrial membrane potential, consistent with mitochondrial dysfunction and the activation of apoptosis, respectively. The induction of apoptosis could be the consequence of direct damage to mitochondria by radiation and cisplatin, or the elevation of ROS leading to the protein, lipid and/or DNA damage in mitochondria. It could also be mediated indirectly, through activation of the intrinsic apoptosis pathway, which is triggered by DNA damage and involves permeabilization of the mitochondrial membrane and release of cytochrome c [51, 255, 256]. One way to tease out the underlying mechanisms (i.e. direct vs indicate mitochondrial damage) would be to study mitochondrial membrane potential in the oocytes of irradiated *Puma*$^{-/-}$ or *Tap63*$^{-/-}$ mice, in which the intrinsic apoptosis pathway is not activated by DNA damage. Of note, at the 24-hour assessment time point, all the small oocytes in the irradiated mice had detectable TMRM signals and normal levels of TMRM intensity, but small oocytes that lost TMRM staining were first observed in cisplatin treated mice, suggesting different apoptosis signal pathways might be triggered by the two treatments.

Compared to small immature oocytes, TMRM signals were detected in all growing immature oocytes after irradiation and cisplatin treatment, which highlights the previous finding that oocytes in primordial follicles are more sensitive to both treatments than oocytes in growing follicles [257, 258]. Although TMRM intensity decreased in growing oocytes at 6 hours after irradiation and at 24 hours after cisplatin exposure, ATP level in these oocytes were similar between groups, indicative of normal functional

outputs. Alternatively, it is possible that the stable ATP content in these oocytes was the result of transport of ATP from granulosa cells through gap junctions at the oolema [259]. It would be interesting to assess oxygen consumption and calcium signaling later in development to further evaluate mitochondrial function.

Mitochondria are mainly maternally inherited and are important for oocyte maturation and embryo development [260]. After evaluating mitochondrial characteristics in immature oocytes in the acute period after exposure to radiation or cisplatin, it was important to determine if any impairment in mitochondrial content or function persisted in mature oocytes as a result of these treatments. In both irradiation and cisplatin treated mice, significant reductions in the number of mature oocytes harvested after superovulation were observed, which could be due to depletion of the primordial follicle reserve, a well-established consequence of these treatments [51, 240, 261]. Although not investigated in detail in this thesis, it is also possible that persistent impairment of mitochondrial function reduced the ability of follicles to grow and mature such that fewer healthy larger preantral follicles were available to be stimulated. However, reported counts of preantral follicles in control and irradiated or cisplatin mice do not support this concept [3, 240]. Alternatively, the reduction of ovulated oocytes number may have been caused by compromised mitochondrial functions in granulosa cells. Indeed, a previous study reported that mitochondrial dysfunction in cumulus cells results in oocyte incompetence and low fertility rates [262]. Therefore, further study could focus on whether mitochondria were affected in granulosa cells. A reduction in the number of mature ovulatory oocytes could also reflect an impaired ability to respond to hormone priming after irradiation or cisplatin. Notably, however, all the mitochondrial parameters investigated in the mature ovulated oocytes (including ATP levels, mtDNA copy number and mitochondrial mass and localisation) were similar between untreated and treated

groups, suggesting the mitochondria were functional. Indeed, fertility studies conducted by others have demonstrated that apoptosis deficient mice (i.e. in which oocytes are unable to undergo apoptosis) receiving irradiation or cisplatin produce comparable litters as control mice by natural mating [51, 218].

It is well established that exposure to exogenous stimuli, such as irradiation and chemotherapy can lead to elevated ROS level in cells [114, 131]. Excessive intracellular ROS can attack mitochondria, which are the main source of ROS, even under physiological conditions, in turn resulting in more ROS production [263]. As discussed earlier, mitochondria are also essential components of the intrinsic apoptosis pathway, and it is the release of cytochrome c from the inner membrane that activates the caspase cascade leading to demolition of the cell [263]. Based on the data presented in the irradiation (Chapter 2) study demonstrating mitochondrial damage in immature oocytes, combined with studies in rats showing that MitoQ prevents radiation-induced damage to the testis [192, 193], it was hypothesized that MitoQ could prevent follicle loss by protecting mitochondria from oxidative damage.

MitoQ is an effective mitochondrial-targeted antioxidant that can rapidly scavenge ROS [264]. It can protect against pathologies associated with various mitochondria-related diseases, such as diabetic kidney disease and chronic hepatitis C virus infection, in rodents and humans [187, 190]. Although previous studies in mice using 5mg/kg MitoQ via ip injection [190] did not report any adverse outcomes, in the present study, 5mg/kg MitoQ given by ip injection for 4 days caused severely swollen intestines and suppressed ovulation in mice. Thus, the dose of MitoQ was decreased to 2mg/kg, based on reports that this dose protects against acute lung injury in rats [207]. In this study, MitoQ conferred no protective effect against radiation-induced follicle depletion. Interestingly, however, the results showed MitoQ delayed primary follicle loss after irradiation, though this effect was transient, suggesting that MitoQ

has protective properties and is worthy of further study. Since MitoQ can be detected in the kidney 5 mins after injection, and the half-life of MitoQ in the liver and kidney is 2 hours and 4 hours, respectively [225], it was possible that MitoQ was not delivered to the ovary with sufficient frequency to reach protective levels over a sustained period of time. Thus, further studies using [^{3}H] MitoQ should be performed, as described [225], to assist with the optimization of the treatment protocol.

One of the mechanisms by which cancer treatments induce cell death is the elevation of intracellular ROS level [140, 198, 265, 266]. Excessive ROS can damage cellular components both within and beyond the mitochondria, such as DNA, lipids and proteins. The oxidative products of these components are associated with aging and the decrease of oocyte quality [235] [155, 156, 234]. Consistent with previous studies [233, 234], the oxidative DNA/RNA damage marker used in this study was only observed in the cytoplasm of oocytes and granulosa cells, not the nucleus. This staining pattern could reflect RNA oxidative damage. Alternatively, since mitochondria contain DNA that has a similar structure to nuclear DNA, this localization pattern might indicate oxidative damage to mtDNA. To support this idea, mtDNA and 8-oxoG were found colocalized under oxidative stress in neurons [209]. In this regard, further studies that co-stain mitochondria and the DNA/RNA oxidative marker in ovarian tissues could help to address this hypothesis. Overall, the studies conducted in this thesis could not confirm that exposure to radiation increases DNA/RNA oxidative damage in the ovary, as it does in other tissues and cells, as no significant differences were observed between groups.

A large amount of lipids accumulate in oocytes during their development to support their growth [236]. In previous studies, the products of lipid peroxidation, such as 4-HNE, have been shown to damage the DNA, spindle and proteins in oocytes, resulting in loss or compromised oocyte quality [153-156]. In

the present study, no significant changes in lipid peroxidative damage in ovarian tissue sections were observed after irradiation, although high inter-animal variations were noted. In addition to the accumulation of lipids, an increase of protein content is observed during oocyte growth [267]. The peroxidation of proteins within cells leads to malfunction of proteins, and especially compromises protein enzymatic activities, resulting in cell death [268]. Even though no significant increase of follicles positively labelled with the marker of protein damage was observed after irradiation, it is worth noting that the localisation of this marker was heavily dependent on follicle stage. Whereas only a small portion of primordial follicles was positive, a much larger cohort of growing follicles was positive. Similar findings were reported in aging mouse ovaries [238], which might indicate that proteins in dormant primordial follicles are less exposed to ROS–than metabolically active growing follicles.

Of note, MitoQ supplementation did not alter localisation or staining patterns of the markers of DNA/RNA, lipids and protein damage used in this study. In addition to the factors mentioned above (dose, uptake rate and half-life of MitoQ), dysfunction of complex II (one of the mitochondrial electron transport chain complexes) might be one explanation for this finding. Since MitoQ can only be efficiently utilized by complex II, mitochondrial function cannot be restored by MitoQ in the absence of complex II [178]. Therefore, further studies, such as Western blots, should be performed to examine complex II levels in ovaries after irradiation.

Overall, this thesis represents the first analysis of the impact of radiation and cisplatin on mitochondria in oocytes. It shows that both γ-irradiation and cisplatin treatment of pre-pubertal mice are associated with 1) loss of mitochondrial membrane potential in a significant proportion of small immature oocytes and 2) a reduction in the number of mature oocytes harvested from adult mice. Importantly, these data

indicate that immature oocytes that survive γ-irradiation or cisplatin treatment can progress to the ovulatory stage and harbor apparently normal mitochondria, although a slight reduction in mitochondrial mass in mature oocytes after γ-irradiation was observed. These results suggest that the long-term impacts of γ-irradiation or cisplatin treatment on mitochondria may be very limited. Though extrapolation from mouse to human should be performed with caution, this knowledge is reassuring to the fertility preservation field, especially those pursuing apoptosis inhibition as a method to prevent treatment-induced follicle depletion. This thesis also reports the first study of mitochondrial protection as a potential strategy to reduce the damaging effects of chemotherapy and radiation on follicles. Although MitoQ did not prevent follicle loss in irradiated mice or reduce the presence of oxidative damage in ovarian tissues, the observed delay in primary follicle depletion indicates some promise. Thus, it is hoped that the data presented in this thesis prompts additional exploration of the therapeutic potential of MitoQ as a novel follicle protectant during cancer treatment.

References

1. Kerr, J.B., et al., *The primordial follicle reserve is not renewed after chemical or gamma-irradiation mediated depletion.* Reproduction, 2012. **143**(4): p. 469-76.
2. Hutt, K., et al., *How to best preserve oocytes in female cancer patients exposed to DNA damage inducing therapeutics.* Cell Death Differ, 2013. **20**(8): p. 967-8.
3. Kerr, J.B., et al., *DNA damage-induced primordial follicle oocyte apoptosis and loss of fertility require TAp63-mediated induction of Puma and Noxa.* Mol Cell, 2012. **48**(3): p. 343-52.
4. Qi, L., et al., *Mitochondria: the panacea to improve oocyte quality?* Ann Transl Med, 2019. **7**(23): p. 789.
5. Kam, W.W. and R.B. Banati, *Effects of ionizing radiation on mitochondria.* Free Radic Biol Med, 2013. **65**: p. 607-19.
6. Barnett, K.R., et al., *Ovarian follicle development and transgenic mouse models.* Hum Reprod Update, 2006. **12**(5): p. 537-55.
7. Smith, P., D. Wilhelm, and R.J. Rodgers, *Development of mammalian ovary.* J Endocrinol, 2014. **221**(3): p. R145-61.
8. Pepling, M.E. and A.C. Spradling, *Female mouse germ cells form synchronously dividing cysts.* Development, 1998. **125**(17): p. 3323-8.
9. Pepling, M.E. and A.C. Spradling, *Mouse ovarian germ cell cysts undergo programmed breakdown to form primordial follicles.* Dev Biol, 2001. **234**(2): p. 339-51.
10. Hartshorne, G.M., et al., *Oogenesis and cell death in human prenatal ovaries: what are the criteria for oocyte selection?* Mol Hum Reprod, 2009. **15**(12): p. 805-19.
11. Pelosi, E., A. Forabosco, and D. Schlessinger, *Genetics of the ovarian reserve.* Front Genet, 2015. **6**: p. 308.
12. Williams, C.J. and G.F. Erickson, *Morphology and Physiology of the Ovary*, in *Endotext*, K.R. Feingold, et al., Editors. 2000: South Dartmouth (MA).
13. Johnson, J., et al., *Germline stem cells and follicular renewal in the postnatal mammalian ovary.* Nature, 2004. **428**(6979): p. 145-50.
14. Kirilly, D. and T. Xie, *The Drosophila ovary: an active stem cell community.* Cell Res, 2007. **17**(1): p. 15-25.
15. White, Y.A., D.C. Woods, and A.W. Wood, *A transgenic zebrafish model of targeted oocyte ablation and de novo oogenesis.* Dev Dyn, 2011. **240**(8): p. 1929-37.
16. Virant-Klun, I., *Postnatal oogenesis in humans: a review of recent findings.* Stem Cells Cloning, 2015. **8**: p. 49-60.
17. Sarraj, M.A. and A.E. Drummond, *Mammalian foetal ovarian development: consequences for health and disease.* Reproduction, 2012. **143**(2): p. 151-63.
18. Sarma, U.C., J.K. Findlay, and K.J. Hutt, *Oocytes from stem cells.* Best Pract Res Clin Obstet Gynaecol, 2019. **55**: p. 14-22.
19. Amleh, A. and J. Dean, *Mouse genetics provides insight into folliculogenesis, fertilization and early embryonic development.* Hum Reprod Update, 2002. **8**(5): p. 395-403.
20. Faddy, M.J., et al., *Accelerated disappearance of ovarian follicles in mid-life: implications for forecasting menopause.* Hum Reprod, 1992. **7**(10): p. 1342-6.
21. Cox, E. and V. Takov, *Embryology, Ovarian Follicle Development*, in *StatPearls*. 2020: Treasure Island (FL).
22. Makker, A., M.M. Goel, and A.A. Mahdi, *PI3K/PTEN/Akt and TSC/mTOR signaling pathways, ovarian dysfunction, and infertility: an update.* J Mol Endocrinol, 2014. **53**(3): p. R103-18.
23. Georges, A., et al., *FOXL2: a central transcription factor of the ovary.* J Mol Endocrinol, 2014. **52**(1): p. R17-33.
24. Griffin, J., et al., *Comparative analysis of follicle morphology and oocyte diameter in four mammalian species (mouse, hamster, pig, and human).* J Exp Clin Assist Reprod, 2006. **3**: p. 2.
25. Tilly, J.L., *Commuting the death sentence: how oocytes strive to survive.* Nat Rev Mol Cell Biol, 2001. **2**(11): p. 838-48.

26. Myers, M., et al., *Methods for quantifying follicular numbers within the mouse ovary.* Reproduction, 2004. **127**(5): p. 569-80.
27. Weenen, C., et al., *Anti-Mullerian hormone expression pattern in the human ovary: potential implications for initial and cyclic follicle recruitment.* Mol Hum Reprod, 2004. **10**(2): p. 77-83.
28. Wang, Y., et al., *Influence of mouse defective zona pellucida in folliculogenesis on apoptosis of granulosa cells and developmental competence of oocytesdagger.* Biol Reprod, 2019. **101**(2): p. 457-465.
29. Gougeon, A., *Human ovarian follicular development: from activation of resting follicles to preovulatory maturation.* Ann Endocrinol (Paris), 2010. **71**(3): p. 132-43.
30. Fraser, H.M., *Regulation of the ovarian follicular vasculature.* Reprod Biol Endocrinol, 2006. **4**: p. 18.
31. Zachut, M., et al., *Proteomic analysis of preovulatory follicular fluid reveals differentially abundant proteins in less fertile dairy cows.* J Proteomics, 2016. **139**: p. 122-9.
32. Edson, M.A., A.K. Nagaraja, and M.M. Matzuk, *The mammalian ovary from genesis to revelation.* Endocr Rev, 2009. **30**(6): p. 624-712.
33. Baird, D.T., *Factors regulating the growth of the preovulatory follicle in the sheep and human.* J Reprod Fertil, 1983. **69**(1): p. 343-52.
34. Cox, E. and V. Takov, *Embryology, Ovarian Follicle Development*, in *StatPearls*. 2021: Treasure Island (FL).
35. Martin-Coello, J., et al., *Superovulation and in vitro oocyte maturation in three species of mice (Mus musculus, Mus spretus and Mus spicilegus).* Theriogenology, 2008. **70**(6): p. 1004-13.
36. Baerwald, A.R., G.P. Adams, and R.A. Pierson, *Form and function of the corpus luteum during the human menstrual cycle.* Ultrasound Obstet Gynecol, 2005. **25**(5): p. 498-507.
37. Rowan, K., et al., *Corpus luteum across the first trimester: size and laterality as observed by ultrasound.* Fertil Steril, 2008. **90**(5): p. 1844-7.
38. Dharma, S.J., S.D. Kholkute, and T.D. Nandedkar, *Apoptosis in endometrium of mouse during estrous cycle.* Indian J Exp Biol, 2001. **39**(3): p. 218-22.
39. Wallace, W.H. and T.W. Kelsey, *Human ovarian reserve from conception to the menopause.* PLoS One, 2010. **5**(1): p. e8772.
40. Findlay, J.K., et al., *How Is the Number of Primordial Follicles in the Ovarian Reserve Established?* Biol Reprod, 2015. **93**(5): p. 111.
41. Hussein, M.R., *Apoptosis in the ovary: molecular mechanisms.* Hum Reprod Update, 2005. **11**(2): p. 162-77.
42. Gao, Q., et al., *How chemotherapy and radiotherapy damage the tissue: Comparative biology lessons from feather and hair models.* Exp Dermatol, 2019. **28**(4): p. 413-418.
43. Welt, C.K., *Primary ovarian insufficiency: a more accurate term for premature ovarian failure.* Clin Endocrinol (Oxf), 2008. **68**(4): p. 499-509.
44. Sklar, C., *Maintenance of ovarian function and risk of premature menopause related to cancer treatment.* J Natl Cancer Inst Monogr, 2005(34): p. 25-7.
45. Popat, V.B., et al., *Bone mineral density in estrogen-deficient young women.* J Clin Endocrinol Metab, 2009. **94**(7): p. 2277-83.
46. Chemaitilly, W., et al., *Premature Ovarian Insufficiency in Childhood Cancer Survivors: A Report From the St. Jude Lifetime Cohort.* J Clin Endocrinol Metab, 2017. **102**(7): p. 2242-2250.
47. Daan, N.M., et al., *Cardiovascular Risk in Women With Premature Ovarian Insufficiency Compared to Premenopausal Women at Middle Age.* J Clin Endocrinol Metab, 2016. **101**(9): p. 3306-15.
48. Marci, R., et al., *Radiations and female fertility.* Reprod Biol Endocrinol, 2018. **16**(1): p. 112.
49. Iorio, R., et al., *Ovarian toxicity: from environmental exposure to chemotherapy.* Curr Pharm Des, 2014. **20**(34): p. 5388-97.
50. Meirow, D., et al., *Toxicity of chemotherapy and radiation on female reproduction.* Clin Obstet Gynecol, 2010. **53**(4):

p. 727-39.
51. Stringer, J.M., et al., *Oocytes can efficiently repair DNA double-strand breaks to restore genetic integrity and protect offspring health.* Proc Natl Acad Sci U S A, 2020. **117**(21): p. 11513-11522.
52. Wallace, W.H., et al., *Predicting age of ovarian failure after radiation to a field that includes the ovaries.* Int J Radiat Oncol Biol Phys, 2005. **62**(3): p. 738-44.
53. Meirow, D. and D. Nugent, *The effects of radiotherapy and chemotherapy on female reproduction.* Hum Reprod Update, 2001. **7**(6): p. 535-43.
54. Rebar, R.W., *Premature ovarian "failure" in the adolescent.* Ann N Y Acad Sci, 2008. **1135**: p. 138-45.
55. Letourneau, J.M., et al., *Acute ovarian failure underestimates age-specific reproductive impairment for young women undergoing chemotherapy for cancer.* Cancer, 2012. **118**(7): p. 1933-9.
56. Jayasinghe, Y.L., W.H.B. Wallace, and R.A. Anderson, *Ovarian function, fertility and reproductive lifespan in cancer patients.* Expert Rev Endocrinol Metab, 2018. **13**(3): p. 125-136.
57. Lee, C.J., et al., *Natural and radiation-induced degeneration of primordial and primary follicles in mouse ovary.* Anim Reprod Sci, 2000. **59**(1-2): p. 109-17.
58. Lee, Y.K., et al., *Effects of gamma-radiation on ovarian follicles.* Arh Hig Rada Toksikol, 1998. **49**(2): p. 147-53.
59. Kam, W.W., et al., *Predicted ionisation in mitochondria and observed acute changes in the mitochondrial transcriptome after gamma irradiation: a Monte Carlo simulation and quantitative PCR study.* Mitochondrion, 2013. **13**(6): p. 736-42.
60. Polyak, K., et al., *Somatic mutations of the mitochondrial genome in human colorectal tumours.* Nat Genet, 1998. **20**(3): p. 291-3.
61. Hong, M., et al., *Mechanism of genotoxicity induced by targeted cytoplasmic irradiation.* Br J Cancer, 2010. **103**(8): p. 1263-8.
62. Deshpande, A., et al., *Alpha-particle-induced sister chromatid exchange in normal human lung fibroblasts: evidence for an extranuclear target.* Radiat Res, 1996. **145**(3): p. 260-7.
63. Wallace, D.C., et al., *Sequence analysis of cDNAs for the human and bovine ATP synthase beta subunit: mitochondrial DNA genes sustain seventeen times more mutations.* Curr Genet, 1987. **12**(2): p. 81-90.
64. Hayashi, T., et al., *MAM: more than just a housekeeper.* Trends Cell Biol, 2009. **19**(2): p. 81-8.
65. May-Panloup, P., et al., *Mitochondrial DNA in the oocyte and the developing embryo.* Curr Top Dev Biol, 2007. **77**: p. 51-83.
66. McBride, H.M., M. Neuspiel, and S. Wasiak, *Mitochondria: more than just a powerhouse.* Curr Biol, 2006. **16**(14): p. R551-60.
67. Herrmann, J.M. and W. Neupert, *Protein transport into mitochondria.* Curr Opin Microbiol, 2000. **3**(2): p. 210-4.
68. Chipuk, J.E., L. Bouchier-Hayes, and D.R. Green, *Mitochondrial outer membrane permeabilization during apoptosis: the innocent bystander scenario.* Cell Death Differ, 2006. **13**(8): p. 1396-402.
69. Kuhlbrandt, W., *Structure and function of mitochondrial membrane protein complexes.* BMC Biol, 2015. **13**: p. 89.
70. Sirey, T.M. and C.P. Ponting, *Insights into the post-transcriptional regulation of the mitochondrial electron transport chain.* Biochem Soc Trans, 2016. **44**(5): p. 1491-1498.
71. Jonckheere, A.I., J.A. Smeitink, and R.J. Rodenburg, *Mitochondrial ATP synthase: architecture, function and pathology.* J Inherit Metab Dis, 2012. **35**(2): p. 211-25.
72. Sazanov, L.A., *A giant molecular proton pump: structure and mechanism of respiratory complex I.* Nat Rev Mol Cell Biol, 2015. **16**(6): p. 375-88.
73. Chatterjee, A., S. Dasgupta, and D. Sidransky, *Mitochondrial subversion in cancer.* Cancer Prev Res (Phila), 2011. **4**(5): p. 638-54.
74. Turrens, J.F., *Mitochondrial formation of reactive oxygen species.* J Physiol, 2003. **552**(Pt 2): p. 335-44.
75. Youle, R.J. and A.M. van der Bliek, *Mitochondrial fission, fusion, and stress.* Science, 2012. **337**(6098): p. 1062-5.

76. Aydin, Z.D., et al., *Sun exposure and age at natural menopause: a cross-sectional study in Turkish women.* Maturitas, 2005. **52**(3-4): p. 235-48.
77. Hoppins, S., L. Lackner, and J. Nunnari, *The machines that divide and fuse mitochondria.* Annu Rev Biochem, 2007. **76**: p. 751-80.
78. Palikaras, K. and N. Tavernarakis, *Mitochondrial homeostasis: the interplay between mitophagy and mitochondrial biogenesis.* Exp Gerontol, 2014. **56**: p. 182-8.
79. Zhu, J., K.Z. Wang, and C.T. Chu, *After the banquet: mitochondrial biogenesis, mitophagy, and cell survival.* Autophagy, 2013. **9**(11): p. 1663-76.
80. Dorn, G.W., 2nd, R.B. Vega, and D.P. Kelly, *Mitochondrial biogenesis and dynamics in the developing and diseased heart.* Genes Dev, 2015. **29**(19): p. 1981-91.
81. Karbowski, M. and R.J. Youle, *Dynamics of mitochondrial morphology in healthy cells and during apoptosis.* Cell Death Differ, 2003. **10**(8): p. 870-80.
82. Twig, G., et al., *Fission and selective fusion govern mitochondrial segregation and elimination by autophagy.* EMBO J, 2008. **27**(2): p. 433-46.
83. Gubina, N.E., O.S. Merekina, and T.E. Ushakova, *Mitochondrial DNA transcription in mouse liver, skeletal muscle, and brain following lethal x-ray irradiation.* Biochemistry (Mosc), 2010. **75**(6): p. 777-83.
84. Shoubridge, E.A. and T. Wai, *Mitochondrial DNA and the mammalian oocyte.* Curr Top Dev Biol, 2007. **77**: p. 87-111.
85. Andrews, R.M., et al., *Reanalysis and revision of the Cambridge reference sequence for human mitochondrial DNA.* Nat Genet, 1999. **23**(2): p. 147.
86. Fernandez-Silva, P., J.A. Enriquez, and J. Montoya, *Replication and transcription of mammalian mitochondrial DNA.* Exp Physiol, 2003. **88**(1): p. 41-56.
87. Clayton, D.A., *Transcription and replication of mitochondrial DNA.* Hum Reprod, 2000. **15 Suppl 2**: p. 11-7.
88. Consortium, E.P., et al., *Identification and analysis of functional elements in 1% of the human genome by the ENCODE pilot project.* Nature, 2007. **447**(7146): p. 799-816.
89. Cao, L., et al., *The mitochondrial bottleneck occurs without reduction of mtDNA content in female mouse germ cells.* Nat Genet, 2007. **39**(3): p. 386-90.
90. Chen, X., et al., *Rearranged mitochondrial genomes are present in human oocytes.* Am J Hum Genet, 1995. **57**(2): p. 239-47.
91. Piko, L. and K.D. Taylor, *Amounts of mitochondrial DNA and abundance of some mitochondrial gene transcripts in early mouse embryos.* Dev Biol, 1987. **123**(2): p. 364-74.
92. Steuerwald, N., et al., *Quantification of mRNA in single oocytes and embryos by real-time rapid cycle fluorescence monitored RT-PCR.* Mol Hum Reprod, 2000. **6**(5): p. 448-53.
93. May-Panloup, P., et al., *Low oocyte mitochondrial DNA content in ovarian insufficiency.* Hum Reprod, 2005. **20**(3): p. 593-7.
94. Reynier, P., et al., *Mitochondrial DNA content affects the fertilizability of human oocytes.* Mol Hum Reprod, 2001. **7**(5): p. 425-9.
95. Borrego-Soto, G., R. Ortiz-Lopez, and A. Rojas-Martinez, *Ionizing radiation-induced DNA injury and damage detection in patients with breast cancer.* Genet Mol Biol, 2015. **38**(4): p. 420-32.
96. Hwang, J.J., et al., *Effect of ionizing radiation on liver mitochondrial respiratory functions in mice.* Chin Med J (Engl), 1999. **112**(4): p. 340-4.
97. Livingston, K., et al., *The Role of Mitochondrial Dysfunction in Radiation-Induced Heart Disease: From Bench to Bedside.* Front Cardiovasc Med, 2020. **7**: p. 20.
98. Nugent, S., et al., *Altered mitochondrial function and genome frequency post exposure to γ-radiation and bystander factors.* Int J Radiat Biol, 2010. **86**(10): p. 829-41.

99. Nugent, S.M., et al., *Increased mitochondrial mass in cells with functionally compromised mitochondria after exposure to both direct gamma radiation and bystander factors.* Radiat Res, 2007. **168**(1): p. 134-42.
100. Yamamori, T., et al., *Ionizing radiation induces mitochondrial reactive oxygen species production accompanied by upregulation of mitochondrial electron transport chain function and mitochondrial content under control of the cell cycle checkpoint.* Free Radic Biol Med, 2012. **53**(2): p. 260-70.
101. Zhou, X., et al., *Effects of X-irradiation on mitochondrial DNA damage and its supercoiling formation change.* Mitochondrion, 2011. **11**(6): p. 886-92.
102. Larsen, N.B., M. Rasmussen, and L.J. Rasmussen, *Nuclear and mitochondrial DNA repair: similar pathways?* Mitochondrion, 2005. **5**(2): p. 89-108.
103. Richter, C., J.W. Park, and B.N. Ames, *Normal oxidative damage to mitochondrial and nuclear DNA is extensive.* Proc Natl Acad Sci U S A, 1988. **85**(17): p. 6465-7.
104. Singh, G., et al., *A method for assessing damage to mitochondrial DNA caused by radiation and epichlorohydrin.* Mol Pharmacol, 1985. **27**(1): p. 167-70.
105. Morita, R., et al., *Molecular characterization of mutations induced by gamma irradiation in rice.* Genes Genet Syst, 2009. **84**(5): p. 361-70.
106. Rogounovitch, T.I., et al., *Large deletions in mitochondrial DNA in radiation-associated human thyroid tumors.* Cancer Res, 2002. **62**(23): p. 7031-41.
107. Zhang, S.B., et al., *The murine common deletion: mitochondrial DNA 3,860-bp deletion after irradiation.* Radiat Res, 2013. **180**(4): p. 407-13.
108. Soong, N.W. and N. Arnheim, *Detection and quantification of mitochondrial DNA deletions.* Methods Enzymol, 1996. **264**: p. 421-31.
109. Evdokimovskii, E.V., et al., *[Sharp changes in the copy number of mtDNA and its transcription in the blood cells of X-ray irradiated mice are observed, and mtDNA fragments appear in the blood serum].* Radiats Biol Radioecol, 2007. **47**(4): p. 402-7.
110. Evdokimovsky, E.V., et al., *Alteration of mtDNA copy number, mitochondrial gene expression and extracellular DNA content in mice after irradiation at lethal dose.* Radiat Environ Biophys, 2011. **50**(1): p. 181-8.
111. Morales, A., et al., *Oxidative damage of mitochondrial and nuclear DNA induced by ionizing radiation in human hepatoblastoma cells.* Int J Radiat Oncol Biol Phys, 1998. **42**(1): p. 191-203.
112. Gubina, N.E., E.V. Evdokimovskii, and T.E. Ushakova, *[Mitochondrial genetic apparatus functioning in mice spleen cells under radiation-induced apoptosis].* Mol Biol (Mosk), 2010. **44**(6): p. 1027-35.
113. Yoshida, K., et al., *Mitochondrial genotypes and radiation-induced micronucleus formation in human osteosarcoma cells in vitro.* Oncol Rep, 2001. **8**(3): p. 615-9.
114. Barjaktarovic, Z., et al., *Radiation-induced signaling results in mitochondrial impairment in mouse heart at 4 weeks after exposure to X-rays.* PLoS One, 2011. **6**(12): p. e27811.
115. Bindoli, A., *Lipid peroxidation in mitochondria.* Free Radic Biol Med, 1988. **5**(4): p. 247-61.
116. Sterniczuk, M. and D.M. Bartels, *Source of Molecular Hydrogen in High-Temperature Water Radiolysis.* J Phys Chem A, 2016. **120**(2): p. 200-9.
117. Pryor, W.A., *Oxy-radicals and related species: their formation, lifetimes, and reactions.* Annu Rev Physiol, 1986. **48**: p. 657-67.
118. Kobashigawa, S., K. Suzuki, and S. Yamashita, *Ionizing radiation accelerates Drp1-dependent mitochondrial fission, which involves delayed mitochondrial reactive oxygen species production in normal human fibroblast-like cells.* Biochem Biophys Res Commun, 2011. **414**(4): p. 795-800.
119. Dasari, S. and P.B. Tchounwou, *Cisplatin in cancer therapy: molecular mechanisms of action.* Eur J Pharmacol, 2014. **740**: p. 364-78.
120. Zhao, C., et al., *Drp1-dependent mitophagy protects against cisplatin-induced apoptosis of renal tubular epithelial*

cells by improving mitochondrial function. Oncotarget, 2017. **8**(13): p. 20988-21000.

121. Cullen, K.J., et al., *Mitochondria as a critical target of the chemotheraputic agent cisplatin in head and neck cancer.* J Bioenerg Biomembr, 2007. **39**(1): p. 43-50.
122. Olivero, O.A., et al., *Preferential binding of cisplatin to mitochondrial DNA of Chinese hamster ovary cells.* Mutat Res, 1995. **346**(4): p. 221-30.
123. Murata, T., et al., *Preferential binding of cisplatin to mitochondrial DNA and suppression of ATP generation in human malignant melanoma cells.* Biochem Int, 1990. **20**(5): p. 949-55.
124. Areti, A., et al., *Oxidative stress and nerve damage: role in chemotherapy induced peripheral neuropathy.* Redox Biol, 2014. **2**: p. 289-95.
125. Kim, H.J., et al., *Roles of NADPH oxidases in cisplatin-induced reactive oxygen species generation and ototoxicity.* J Neurosci, 2010. **30**(11): p. 3933-46.
126. Lomeli, N., et al., *Cisplatin-induced mitochondrial dysfunction is associated with impaired cognitive function in rats.* Free Radic Biol Med, 2017. **102**: p. 274-286.
127. Podratz, J.L., et al., *Cisplatin induced mitochondrial DNA damage in dorsal root ganglion neurons.* Neurobiol Dis, 2011. **41**(3): p. 661-8.
128. Kruidering, M., et al., *Cisplatin-induced nephrotoxicity in porcine proximal tubular cells: mitochondrial dysfunction by inhibition of complexes I to IV of the respiratory chain.* J Pharmacol Exp Ther, 1997. **280**(2): p. 638-49.
129. Waseem, M., et al., *Ameliorative efficacy of quercetin against cisplatininduced mitochondrial dysfunction: Study on isolated rat liver mitochondria.* Mol Med Rep, 2017. **16**(3): p. 2939-2945.
130. Mapuskar, K.A., et al., *Mitochondrial Superoxide Increases Age-Associated Susceptibility of Human Dermal Fibroblasts to Radiation and Chemotherapy.* Cancer Res, 2017. **77**(18): p. 5054-5067.
131. Ma, J., et al., *Emodin augments cisplatin cytotoxicity in platinum-resistant ovarian cancer cells via ROS-dependent MRP1 downregulation.* Biomed Res Int, 2014. **2014**: p. 107671.
132. Berndtsson, M., et al., *Acute apoptosis by cisplatin requires induction of reactive oxygen species but is not associated with damage to nuclear DNA.* Int J Cancer, 2007. **120**(1): p. 175-80.
133. Custodio, J.B., et al., *Cisplatin impairs rat liver mitochondrial functions by inducing changes on membrane ion permeability: prevention by thiol group protecting agents.* Toxicology, 2009. **259**(1-2): p. 18-24.
134. Huang, H.L., et al., *DNA-damaging reagents induce apoptosis through reactive oxygen species-dependent Fas aggregation.* Oncogene, 2003. **22**(50): p. 8168-77.
135. Stewart, D.J., *Mechanisms of resistance to cisplatin and carboplatin.* Crit Rev Oncol Hematol, 2007. **63**(1): p. 12-31.
136. Jing, X.B., et al., *Reactive oxygen species and mitochondrial membrane potential are modulated during CDDP-induced apoptosis in EC-109 cells.* Biochem Cell Biol, 2007. **85**(2): p. 265-71.
137. Fulda, S. and K.M. Debatin, *Extrinsic versus intrinsic apoptosis pathways in anticancer chemotherapy.* Oncogene, 2006. **25**(34): p. 4798-811.
138. Kleih, M., et al., *Direct impact of cisplatin on mitochondria induces ROS production that dictates cell fate of ovarian cancer cells.* Cell Death Dis, 2019. **10**(11): p. 851.
139. Pizzino, G., et al., *Oxidative Stress: Harms and Benefits for Human Health.* Oxid Med Cell Longev, 2017. **2017**: p. 8416763.
140. Perillo, B., et al., *ROS in cancer therapy: the bright side of the moon.* Exp Mol Med, 2020. **52**(2): p. 192-203.
141. Kim, H.K. and J. Han, *Mitochondria-Targeted Antioxidants for the Treatment of Cardiovascular Disorders.* Adv Exp Med Biol, 2017. **982**: p. 621-646.
142. Kim, S.J., H.S. Kim, and Y.R. Seo, *Understanding of ROS-Inducing Strategy in Anticancer Therapy.* Oxid Med Cell Longev, 2019. **2019**: p. 5381692.
143. Song, J., N. Pfanner, and T. Becker, *Assembling the mitochondrial ATP synthase.* Proc Natl Acad Sci U S A, 2018.

115(12): p. 2850-2852.
144. Zhao, R.Z., et al., *Mitochondrial electron transport chain, ROS generation and uncoupling (Review).* Int J Mol Med, 2019. **44**(1): p. 3-15.
145. Yang, S. and G. Lian, *ROS and diseases: role in metabolism and energy supply.* Mol Cell Biochem, 2020. **467**(1-2): p. 1-12.
146. Hamanaka, R.B. and N.S. Chandel, *Mitochondrial reactive oxygen species regulate cellular signaling and dictate biological outcomes.* Trends Biochem Sci, 2010. **35**(9): p. 505-13.
147. Hawkins, C.L. and M.J. Davies, *Detection, identification, and quantification of oxidative protein modifications.* J Biol Chem, 2019. **294**(51): p. 19683-19708.
148. Cai, Z. and L.J. Yan, *Protein Oxidative Modifications: Beneficial Roles in Disease and Health.* J Biochem Pharmacol Res, 2013. **1**(1): p. 15-26.
149. Maruo, A., et al., *Protein tyrosine kinase Lyn mediates apoptosis induced by topoisomerase II inhibitors in DT40 cells.* Int Immunol, 1999. **11**(9): p. 1371-80.
150. Campolo, N., et al., *3-Nitrotyrosine and related derivatives in proteins: precursors, radical intermediates and impact in function.* Essays Biochem, 2020. **64**(1): p. 111-133.
151. Su, L.J., et al., *Reactive Oxygen Species-Induced Lipid Peroxidation in Apoptosis, Autophagy, and Ferroptosis.* Oxid Med Cell Longev, 2019. **2019**: p. 5080843.
152. Ayala, A., M.F. Munoz, and S. Arguelles, *Lipid peroxidation: production, metabolism, and signaling mechanisms of malondialdehyde and 4-hydroxy-2-nonenal.* Oxid Med Cell Longev, 2014. **2014**: p. 360438.
153. Zhong, H. and H. Yin, *Role of lipid peroxidation derived 4-hydroxynonenal (4-HNE) in cancer: focusing on mitochondria.* Redox Biol, 2015. **4**: p. 193-9.
154. West, J.D. and L.J. Marnett, *Endogenous reactive intermediates as modulators of cell signaling and cell death.* Chem Res Toxicol, 2006. **19**(2): p. 173-94.
155. Oberley, T.D., S. Toyokuni, and L.I. Szweda, *Localization of hydroxynonenal protein adducts in normal human kidney and selected human kidney cancers.* Free Radic Biol Med, 1999. **27**(5-6): p. 695-703.
156. Mihalas, B.P., et al., *The lipid peroxidation product 4-hydroxynonenal contributes to oxidative stress-mediated deterioration of the ageing oocyte.* Sci Rep, 2017. **7**(1): p. 6247.
157. Davalli, P., et al., *Targeting Oxidatively Induced DNA Damage Response in Cancer: Opportunities for Novel Cancer Therapies.* Oxid Med Cell Longev, 2018. **2018**: p. 2389523.
158. Salehi, F., et al., *Oxidative DNA damage induced by ROS-modulating agents with the ability to target DNA: A comparison of the biological characteristics of citrus pectin and apple pectin.* Sci Rep, 2018. **8**(1): p. 13902.
159. Moloney, J.N. and T.G. Cotter, *ROS signalling in the biology of cancer.* Semin Cell Dev Biol, 2018. **80**: p. 50-64.
160. Srinivas, U.S., et al., *ROS and the DNA damage response in cancer.* Redox Biol, 2019. **25**: p. 101084.
161. Pacher, P., J.S. Beckman, and L. Liaudet, *Nitric oxide and peroxynitrite in health and disease.* Physiol Rev, 2007. **87**(1): p. 315-424.
162. Butterfield, D.A., *Amyloid beta-peptide (1-42)-induced oxidative stress and neurotoxicity: implications for neurodegeneration in Alzheimer's disease brain. A review.* Free Radic Res, 2002. **36**(12): p. 1307-13.
163. Hoshino, Y. and M. Mishima, *Redox-based therapeutics for lung diseases.* Antioxid Redox Signal, 2008. **10**(4): p. 701-4.
164. Galle, J., *Oxidative stress in chronic renal failure.* Nephrol Dial Transplant, 2001. **16**(11): p. 2135-7.
165. Samuel, J.B., et al., *Gestational cadmium exposure-induced ovotoxicity delays puberty through oxidative stress and impaired steroid hormone levels.* J Med Toxicol, 2011. **7**(3): p. 195-204.
166. Lobo, V., et al., *Free radicals, antioxidants and functional foods: Impact on human health.* Pharmacogn Rev, 2010. **4**(8): p. 118-26.
167. Steinhubl, S.R., *Why have antioxidants failed in clinical trials?* Am J Cardiol, 2008. **101**(10A): p. 14D-19D.

168. Glasauer, A. and N.S. Chandel, *Targeting antioxidants for cancer therapy.* Biochem Pharmacol, 2014. **92**(1): p. 90-101.
169. Smith, R.A. and M.P. Murphy, *Mitochondria-targeted antioxidants as therapies.* Discov Med, 2011. **11**(57): p. 106-14.
170. Dashdorj, A., et al., *Mitochondria-targeted antioxidant MitoQ ameliorates experimental mouse colitis by suppressing NLRP3 inflammasome-mediated inflammatory cytokines.* BMC Med, 2013. **11**: p. 178.
171. Mitchell, W., et al., *The mitochondria-targeted peptide SS-31 binds lipid bilayers and modulates surface electrostatics as a key component of its mechanism of action.* J Biol Chem, 2020. **295**(21): p. 7452-7469.
172. Rocha, M., et al., *Mitochondria-targeted antioxidant peptides.* Curr Pharm Des, 2010. **16**(28): p. 3124-31.
173. Broome, S.C., J.S.T. Woodhead, and T.L. Merry, *Mitochondria-Targeted Antioxidants and Skeletal Muscle Function.* Antioxidants (Basel), 2018. **7**(8).
174. Szeto, H.H. and A.V. Birk, *Serendipity and the discovery of novel compounds that restore mitochondrial plasticity.* Clin Pharmacol Ther, 2014. **96**(6): p. 672-83.
175. Chatfield, K.C., et al., *Elamipretide Improves Mitochondrial Function in the Failing Human Heart.* JACC Basic Transl Sci, 2019. **4**(2): p. 147-157.
176. Saini, R., *Coenzyme Q10: The essential nutrient.* J Pharm Bioallied Sci, 2011. **3**(3): p. 466-7.
177. Smith, R.A., et al., *Targeting coenzyme Q derivatives to mitochondria.* Methods Enzymol, 2004. **382**: p. 45-67.
178. Murphy, M.P. and R.A. Smith, *Targeting antioxidants to mitochondria by conjugation to lipophilic cations.* Annu Rev Pharmacol Toxicol, 2007. **47**: p. 629-56.
179. Smith, R.A. and M.P. Murphy, *Animal and human studies with the mitochondria-targeted antioxidant MitoQ.* Ann N Y Acad Sci, 2010. **1201**: p. 96-103.
180. Koopman, W.J., et al., *Inhibition of complex I of the electron transport chain causes O2-. -mediated mitochondrial outgrowth.* Am J Physiol Cell Physiol, 2005. **288**(6): p. C1440-50.
181. Yang, Y., et al., *Mitochondria and Mitochondrial ROS in Cancer: Novel Targets for Anticancer Therapy.* J Cell Physiol, 2016. **231**(12): p. 2570-81.
182. Fouret, G., et al., *The mitochondrial-targeted antioxidant, MitoQ, increases liver mitochondrial cardiolipin content in obesogenic diet-fed rats.* Biochim Biophys Acta, 2015. **1847**(10): p. 1025-35.
183. James, A.M., et al., *Interactions of mitochondria-targeted and untargeted ubiquinones with the mitochondrial respiratory chain and reactive oxygen species. Implications for the use of exogenous ubiquinones as therapies and experimental tools.* J Biol Chem, 2005. **280**(22): p. 21295-312.
184. Radi, R., *Oxygen radicals, nitric oxide, and peroxynitrite: Redox pathways in molecular medicine.* Proc Natl Acad Sci U S A, 2018. **115**(23): p. 5839-5848.
185. Zhang, Z.W., et al., *Mitochondrion-Permeable Antioxidants to Treat ROS-Burst-Mediated Acute Diseases.* Oxid Med Cell Longev, 2016. **2016**: p. 6859523.
186. Gane, E.J., et al., *The mitochondria-targeted anti-oxidant mitoquinone decreases liver damage in a phase II study of hepatitis C patients.* Liver Int, 2010. **30**(7): p. 1019-26.
187. Rossman, M.J., et al., *Chronic Supplementation With a Mitochondrial Antioxidant (MitoQ) Improves Vascular Function in Healthy Older Adults.* Hypertension, 2018. **71**(6): p. 1056-1063.
188. McManus, M.J., M.P. Murphy, and J.L. Franklin, *The mitochondria-targeted antioxidant MitoQ prevents loss of spatial memory retention and early neuropathology in a transgenic mouse model of Alzheimer's disease.* J Neurosci, 2011. **31**(44): p. 15703-15.
189. Ribeiro Junior, R.F., et al., *MitoQ improves mitochondrial dysfunction in heart failure induced by pressure overload.* Free Radic Biol Med, 2018. **117**: p. 18-29.
190. Xiao, L., et al., *The mitochondria-targeted antioxidant MitoQ ameliorated tubular injury mediated by mitophagy in diabetic kidney disease via Nrf2/PINK1.* Redox Biol, 2017. **11**: p. 297-311.

191. Kyei, G., et al., *Assessing the effect of MitoQ10 and Vitamin D3 on ovarian oxidative stress, steroidogenesis and histomorphology in DHEA induced PCOS mouse model.* Heliyon, 2020. **6**(7): p. e04279.
192. Zhang, J., et al., *MitoQ ameliorates testis injury from oxidative attack by repairing mitochondria and promoting the Keap1-Nrf2 pathway.* Toxicol Appl Pharmacol, 2019. **370**: p. 78-92.
193. Ibrahim, A.A., et al., *MitoQ ameliorates testicular damage induced by gamma irradiation in rats: Modulation of mitochondrial apoptosis and steroidogenesis.* Life Sci, 2019. **232**: p. 116655.
194. Zhang, J., et al., *ROS and ROS-Mediated Cellular Signaling.* Oxid Med Cell Longev, 2016. **2016**: p. 4350965.
195. Thannickal, V.J. and B.L. Fanburg, *Reactive oxygen species in cell signaling.* Am J Physiol Lung Cell Mol Physiol, 2000. **279**(6): p. L1005-28.
196. Marusich, M.F., et al., *Expression of mtDNA and nDNA encoded respiratory chain proteins in chemically and genetically-derived Rho0 human fibroblasts: a comparison of subunit proteins in normal fibroblasts treated with ethidium bromide and fibroblasts from a patient with mtDNA depletion syndrome.* Biochim Biophys Acta, 1997. **1362**(2-3): p. 145-59.
197. Kim, W., et al., *Cellular Stress Responses in Radiotherapy.* Cells, 2019. **8**(9).
198. Brozovic, A., A. Ambriovic-Ristov, and M. Osmak, *The relationship between cisplatin-induced reactive oxygen species, glutathione, and BCL-2 and resistance to cisplatin.* Crit Rev Toxicol, 2010. **40**(4): p. 347-59.
199. Baskar, R., et al., *Cancer and radiation therapy: current advances and future directions.* Int J Med Sci, 2012. **9**(3): p. 193-9.
200. Kawamura, K., F. Qi, and J. Kobayashi, *Potential relationship between the biological effects of low-dose irradiation and mitochondrial ROS production.* J Radiat Res, 2018. **59**(suppl_2): p. ii91-ii97.
201. Yusoff, A.A.M., et al., *A comprehensive overview of mitochondrial DNA 4977-bp deletion in cancer studies.* Oncol Rev, 2019. **13**(1): p. 409.
202. Guo, Z.S., et al., *Analysis of the Mitochondrial 4977 Bp Deletion in Patients with Hepatocellular Carcinoma.* Balkan J Med Genet, 2017. **20**(1): p. 81-86.
203. Murphy, M.P., *Understanding and preventing mitochondrial oxidative damage.* Biochem Soc Trans, 2016. **44**(5): p. 1219-1226.
204. Wang, Q., et al., *Evaluation of mitochondria in oocytes following gamma-irradiation.* Sci Rep, 2019. **9**(1): p. 19941.
205. Winship, A.L., et al., *Accurate Follicle Enumeration in Adult Mouse Ovaries.* J Vis Exp, 2020(164).
206. Sarma, U.C., A.L. Winship, and K.J. Hutt, *Comparison of methods for quantifying primordial follicles in the mouse ovary.* J Ovarian Res, 2020. **13**(1): p. 121.
207. Li, R., T. Ren, and J. Zeng, *Mitochondrial Coenzyme Q Protects Sepsis-Induced Acute Lung Injury by Activating PI3K/Akt/GSK-3beta/mTOR Pathway in Rats.* Biomed Res Int, 2019. **2019**: p. 5240898.
208. Sasaki, H., et al., *Impact of Oxidative Stress on Age-Associated Decline in Oocyte Developmental Competence.* Front Endocrinol (Lausanne), 2019. **10**: p. 811.
209. Leon, J., et al., *8-Oxoguanine accumulation in mitochondrial DNA causes mitochondrial dysfunction and impairs neuritogenesis in cultured adult mouse cortical neurons under oxidative conditions.* Sci Rep, 2016. **6**: p. 22086.
210. Bernard, M.E., et al., *Role of the esophageal vagus neural pathway in ionizing irradiation-induced seizures in nitric oxide synthase-1 homologous recombinant negative NOS1-/- mice.* In Vivo, 2011. **25**(6): p. 861-9.
211. Said, R.S., A.S. Nada, and E. El-Demerdash, *Sodium selenite improves folliculogenesis in radiation-induced ovarian failure: a mechanistic approach.* PLoS One, 2012. **7**(12): p. e50928.
212. Yilmaz, S. and E. Yilmaz, *Effects of melatonin and vitamin E on oxidative-antioxidative status in rats exposed to irradiation.* Toxicology, 2006. **222**(1-2): p. 1-7.
213. Lord, T., J.H. Martin, and R.J. Aitken, *Accumulation of electrophilic aldehydes during postovulatory aging of mouse oocytes causes reduced fertility, oxidative stress, and apoptosis.* Biol Reprod, 2015. **92**(2): p. 33.
214. Bradley, J., et al., *Quantitative imaging of lipids in live mouse oocytes and early embryos using CARS microscopy.*

Development, 2016. **143**(12): p. 2238-47.
215. Nita, M. and A. Grzybowski, *The Role of the Reactive Oxygen Species and Oxidative Stress in the Pathomechanism of the Age-Related Ocular Diseases and Other Pathologies of the Anterior and Posterior Eye Segments in Adults.* Oxid Med Cell Longev, 2016. **2016**: p. 3164734.
216. Azzam, E.I., J.P. Jay-Gerin, and D. Pain, *Ionizing radiation-induced metabolic oxidative stress and prolonged cell injury.* Cancer Lett, 2012. **327**(1-2): p. 48-60.
217. Wu, M., et al., *Resveratrol alleviates chemotherapy-induced oogonial stem cell apoptosis and ovarian aging in mice.* Aging (Albany NY), 2019. **11**(3): p. 1030-1044.
218. Nguyen, Q.N., et al., *Loss of PUMA protects the ovarian reserve during DNA-damaging chemotherapy and preserves fertility.* Cell Death Dis, 2018. **9**(6): p. 618.
219. Li, M., *The role of P53 up-regulated modulator of apoptosis (PUMA) in ovarian development, cardiovascular and neurodegenerative diseases.* Apoptosis, 2021.
220. Wang, Q. and K.J. Hutt, *Evaluation of mitochondria in mouse oocytes following cisplatin exposure.* J Ovarian Res, 2021. **14**(1): p. 65.
221. Muntean, D.M., et al., *The Role of Mitochondrial Reactive Oxygen Species in Cardiovascular Injury and Protective Strategies.* Oxid Med Cell Longev, 2016. **2016**: p. 8254942.
222. Redza-Dutordoir, M. and D.A. Averill-Bates, *Activation of apoptosis signalling pathways by reactive oxygen species.* Biochim Biophys Acta, 2016. **1863**(12): p. 2977-2992.
223. Snow, B.J., et al., *A double-blind, placebo-controlled study to assess the mitochondria-targeted antioxidant MitoQ as a disease-modifying therapy in Parkinson's disease.* Mov Disord, 2010. **25**(11): p. 1670-4.
224. Chandran, K., et al., *Doxorubicin inactivates myocardial cytochrome c oxidase in rats: cardioprotection by Mito-Q.* Biophys J, 2009. **96**(4): p. 1388-98.
225. Porteous, C.M., et al., *Rapid uptake of lipophilic triphenylphosphonium cations by mitochondria in vivo following intravenous injection: implications for mitochondria-specific therapies and probes.* Biochim Biophys Acta, 2010. **1800**(9): p. 1009-17.
226. Pokrzywinski, K.L., et al., *Therapeutic Targeting of the Mitochondria Initiates Excessive Superoxide Production and Mitochondrial Depolarization Causing Decreased mtDNA Integrity.* PLoS One, 2016. **11**(12): p. e0168283.
227. Sun, C., et al., *MitoQ regulates autophagy by inducing a pseudo-mitochondrial membrane potential.* Autophagy, 2017. **13**(4): p. 730-738.
228. Gottwald, E.M., et al., *The targeted anti-oxidant MitoQ causes mitochondrial swelling and depolarization in kidney tissue.* Physiol Rep, 2018. **6**(7): p. e13667.
229. Al-Zubaidi, U., et al., *Mitochondria-targeted therapeutics, MitoQ and BGP-15, reverse aging-associated meiotic spindle defects in mouse and human oocytes.* Hum Reprod, 2021. **36**(3): p. 771-784.
230. Zhou, J., et al., *Mitochondrial-targeted antioxidant MitoQ provides neuroprotection and reduces neuronal apoptosis in experimental traumatic brain injury possibly via the Nrf2-ARE pathway.* Am J Transl Res, 2018. **10**(6): p. 1887-1899.
231. Sapmaz-Metin, M., M. Kanter, and C. Uzal, *The role of ionizing radiaton on ovulation rate and oocyte morphology in mouse.* Acta Biol Hung, 2014. **65**(1): p. 27-37.
232. Hosseinzadeh Shirzeyli, M., et al., *Exposing Mouse Oocytes to MitoQ During In Vitro Maturation Improves Maturation and Developmental Competence.* Iran J Biotechnol, 2020. **18**(3): p. e2454.
233. Shi, L., et al., *Long-Term Moderate Oxidative Stress Decreased Ovarian Reproductive Function by Reducing Follicle Quality and Progesterone Production.* PLoS One, 2016. **11**(9): p. e0162194.
234. Lim, J. and U. Luderer, *Oxidative damage increases and antioxidant gene expression decreases with aging in the mouse ovary.* Biol Reprod, 2011. **84**(4): p. 775-82.
235. Agarwal, A., et al., *The effects of oxidative stress on female reproduction: a review.* Reprod Biol Endocrinol, 2012.

10: p. 49.

236. Warzych, E. and P. Lipinska, *Energy metabolism of follicular environment during oocyte growth and maturation.* J Reprod Dev, 2020. **66**(1): p. 1-7.
237. Mihalas, B.P., et al., *Oxidative damage in naturally aged mouse oocytes is exacerbated by dysregulation of proteasomal activity.* J Biol Chem, 2018. **293**(49): p. 18944-18964.
238. Mishra, B., L. Ortiz, and U. Luderer, *Charged iron particles, components of space radiation, destroy ovarian follicles.* Hum Reprod, 2016. **31**(8): p. 1816-26.
239. Wang, Y.F., et al., *Protective effects of melatonin against nicotine-induced disorder of mouse early folliculogenesis.* Aging (Albany NY), 2018. **10**(3): p. 463-480.
240. Nguyen, Q.N., et al., *Cisplatin- and cyclophosphamide-induced primordial follicle depletion is caused by direct damage to oocytes.* Mol Hum Reprod, 2019. **25**(8): p. 433-444.
241. Waimey, K.E., et al., *Understanding Fertility in Young Female Cancer Patients.* J Womens Health (Larchmt), 2015. **24**(10): p. 812-8.
242. Gorini, S., et al., *Chemotherapeutic Drugs and Mitochondrial Dysfunction: Focus on Doxorubicin, Trastuzumab, and Sunitinib.* Oxid Med Cell Longev, 2018. **2018**: p. 7582730.
243. Sabharwal, S.S. and P.T. Schumacker, *Mitochondrial ROS in cancer: initiators, amplifiers or an Achilles' heel?* Nat Rev Cancer, 2014. **14**(11): p. 709-21.
244. Bavister, B.D. and J.M. Squirrell, *Mitochondrial distribution and function in oocytes and early embryos.* Hum Reprod, 2000. **15 Suppl 2**: p. 189-98.
245. Stojkovic, M., et al., *Mitochondrial distribution and adenosine triphosphate content of bovine oocytes before and after in vitro maturation: correlation with morphological criteria and developmental capacity after in vitro fertilization and culture.* Biol Reprod, 2001. **64**(3): p. 904-9.
246. Wang, L.Y., et al., *Mitochondrial functions on oocytes and preimplantation embryos.* J Zhejiang Univ Sci B, 2009. **10**(7): p. 483-92.
247. Westermann, B., *Bioenergetic role of mitochondrial fusion and fission.* Biochim Biophys Acta, 2012. **1817**(10): p. 1833-8.
248. Sirago, G., et al., *Growth hormone secretagogues hexarelin and JMV2894 protect skeletal muscle from mitochondrial damages in a rat model of cisplatin-induced cachexia.* Sci Rep, 2017. **7**(1): p. 13017.
249. Sheng, J., et al., *Inhibition of PI3K/mTOR increased the sensitivity of hepatocellular carcinoma cells to cisplatin via interference with mitochondrial-lysosomal crosstalk.* Cell Prolif, 2019. **52**(3): p. e12609.
250. Perry, S.W., et al., *Mitochondrial membrane potential probes and the proton gradient: a practical usage guide.* Biotechniques, 2011. **50**(2): p. 98-115.
251. Adrie, C., et al., *Mitochondrial membrane potential and apoptosis peripheral blood monocytes in severe human sepsis.* Am J Respir Crit Care Med, 2001. **164**(3): p. 389-95.
252. Ly, J.D., D.R. Grubb, and A. Lawen, *The mitochondrial membrane potential (deltapsi(m)) in apoptosis; an update.* Apoptosis, 2003. **8**(2): p. 115-28.
253. Hacker, G., *The morphology of apoptosis.* Cell Tissue Res, 2000. **301**(1): p. 5-17.
254. Zorova, L.D., et al., *Mitochondrial membrane potential.* Anal Biochem, 2018. **552**: p. 50-59.
255. Boengler, K., G. Heusch, and R. Schulz, *Nuclear-encoded mitochondrial proteins and their role in cardioprotection.* Biochim Biophys Acta, 2011. **1813**(7): p. 1286-94.
256. Nguyen, Q.N., et al., *DNA repair in primordial follicle oocytes following cisplatin treatment.* J Assist Reprod Genet, 2021.
257. Adriaens, I., J. Smitz, and P. Jacquet, *The current knowledge on radiosensitivity of ovarian follicle development stages.* Hum Reprod Update, 2009. **15**(3): p. 359-77.
258. Rossi, V., et al., *LH prevents cisplatin-induced apoptosis in oocytes and preserves female fertility in mouse.* Cell

Death Differ, 2017. **24**(1): p. 72-82.
259. Dalton, C.M., G. Szabadkai, and J. Carroll, *Measurement of ATP in single oocytes: impact of maturation and cumulus cells on levels and consumption.* J Cell Physiol, 2014. **229**(3): p. 353-61.
260. Babayev, E. and E. Seli, *Oocyte mitochondrial function and reproduction.* Curr Opin Obstet Gynecol, 2015. **27**(3): p. 175-81.
261. Kerr, J.B., et al., *Cisplatin-induced primordial follicle oocyte killing and loss of fertility are not prevented by imatinib.* Nat Med, 2012. **18**(8): p. 1170-2; author reply 1172-4.
262. Wang, Q., et al., *Mitochondrial dysfunction and apoptosis in cumulus cells of type I diabetic mice.* PLoS One, 2010. **5**(12): p. e15901.
263. Murphy, M.P., *How mitochondria produce reactive oxygen species.* Biochem J, 2009. **417**(1): p. 1-13.
264. Jin, H., et al., *Mitochondria-targeted antioxidants for treatment of Parkinson's disease: preclinical and clinical outcomes.* Biochim Biophys Acta, 2014. **1842**(8): p. 1282-94.
265. So, H., et al., *Cisplatin cytotoxicity of auditory cells requires secretions of proinflammatory cytokines via activation of ERK and NF-kappaB.* J Assoc Res Otolaryngol, 2007. **8**(3): p. 338-55.
266. Yang, Z., et al., *Cisplatin preferentially binds mitochondrial DNA and voltage-dependent anion channel protein in the mitochondrial membrane of head and neck squamous cell carcinoma: possible role in apoptosis.* Clin Cancer Res, 2006. **12**(19): p. 5817-25.
267. Schultz, R.M. and P.M. Wassarman, *Biochemical studies of mammalian oogenesis: Protein synthesis during oocyte growth and meiotic maturation in the mouse.* J Cell Sci, 1977. **24**: p. 167-94.
268. Pickering, A.M. and K.J. Davies, *Degradation of damaged proteins: the main function of the 20S proteasome.* Prog Mol Biol Transl Sci, 2012. **109**: p. 227-48.